UNIVERSITÉ DU QUÉBEC À CHICOUTIMI

MÉMOIRE PRÉSENTÉ À
L'UNIVERSITÉ DU QUÉBEC À CHICOUTIMI
COMME EXIGENCE PARTIELLE
DE LA MAÎTRISE EN INGÉNIERIE

PAR
DEYU YANG

# RÔLE D'ADDITION DE MAGNÉSIUM SUR L'OCCURRENCE DE LA FONTE NAISSANTE DANS LES ALLIAGES EXPÉRIMENTAUX ET COMMERCIAUX AL-SI-CU ET SON INFLUENCE SUR LA MICROSTRUCTURE ET LES PROPRIÉTÉS DE TRACTION DE L'ALLIAGE

MARS 2006

Bibliothèque Paul-Émile-Boulet

UQAC Université du Québec à Chicoutimi

# ***Mise en garde/Advice***

Afin de rendre accessible au plus grand nombre le résultat des travaux de recherche menés par ses étudiants gradués et dans l'esprit des règles qui régissent le dépôt et la diffusion des mémoires et thèses produits dans cette Institution, **l'Université du Québec à Chicoutimi (UQAC)** est fière de rendre accessible une version complète et gratuite de cette œuvre.

Motivated by a desire to make the results of its graduate students' research accessible to all, and in accordance with the rules governing the acceptation and diffusion of dissertations and theses in this Institution, the **Université du Québec à Chicoutimi (UQAC)** is proud to make a complete version of this work available at no cost to the reader.

L'auteur conserve néanmoins la propriété du droit d'auteur qui protège ce mémoire ou cette thèse. Ni le mémoire ou la thèse ni des extraits substantiels de ceux-ci ne peuvent être imprimés ou autrement reproduits sans son autorisation.

The author retains ownership of the copyright of this dissertation or thesis. Neither the dissertation or thesis, nor substantial extracts from it, may be printed or otherwise reproduced without the author's permission.

UNIVERSITÉ DU QUÉBEC À CHICOUTIMI

MÉMOIRE PRÉSENTÉ À
L'UNIVERSITÉ DU QUÉBEC À CHICOUTIMI
COMME EXIGENCE PARTIELLE
DE LA MAÎTRISE EN INGÉNIERIE

BY
DEYU YANG

# ROLE OF MAGNESIUM ADDITION ON THE OCCURRENCE OF INCIPIENT MELTING IN EXPERIMENTAL AND COMMERCIAL AL-SI-CU ALLOYS AND ITS INFLUENCE ON THE ALLOY MICROSTRUCTURE AND TENSILE PROPERTIES

MARCH 2006

*Dedicated to my parents*

*谨以此献给我的父母*

# RESUME

Les alliages de fonderie Al-Si sont largement répandus dans des applications des véhicules à moteur à cause de leur rapport résistance/poids et capacité élevée d'être moulé dans des formes complexes. Parmi ces alliages, on trouve l'alliage de type 319, appartenant au système Al-Si-Cu qui est populairement utilisé dans de telles applications, où du magnésium est souvent ajouté à l'alliage pour renforcer ses propriétés. Ces alliages sont habituellement soumis à un traitement thermique afin d'obtenir une combinaison optimale de résistance et de ductilité. L'excellente coulabilité et les propriétés mécaniques de tels alliages Al-Si-Cu-Mg les ont rendus commercialement populaires pour des applications industrielles.

Les propriétés mécaniques d'un alliage coulé sont commandées par sa microstructure qui, alternativement, est influencée par la composition en éléments d'alliage et les conditions de solidifications utilisées. Dans le cas des alliages de type 319 (Al-Si-Cu-Mg), plusieurs facteurs se mettent en jeu, à savoir, la finesse des dendrites primaires de la phase $\alpha$-Al (déterminée par la valeur de l'espace interdendritique (DAS)), la structure du silicium eutectique Al-Si dont sa morphologie brute passant d'une forme aciculaire à une forme fibreuse lors d'une modification, les $CuAl_2$ et tous autres intermétalliques de cuivre, autres constituants de deuxième phase comme les intermétalliques de fer et les phases $Mg_2Si$ dépendant de l'alliage et les éléments de trace actuels dans celui-ci. La forme du silicium eutectique normalement aciculaire peut être transformée ou modifiée à une forme fibreuse par l'addition d'un modificateur comme le sodium Na ou le strontium Sr au métal liquide; ceci permet d'améliorer la ductilité et la résistance de l'alliage. On observe également du magnésium pour modifier le silicium eutectique. Cependant, il cause également une ségrégation des phases de cuivre, ceci peut mener aux problèmes au métal liquide (fonte naissante).

Les propriétés des alliages contenant des éléments tels que le Cu et le Mg peuvent également être améliorées par un traitement thermique, où la formation des précipités fins de type $CuAl_2$ et $Mg_2Si$ pendant le vieillissement ont comme conséquence un durcissement de l'alliage. Un traitement thermique typique se compose d'un traitement de mise en solution, suivi d'une trempe et d'un vieillissement artificiel. Le traitement thermique de mise en solution est effectué pour réaliser une dissolution maximale du cuivre et du magnésium dans la matrice en aluminium. Pour ceci, la température de traitement de mise en solution doit être gardée aussi étroitement que possible à la température eutectique de

Al-$CuAl_2$, mais, en même temps, doit être limitée à un niveau sûr au-dessous du maximum pour éviter une fonte naissante des phases de cuivre qui auraient comme conséquence la formation des cavités après la trempe et abaisseraient la solidité de l'alliage.

Le procédé de traitement thermique de mise en solution peut être suivi étape par étape ou dans des étapes multiples. Malheureusement, une seule étape ou un traitement thermique conventionnel de mise en solution utilisé pour un alliage de type 319 (~498°C) n'est ni capable de maximiser la dissolution des phases riches en cuivre ni capable de modifier suffisamment la morphologie des particules de silicium où tous les deux sont exigés pour améliorer les propriétés de l'alliage. Pour surmonter ceci, un traitement de mise en solution en deux étapes (traitement conventionnel de mise en solution suivi d'un traitement de mise en solution de température plus élevée) a été suggéré, qui améliore de manière significative la dissolution de la phase riche en cuivre, provoquant une meilleure homogénéisation avant le vieillissement, et de ce fait améliorant les propriétés mécaniques.

La présente étude a été entreprise pour étudier l'effet du magnésium sur l'occurrence de la fonte naissante dans les alliages expérimentaux et industriels de type 319, en utilisant l'analyse thermique, des essais de traction, l'analyse microstructurale et des mesures de porosité. Des échantillons ont été préparés à partir des fontes expérimentales et industrielles d'alliage contenant des niveaux de magnésium variant de 0 à 0.6 % en poids. Les barreaux pour des essais de traction ont été moulés en utilisant un moule permanent de type ASTM B-108. Les barreaux ont subi un traitement thermique de mise en solution dans la gamme de 490°C à 540°C pour le traitement de mise en solution de pas à pas, et à 505°C suivi de 520°C ou de 530°C pour le traitement thermique de mise en solution à deux étages. Des essais de traction ont été effectués à l'aide d'une machine d'essai mécanique MTS. La porosité qui est dûe à la fonte naissante a été également mesurée pour surveiller l'occurrence de la fonte naissante. La microscopie, l'analyse d'image et les techniques optiques d'EPMA ont été employées pour l'analyse, la quantification, et l'identification microstructurale des phases.

Les résultats ont montré que la concentration en magnésium et la température de mise en solution jouent un rôle important dans l'occurrence de la fonte naissante. Les mesures de porosité ont prouvé qu'elles sont en relation avec les propriétés de traction et ont confirmé les résultats obtenus en termes de fonte naissante observée pour chaque condition de l'alliage ou de traitement de mise en solution. L'addition du magnésium mène à la ségrégation de la phase de cuivre, ayant pour résultat la formation de la phase eutectique $CuAl_2$ sous forme de blocs plutôt qu'à sa plus fine forme. Ceci rend plus difficile de dissoudre la phase $CuAl_2$ pendant le traitement thermique de mise en solution. L'addition du magnésium aux alliages de type 319, indépendamment de la source d'alliage, modifie la morphologie de particules de silicium. On observe cet effet très clair à 0.6 % en poids de magnésium, avec une diminution correspondante de la température eutectique Al-Si comparée à l'alliage de base. Comme prévu, l'effet de modification du magnésium n'est pas très évident à la faible addition de magnésium.

L'addition du magnésium mène également à la précipitation de la phase $Al_5Mg_8Cu_2Si_6$. Cette phase précipite normalement après la phase $CuAl_2$. Néanmoins, quand l'addition du magnésium excède 0.4 % en poids, la précipitation de la phase $Al_5Mg_8Cu_2Si_6$ a eu lieu également dans une autre réaction, avant la précipitation de la phase $CuAl_2$. La morphologie des particules de la phase $Al_5Mg_8Cu_2Si_6$ est dans ce cas-ci de forme manuscrite plutôt que les particules de forme irrégulière normalement observées. Les propriétés mécaniques sont également commandées par le niveau de magnésium et la température de traitement de mise en solution. En plus de la fonte naissante, une température élevée de mise en solution produit également des microcraques et des boucles (déformation de forme) dans les barreaux d'essai de traction. En ce qui concerne le traitement de mise en solution à deux étages, la température de mise en solution de la deuxième étape ne devrait pas excéder 520°C même si une température plus élevée homogénéise l'alliage.

Comparé aux alliages expérimentaux, l'alliage industriel montre une plus grande résistance à la fonte naissante, ceci peut être expliqué en termes de la réaction entre le Cu et les éléments de trace actuels dans l'alliage tels que le Fe et le Ni, menant à une augmentation de la température de la fonte naissante.

D'après l'analyse des essais de traction, les données microstructurales et de porosité obtenues, les températures de traitement de mise en solution suivantes sont suggérées pour les divers alliages expérimentaux de type 319 et les alliages industriels, pour éviter ou réduire au minimum l'occurrence de la fonte naissante. On le suggère que les températures utilisées ne devraient jamais dépasser ces valeurs.

| Alliage | E0 | E1 | E2 | E3 | E4 | E6 | I3 | I6 |
|---|---|---|---|---|---|---|---|---|
| Température suggérée (°C) | 535 | 530 | 525 | 525 | 520 | 510 | 520 | 520 |

# ABSTRACT

Aluminum-silicon (Al-Si) casting alloys are widely used in automotive applications on account of their high strength-to-weight ratio and ability to be cast into complex shapes. Among these alloys, 319 alloy, belonging to the Al-Si-Cu system is popularly employed in such applications, where magnesium is often added to the alloy for strengthening purposes. These alloys are usually heat treated in order to obtain an optimum combination of strength and ductility. The excellent castability and mechanical properties of such Al–Si–Cu–Mg alloys has made them commercially popular for industrial applications.

The mechanical properties of a casting are controlled by its microstructure which, in turn, is influenced by the alloy composition and the solidification conditions employed. In the case of 319 type Al-Si-Cu-Mg alloys, this would involve the fineness of the primary α-Al dendrites (as determined by the dendrite arm spacing (DAS) value), the Al-Si eutectic structure *(i.e.*, an acicular *vs.* a fibrous Si morphology), the $CuAl_2$ and other copper intermetallics, as well as other second phase constituents (Fe-intermetallics, $Mg_2Si$, etc.), depending upon the alloying and trace elements present in the alloy. The normally acicular form of the eutectic Si can be transformed or 'modified' to the fibrous form by the addition of certain 'modifiers' such as Na or Sr to the alloy melt, to improve the alloy ductility and strength. Magnesium is also observed to modify the Si eutectic. However, as it also causes segregation of the copper phases, this can lead to problems related to the melting of the latter (termed 'incipient melting').

The properties of alloys containing elements such as Cu and Mg can also be enhanced through heat treatment, where the formation of fine precipitates of $CuAl_2$ and $Mg_2Si$ during aging result in the precipitation hardening of the alloy. A typical heat treatment consists of solution treatment and quenching, followed by artificial aging. Solution heat treatment is carried out to achieve maximum dissolution of the Cu and Mg into the aluminum matrix. For this purpose, the solution treatment temperature must be kept as close as possible to the Al-$CuAl_2$ eutectic temperature, but, at the same time, limited to a safe level below the maximum to avoid incipient melting of the copper phases which would result in the formation of cavities after quenching and lower the alloy soundness.

The solution heat treatment process can be carried out in either a single step or in multiple steps. Unfortunately, the single step or conventional solution heat treatment used for 319 alloys (~498°C) is not capable of maximizing the dissolution of the Cu-rich phases, nor is it able to sufficiently modify the Si particle morphology, both of which are required

for enhancing the alloy properties. To overcome this, a two-step solution treatment (conventional solution treatment followed by a higher temperature solution treatment) was suggested, that significantly improves the dissolution of the Cu-rich phase, giving rise to better homogenization prior to aging, and thus improving the mechanical properties.

The present study was undertaken to investigate the effect of Mg on the occurrence of incipient melting in experimental and industrial 319 alloys, using thermal analysis, tensile testing, microstructural analysis and porosity measurements. Castings were prepared from experimental and industrial alloy melts containing Mg levels of 0 to 0.6 wt%. Tensile test bars were cast using an ASTM B-108 type permanent mold. The bars were solution heat treated in the range of 490°C to 540°C for the single step solution treatment, and at 505°C followed by 520°C or 530°C for the two-stage solution heat treatment. Tensile tests were carried out using an MTS Servohydraulic mechanical testing machine. Porosity (arising due to incipient melting) was also measured to monitor the occurrence of the incipient melting. Optical microscopy, image analysis and EPMA techniques were used for microstructural analysis, quantification, and phase identification purposes.

The results showed that both Mg concentration and solution temperature play an important role in the occurrence of incipient melting. The porosity measurements were found to be in accordance with the tensile properties and confirmed the results obtained in terms of the incipient melting observed for each alloy/solution treatment condition.

The addition of Mg leads to the segregation of the copper phase, resulting in the formation of the block-like form of the $CuAl_2$ phase rather than its finer eutectic-like form. This makes it more difficult to dissolve the $CuAl_2$ phase during solution heat treatment. Addition of Mg to 319 alloy, irrespective of the alloy source, modifies the Si particle morphology. This effect is observed very clearly at 0.6 wt% Mg, with a corresponding decrease in the Al-Si eutectic temperature compared to the base alloy. As expected, the modification effect of Mg is not very obvious at low Mg addition.

Addition of Mg also leads to the precipitation of the $Al_5Mg_8Cu_2Si_6$ phase. This phase normally precipitates after the $CuAl_2$ phase. Nevertheless, when addition of Mg exceeds 0.4 wt%, the precipitation of the $Al_5Mg_8Cu_2Si_6$ phase also takes place in another reaction, *before* the precipitation of the $CuAl_2$ phase. The morphology of the $Al_5Mg_8Cu_2Si_6$ phase particles in this case is script-like rather than the irregular-shaped particles normally observed.

The mechanical properties are also controlled by the Mg level and the solution treatment temperature. In addition to the incipient melting, a high solution temperature also produces macrocracking and buckling (shape deformation) in the test bars. With respect to the two-stage solution treatment, the second stage solution temperature should not exceed 520°C even if a higher temperature homogenizes the alloy.

Compared to the experimental alloys, the industrial alloy shows a greater resistance to incipient melting, which may be accounted for in terms of the reaction between Cu and trace elements such as Fe and Ni present in the alloy, leading to an increase in the incipient melting temperature.

From an analysis of the tensile test, microstructural and porosity data obtained, the following solution treatment temperatures are suggested for the various 319 experimental and industrial alloys, to avoid or minimize the occurrence of incipient melting. It is suggested that the temperatures used should never exceed these values.

| Alloy | E0 | E1 | E2 | E3 | E4 | E6 | I3 | I6 |
|---|---|---|---|---|---|---|---|---|
| Suggested temperature (°C) | 535 | 530 | 525 | 525 | 520 | 510 | 520 | 520 |

# ACKNOWLEDGMENTS

It is a great pleasure to finally have the chance to convey my thanks to all those who were involved, directly or indirectly, in making this work a success. I would like to express my sincere thanks to my supervisors, Professors F. H. Samuel and A.M. Samuel, for their invaluable guidance and help during the different stages of my work.

Financial assistance (in the form of scholarships) and in-kind support received from the Natural Sciences and Engineering Research Council of Canada (NSERC), General Motors Powertrain Group (U.S.A.), Corporativo Nemak (Mexico), and the Fondation de l'Université du Québec à Chicoutimi (FUQAC) is gratefully acknowledged.

I would like to express my appreciation to several colleagues, particularly Mr. Alain Bérubé and Mr. Mathieu Paradis, for their help and for creating an enjoyable working atmosphere. Many thanks go to Dr. Zheyuan Ma who recommended me to join UQAC and who has been a constant source of encouragement.

Finally, I would like to record my deep gratitude to the members of my family, especially my parents. Without their encouragement and support, I would not have been able to fulfill my goal of completing my Master's degree successfully.

# TABLE OF CONTENTS

# LIST OF FIGURES

## CHAPTER 2

**CHAPTER 3**



**CHAPTER 4**

**CHAPTER 5**

# LIST OF TABLES

## CHAPTER 2



## CHAPTER 3



## CHAPTER 4

# CHAPTER 1

# DEFINITION OF THE PROBLEM

# CHAPTER 1

# DEFINITION OF THE PROBLEM

## 1.1 INTRODUCTION

Aluminum-silicon (Al-Si) alloys are popularly used in many applications. They are characterized by their low specific gravity, low melting point, negligible gas solubility (with the exception of hydrogen), excellent castability and good corrosion resistance. These characteristics make them excellent candidates for such applications.

Copper (Cu) and magnesium (Mg) are often added as alloying elements to increase the strength and hardenability, while iron (Fe), manganese (Mn), nickel (Ni) and chromium (Cr) are usually present as impurity elements.

The excellent castability and mechanical properties of Al–Si–Cu–Mg cast alloys make them popular foundry alloys for industrial applications. These alloys are usually heat treated in order to obtain an optimum combination of strength and ductility. The heat treatment consists of solution treatment and quenching, followed by artificial aging. Solution heat treatment is carried out to achieve maximum dissolution of the magnesium and copper into the aluminum matrix. The dissolution rate of intermetallic compounds is temperature sensitive and even a 10°C increase in temperature can have an appreciable effect on the optimum solution time and mechanical properties.

The mechanical properties, in particular the ductility, can also be enhanced by changing the morphology of the eutectic silicon particles from their normally acicular brittle form to a more fibrous and rounded form. The 'modification' is achieved by the addition of a chemical modifier such as Na or Sr to the alloy, or also through solution heat treatment during which the Si particles are fragmented and become spheroidized. Long solution treatment times can lead to particle coarsening.

In the case of Al-Si-Cu alloys such as 319 alloys, the presence of copper leads to the formation of the copper intermetallic, $CuAl_2$. Three different copper-rich phases can be present in Al-Si-Cu alloys: block-like $CuAl_2$, eutectic Al-$CuAl_2$, and $Al_5Mg_8Cu_2Si_6$. If the solution heat treatment temperature is not properly controlled, it can induce melting of the copper phases ("incipient melting"), resulting in the formation of cavities and lowering the alloy soundness.

The solution heat treatment can be carried out in either a single step or in multiple steps. Single-step solution treatment is normally limited to about 495°C, because higher temperatures lead to the incipient melting of the copper phase. This tends to lower the mechanical properties of the casting. However, solution treatment at temperatures of 495°C or less is not capable of maximizing the dissolution of the copper-rich phases, nor is it able to sufficiently modify the silicon particle morphology.

A two-step solution treatment (conventional solution treatment followed by a high-temperature solution treatment) suggested by Sokolowski *et al.*[1] is reported to significantly reduce the amount of the copper-rich phase in 319 alloys, giving rise to better homogenization prior to aging and thus improving the mechanical properties. The holding

time of the first stage and the solution temperature of the second stage are very important parameters.

Iron is normally present in the form of iron intermetallics, in particular, the $\beta$-$Al_5FeSi$ platelet phase. The platelet-like $\beta$-$Al_5FeSi$ iron intermetallic is quite deleterious to the alloy properties due to its brittle nature. At the same time, the platelet-like $\beta$-$Al_5FeSi$ iron intermetallic also acts as a nucleant for the $CuAl_2$ phase, which helps to reduce $CuAl_2$ segregation.[2]

The addition of Mg can cause the segregation of the copper phase which aggravates the problem in that it becomes more difficult to dissolve the $CuAl_2$ phase. The addition of Mg in quantities up to 0.5 wt% leads to a significant increase in the volume fraction of the Cu-containing phase with a clear tendency to segregation in localized areas, leading to the formation of the block-like rather than the fine eutectic-like $CuAl_2$ phase.[3] "Burn spots" that rise from the burning of the molten copper phase in alloy test bars containing a high Mg level can occur when the test bars are solution heat treated at a temperature higher than 520°C.[4] One must be careful to avoid segregation of the copper phases in order to prevent the occurrence of incipient melting, so that the alloy properties and castings remain sound.

In view of the importance of 319 alloys in automotive applications, the present work was undertaken to investigate the occurrence of incipient melting in these alloys in terms of the solution heat treatment conditions and the Mg content of the alloy, and also to study the porosity arising as a result, and the effect on the alloy tensile properties.

## 1.2 OBJECTIVES

The aim of the present work was to study the metallurgical parameters controlling the occurrence of the incipient melting of the copper phases in Al-Si-Cu-Mg alloys, and their effect on the tensile properties. This was undertaken through an investigation of the following:

i) The solidification behavior of various Mg-containing 319 experimental alloys using thermal analysis, to determine the reaction temperatures of the copper-rich eutectic phases.

ii) The dissolution behavior of the copper-rich phases in these alloys.

iii) Optimization of the solution treatment parameters in the different heat treatment processes applied.

iv) Comparison of the effect of different solution heat treatments on the mechanical properties of these alloys.

v) Effect of magnesium on the tensile properties in relation to the precipitation of copper phases.

# CHAPTER 2

# LITERATURE REVIEW

# CHAPTER 2

# LITERATURE REVIEW

## 2.1 ALUMINUM-SILICON ALLOYS

Worldwide, aluminum-silicon (Al-Si) base casting alloys are widely used in automotive applications on account of their low density and ability to be cast in complex shapes. Today, Al-Si alloys are used extensively in the automobile industry for engine components including blocks, cylinder heads, pistons, intake manifolds and brackets, and have replaced cast iron components in many cases.[5]

Compared with aluminum, silicon has a lower density, and is one of the few elements that may be added to aluminum without the loss of a weight advantage.[6] Only a few elements with sufficient solubilities such as silicon, zinc, magnesium, and copper can be used as major alloying additions. Alloys with silicon as a major alloying element are important alloys, widely employed because of their superior casting characteristics. These Al-Si base alloys constitute 85% to 90% of all aluminum castings. Their other outstanding features include their high corrosion resistance, low thermal expansion coefficient, weldability, and elevated mechanical properties.

With the increasing demands of the automotive industry for smaller, lighter-weight high-performance components, Al-Si alloys have today replaced iron and steel in many

components such as transmission cases, intake manifolds, and even in more critical components such as engine blocks, cylinder-heads and wheels. Such applications require that the casting parts exhibit consistent strength-ductility properties throughout the casting.

Depending on the amount of silicon, Al-Si alloys are divided into three groups: hypoeutectic alloys with a Si content between 5 and 10%, eutectic alloys with 11-13% Si, and hypereutectic alloys, commonly with a Si content between 14 and 20%, as shown in Figure 2.1.[7]

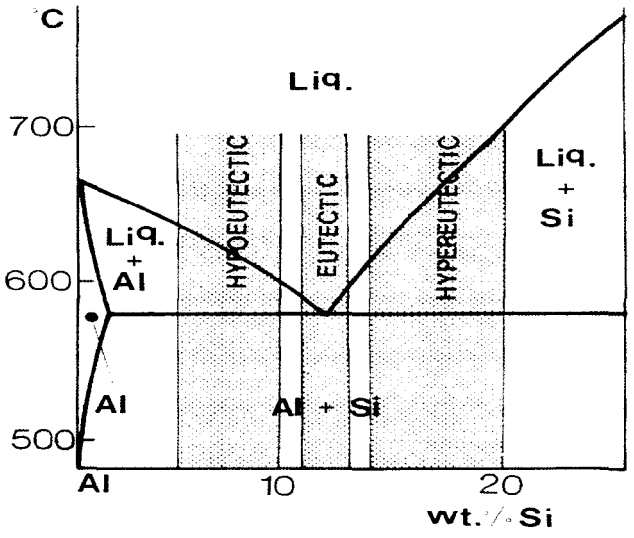


**Figure 2.1** Part of the Al-Si phase diagram showing composition ranges of various alloy types.[7]

The solidification process of Al-Si alloys involves the following main reactions:

1) Formation of a dendritic network of the $\alpha$-aluminum phase.

2) The aluminum-silicon eutectic reaction when the Al-Si eutectic is precipitated.

3) Precipitation of a secondary eutectic phase such as $Mg_2Si$ and $CuAl_2$.

In addition to the main reactions, due to the presence of some impurity elements such as Fe and Mn, some intermetallic phases can also precipitate during solidification. The iron intermetallics $Al_5FeSi$ and $Al_{15}(Mn,Fe)_3Si_2$ are two phases often seen in Al-Si alloys.

Casting alloys are defined by their chemical compositions. Each country has developed its own aluminum casting alloy nomenclature and designation. In the United States, the three-digit registration system of the Aluminum Association is used widely.

In the Aluminum Association (AA) system, casting alloys are divided into nine series, according to the major alloying elements present in the alloy. These are shown in Table 2.1.[8]

**Table 2.1** Classification of aluminum casting alloys[8]

| Series | Alloy family |
|---|---|
| 1XX | 99.0% min Al |
| 2XX | Al-Cu |
| 3XX | Al-Si-Mg, Al-Si-Cu, Al-Si-Cu-Mg |
| 4XX | Al-Si |
| 5XX | Al-Mg |
| 6XX | Unused |
| 7XX | Al-Zn |
| 8XX | Al-Sn |
| 9XX | Unused |

No commercial alloys are established currently in the 6XX and 9XX series. XXX.0 represents the chemical composition limit for castings, and XXX.1 and XXX.2 represent those for ingots. Al-Si base alloys belong to the 3XX and 4XX series of aluminium casting

alloys. Al-Si-Mg, Al-Si-Cu, and Al-Si-Cu-Mg are the three major alloy systems in the 3XX series, where Mg and Cu are two important alloying additions which act as effective strengtheners. Some alloys include a prefix letter in their denomination. Different letters used with the same alloy number distinguish alloys of a general composition that differ in their percentage of impurities of minor alloying elements, for example 356 and A356, or 380, A380 and B380.

### 2.1.1 Al-Si-Cu Alloy System

Al-Si-Cu alloys are employed extensively in a wide variety of applications on account of their excellent castability, high thermal conductivity and low thermal expansion coefficient.[9] In addition, they can be heat treated to obtain an optimum combination of strength and ductility. With heat treatment, Al-Si-Cu alloys can provide a wide range of physical and mechanical properties. The heat treatment includes the processes of solution heat treatment, quenching, and natural or artificial aging. In these alloys, silicon provides good casting characteristics and copper gives high strength and machinability. One of the well-known alloys belonging to the Al-Si-Cu alloy system is 319 alloy. The chemical compositions of various 319 type alloys are given in Table 2.2.

The 319 alloys contain both copper and magnesium as the hardening element, together with various impurities such as Fe, Mn or Zn. During solution heat treatment, copper forms an intermetallic phase with aluminum that precipitates during solidification in the form of block-like $CuAl_2$ or in the form of eutectic (Al-$CuAl_2$) phase. The Si particle

**Table 2.2** Chemical compositions of 319 alloys (wt %)[10]

| AA | Si % | Fe % | Cu% | Mg % | Mn% | Zn% | Ti% | Ni% |
|---|---|---|---|---|---|---|---|---|
| 319.0 | 5.5-6.5 | 1.0 | 3.0-4.0 | 0.10 | 0.5 | 1.0 | 0.25 | 0.35 |
| 319.1 | 5.5-6.5 | 0.8 | 3.0-4.0 | 0.10 | 0.5 | 1.0 | 0.25 | 0.35 |
| 319.2 | 5.5-6.5 | 0.6 | 3.0-4.0 | 0.10 | 0.1 | 1.0 | 0.20 | 0.10 |
| A 319.0 | 5.5-6.5 | 1.0 | 3.0-4.0 | 0.10 | 0.5 | 3.0 | 0.25 | 0.35 |
| A 319.1 | 5.5-6.5 | 0.8 | 3.0-4.0 | 0.10 | 0.5 | 3.0 | 0.25 | 0.35 |
| B 319.0 | 5.5-6.5 | 1.2 | 3.0-4.0 | 0.10-0.5 | 0.8 | 1.0 | 0.25 | 0.5 |
| B 319.1 | 5.5-6.5 | 0.9 | 3.0-4.0 | 0.10-0.5 | 0.8 | 1.0 | 0.25 | 0.5 |

characteristics also influence the mechanical properties; with a successful strontium modification treatment, the silicon can assume a fine fibrous structure which improves the mechanical properties.

## 2.2 SOLIDIFICATION OF AL-SI-CU 319 TYPE ALLOYS

All commercial solidification processes involve some non-equilibrium effects. True stable equilibrium conditions seldom exist in a metal field. However, the study of equilibrium systems is extremely valuable, because it constitutes a limiting condition from which actual conditions can be estimated.[11] In real casting processes, the extent of deviation from equilibrium conditions has a significant effect on the actual microstructure observed.

During the solidification of unmodified 319 alloy, the following main sequence of phase precipitation will occur:

i. the formation of primary aluminum at about 608°C;

ii. the main silicon-forming eutectic reaction at about 563°C;

iii. a $CuAl_2$-forming reaction at about 550°C; and

iv. a complex eutectic reaction at about 525°C.

The solidification rate during casting is important in that it affects almost all the microstructural parameters, such as dendrite arm spacing, the degree of eutectic silicon modification, and the porosity and intermetallics that occur in the microstructure.

At the end of the solidification process, $Mg_2Si$, $CuAl_2$ and other more complex phases precipitate from the remaining liquid. Table 2.3 summarizes the sequence of phase precipitation in hypoeutectic Al-Si alloys.[12]

**Table 2.3** Sequence of phase precipitation in hypoeutectic Al-Si alloys[12]

| Temperature (°C) | Phases precipitated | Suffix |
|---|---|---|
| 650 | Primary $Al_{15}(Mn, Fe)_3Si_2$ (sludge) | Pre-dendrite |
| 600 | Aluminum dendrites<br>and ($Al_{15}(Mn, Fe)_3Si_2$)<br>and /or $Al_5FeSi$ | Dendritic<br>Post-dendritic<br>Pre-eutectic |
| 550 | Eutectic Al + Si<br>and $Al_5FeSi$<br>$Mg_2Si$ | Eutectic<br>Co-eutectic |
| 500 | $CuAl_2$ and more complex phases | Post-eutectic |

In our work, a preheated graphite mold (600°C) was used for microstructural characterization purposes, which provided close-to-equilibrium cooling conditions and enough time for the precipitating phases to grow, to facilitate their identification using electron microscopic techniques. Thermal analysis could also be carried out simultaneously with the graphite mold set-up, which assisted in determining the precipitation reactions taking place during solidification.

## 2.3 ROLE OF MODIFICATION

As mentioned previously, Al-Si alloys are widely used in applications where good strength and light weight are required, or where corrosion resistance or castability is desired. However, the commercial application of these alloys often depends on the successful modification of the eutectic silicon. Modification is one of the melt treatments carried out to alter the structure of the eutectic silicon particles, in order to improve the mechanical properties.

An unmodified alloy contains an acicular eutectic silicon structure. Such brittle, acicular Si particles act as internal stress raisers in the microstructure and provide easy paths for fracture. With modification, the eutectic structure becomes finer and the silicon becomes rounded, which contribute to higher values of ultimate tensile strength and greatly increased values of ductility. During modification, the aluminum phase is not affected structurally. For the silicon phase, modification results in a change from a faceted to a more isotropic growth morphology.

The eutectic silicon can also be 'modified' through solution heat treatment or the use of high cooling rates. Fast cooling rates are used to reduce the size and the distance between eutectic silicon particles, rather than their shape or morphology.[13] However, full modification is difficult to achieve by simply increasing the solidification rate of the casting alone, and thus Al-Si alloys are generally modified chemically, using modifying agents.[14] These are normally added to the alloy melt in the form of master alloys in desired quantities, to achieve a well-modified eutectic structure.

Apelian et *al.*[15] assessed the grain refinement and modification of Al-Si foundry alloys using thermal analysis. Figure 2.2 depicts the range of microstructures observed by the authors on the polished surfaces of a modified hypoeutectic Al-Si alloy. The structures are divided into six classes, with the unmodified structure represented by class 1, lamellar by class 2, undermodified by classes 2-4, well modified structures by class 5, and overmodified structures by class 6.

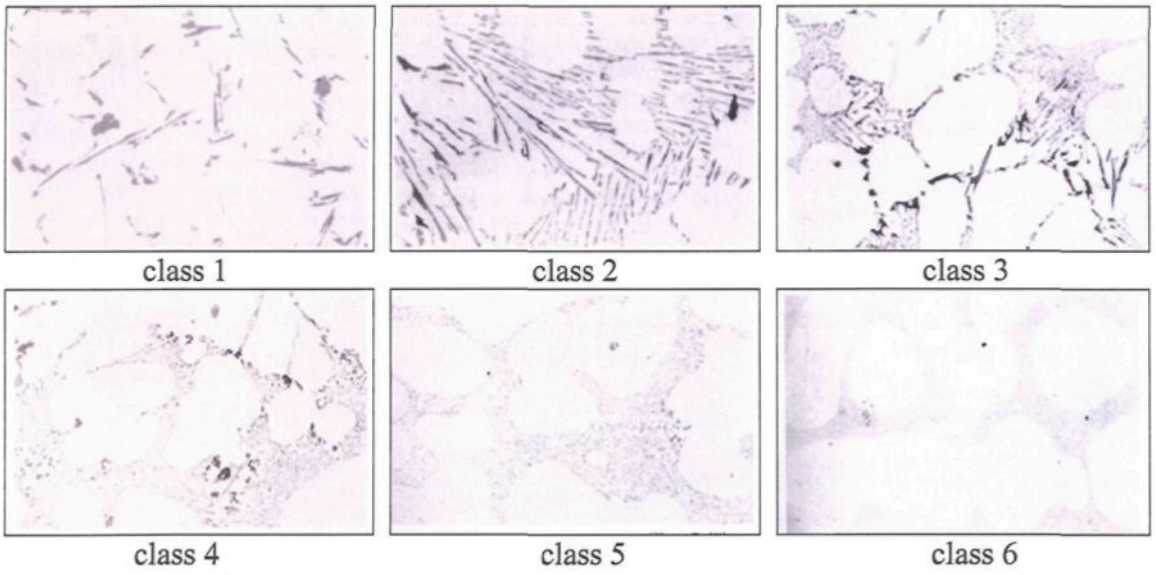


**Figure 2.2** Rating system for a modified microstructure.[15]

Five variables determine the exact microstructure which will form: i) the type of modifier used, ii) the impurities present in the melt, iii) amount of modifier used, iv) the freezing rate, and v) the silicon content of the alloy. These five variables interact in a highly complex manner, so that an exact quantitative prediction of the microstructure in terms of a modification rating is made difficult.

In 1921, Pacz[16] discovered that Al-Si alloys containing 5 to 15% Si could be treated with alkali fluoride (*viz.*, sodium fluoride) to improve their ductility and machinability. Some researchers[17, 18] found that modification by sodium addition is a combination of two effects: neutralization of AlP so that easy nucleation of silicon is prevented, and a change in the mode of solidification of the eutectic so that the modified eutectic crystallizes with aluminum crystals in the lead instead of silicon crystals, as in the case of non-modified alloys. In the 1970s, Hess and Blackmun[19] reported that strontium is an effective modifying agent for hypoeutectic Al-Si alloys.

Several elements are known to cause silicon modification. Group IA and Group IIA elements of the Periodic Table, rare earths, (*e.g.*, La and Ce), As, Sb, Se and Cd have all been reported to exert a modification effect.[20, 21, 22] However, only Na, Sr and Sb are currently the most effective within economic constraints.[23] Among them, Sb is not used in North American foundries due to its toxic effects. The amount of each modifier element required depends on the alloy composition, in that a higher silicon content requires a larger amount of the modifier.

It is well known that sodium can modify the eutectic structure greatly. Due to its low melting point, sodium is easily incorporated into Al-Si melts, but its high vapor pressure makes it boil off almost immediately (called "fading"). As sodium is also sensitive to porosity and has adverse effects in terms of oxidation and aggressiveness against mold coatings, *etc.*,[24] it is difficult to control the Na-modification process, and its use is therefore limited.

Compared with Na, Sr as a modifier has been widely used because of its greater stability in the melt. The addition of Sr neutralizes the effect of phosphorus and promotes the formation of a fibrous silicon structure by retarding the growth rate of silicon.[25, 26] The eutectic structure becomes finer and the silicon particles become rounded, which contribute to higher values of ultimate tensile strength and greatly increased values of ductility. Also, because of its low vapor pressure and tendency for oxidation, the loss rate of strontium is distinctly less than that of sodium.

It has also been reported that an initial incubation period is required for maximum modification. Strontium retains its modifying action longer than Na in spite of a continual loss of Sr during holding, provided a sufficient amount of Sr remains in the alloy. The modifying effect of Sr actually appears to improve with holding time, again provided a sufficient amount remains in the melt.[19]

Although the presence of strontium can change the morphology of the silicon particles, when the Al-Si alloy contains more than 0.05 wt% Sr, the formation of undesirable Sr-compounds such as $Al_2SrSi_2$ contribute to a decrease in mechanical properties.[27]

Modification with Sr considerably lowers the actual eutectic temperature.[28, 29] The depression in the eutectic temperature can be used as an indicator of the extent of the Si structure modification expected in the casting: the lower the eutectic temperature, the greater the modification effect. Sokolowski *et al.*[30] have reported that additional strontium raises the eutectic temperature of the copper-rich phases. It is likely that high strontium melts need to be subjected to higher temperature solution treatment. An additional benefit

of Sr modification is that it considerably lowers solution treatment time necessary to attain the desired property level.[31] On the other hand, Sr modification also results in the segregation of the interdendritic blocky $CuAl_2$ structure in 319 alloys,[32] in addition to increasing porosity in the modified alloy.[33]

## 2.4 ROLE OF MAGNESIUM

Magnesium is used extensively in Al-Si alloys to improve the mechanical properties. The addition of Mg increases the strength during ageing due to the precipitation of submicroscopic and metastable phases containing Mg and Si which provide excellent obstacles for dislocation movement.

In their studies of the influence of alloying elements on the thermal analysis results of Al-Si cast alloys, Heusler and Schneider[29] observed that the Sr-modified microstructure is clearly affected when magnesium is present. Microstructural parameters obtained from image analysis, such as the silicon particle size and aspect ratio, were found to increase with an increasing Mg content and became more inhomogeneous. The reason for the degradation in modification was believed to be due to the formation of intermetallic phases of the type $Mg_2SrAl_4Si_3$. The addition of Mg also lowers the eutectic temperature. As Figure 2.3 shows, the eutectic temperature decreases with increasing Mg content. It has also been reported, however, that a magnesium content of ~1 wt% itself acts as a refiner for the eutectic silicon in unmodified Al–Si alloys.[34]

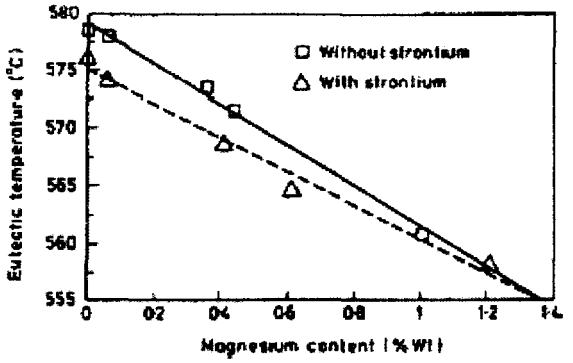


**Figure 2.3** Depression of the eutectic temperature as a function of magnesium level for the unmodified and strontium modified Al-Si alloy.[29]

De la Sablonnière and Samuel[3] studied the solution heat treatment of 319 aluminium alloy containing ~0.5 wt% Mg. Their results showed that increasing the Mg content to ~0.5 wt% led to a significant decrease in the eutectic silicon temperature (about 1.5°C per 0.1 wt% Mg). Addition of Mg also led to the precipitation of the $Al_5Mg_8Cu_2Si_6$ phase, and to the splitting of the copper phase formation temperature range into two explicit peaks representing the precipitation of $CuAl_2$ and $Al_5Mg_8Cu_2Si_6$ phases.

Thus, addition of Mg is seen to result in an increase in the volume fraction of Cu-containing phases, with a clear tendency for segregation in localized areas, leading to the formation of the block-like rather than the fine eutectic-like $CuAl_2$ phase.[3] This makes it more difficult to dissolve the $CuAl_2$ phase during solution heat treatment. It is also important to avoid such segregation to prevent the occurrence of incipient melting, and ensure that the alloy properties and castings remain sound.

In another study, Samuel *et al.*[34] showed that the addition of Mg to molten 319 type alloys, in amounts up to 0.5 wt pct, leads to the precipitation of $Mg_2Si$ (or a Mg-rich) phase

that appears in the form of rounded black particles dotted along the sides of the eutectic Si particles. Noticeable fragmentation of the eutectic Si (*i.e.* its modification), and transformation of a large proportion of the β-$Al_5FeSi$ iron intermetallic phase into a Chinese script-like phase with a composition close to $Al_8Mg_3FeSi_6$ is also observed.

In the context of alloy properties, de la Sablonnière and Samuel[3] obtained some interesting results from the tensile testing carried out for solution heat treated 319 alloys containing 0.5 wt% Mg. They found that two types of defects can occur during solution heat treatment: "dark spots" with no distinct boundaries with the surrounding matrix when the alloy test bars are heat treated at a temperature close to 520°C (irrespective of the Mg level), and "burn spots" that result from the burning (or fusion) of the molten phases in alloy test bars containing a high Mg level (0.5 wt%) subjected to solution treatment at a higher temperature (i.e. greater than 520°C).

The darks spots were always observed near the periphery of the test bars, indicating that they acted as a source for crack initiation. Also, the size of these dark spots was found to increase with increase in solution temperature. The occurrence of the 'burn spots', however, was not restricted to the fracture surface. Nonetheless, the incipient melting related to these burn spots resulted in a degradation in the tensile properties. Figure 2.4 shows examples of such dark spots observed on the fractured surface of 319+0.5 wt% Mg alloy test bars that were solution heat treated for (a) 12 h/510°C and (b) 12 h/520°C.

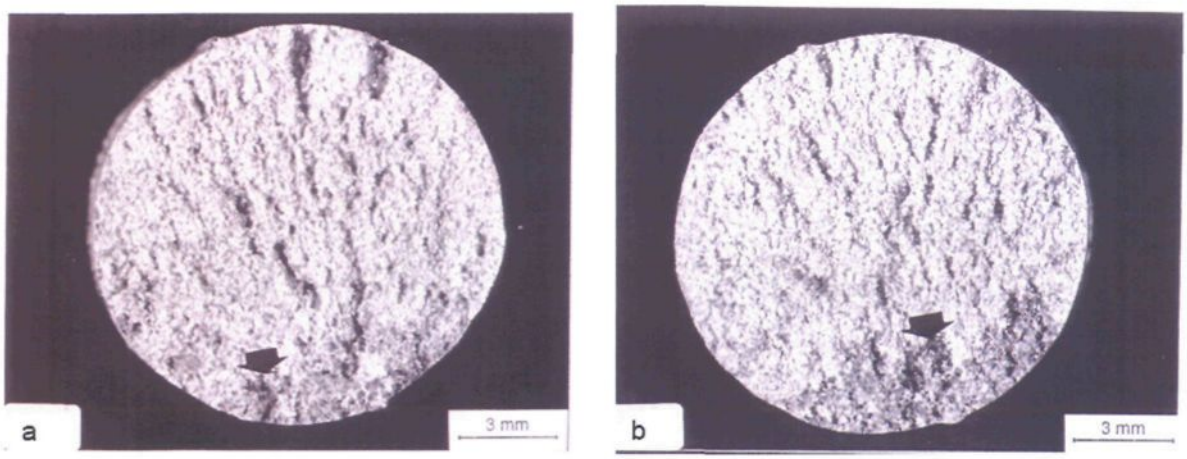


**Figure 2.4** Dark spots observed on the fracture surfaces of test bars of 319+0.5 wt% Mg alloy, solutionized for (a) 12h/510°C and (b) 12h/520°C. Arrows show the progress in the size of the dark spot.[4]

## 2.5 INTERMETALLIC PHASES IN AL-SI-CU ALLOYS

In the case of Al-Si-Cu alloys, the presence of copper leads to the formation of the copper intermetallic, $CuAl_2$. If iron is also present in the alloy, then, during solidification, together with other alloying elements, the iron partly goes into solid solution in the matrix and partly forms intermetallic compounds, among them the plate-like β-$Al_5FeSi$ and the script–like α-$Al_{15}(Mn,Fe)_3Si_2$ phases. In the solidification process, $\beta$-$Al_5FeSi$ platelets are very active sites for the nucleation of the $CuAl_2$ phase. These copper and iron intermetallics are discussed below in further detail.

### 2.5.1 Copper Intermetallic Phases

Three different copper-rich phases can be present in the Al-Si-Cu alloys: block-like $CuAl_2$, eutectic Al-$CuAl_2$, and $Al_5Mg_8Cu_2Si_6$ phase, as shown in Figure 2.5.[35] If the

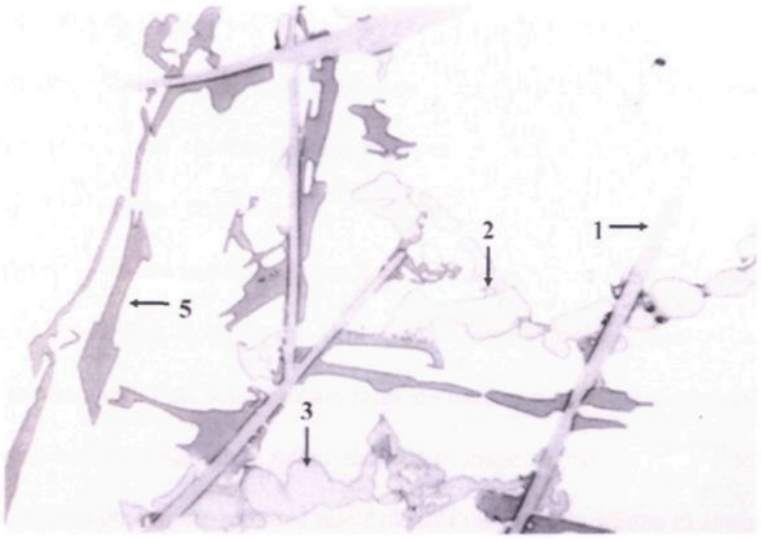


(a)

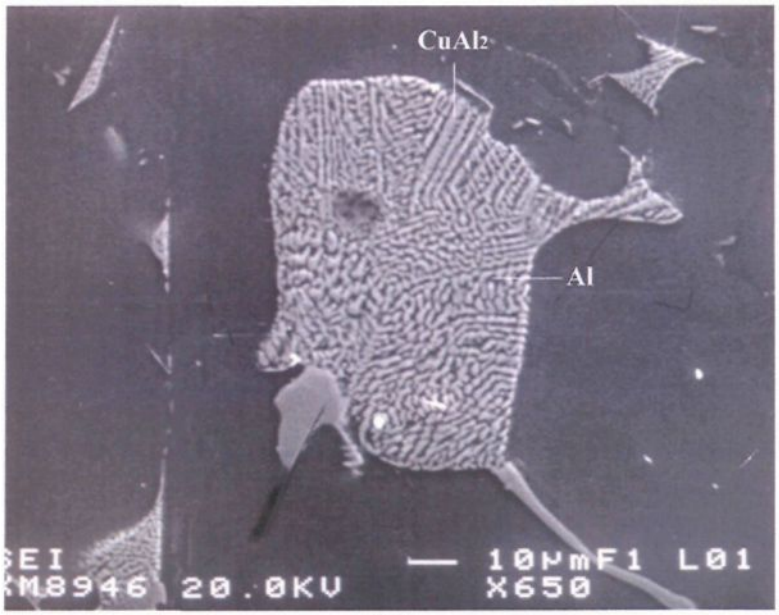


(b)

**Figure 2.5** (a) Microstructure of a sample from 319.1 alloy, X560: 1) $\beta$-$Al_5FeSi$, 2) blocky $CuAl_2$ phase, 3) $Al_5Mg_8Cu_2Si_6$ phase, 5) acicular Si phase.[35] (b) Secondary electron image of 319 alloy showing the eutectic Al-$CuAl_2$ phase (round).[37]

solution heat treatment temperature is not properly controlled, it can induce melting of the copper phases, resulting in the formation of cavities and lowering the alloy soundness.

The mechanism of $CuAl_2$ precipitation has been proposed by Samuel *et al.*[36] as follows. During the first stages of solidification, the formation of the $\alpha$-Al dendritic network is associated with the segregation of the Si and Cu in the melt, ahead of the progressing dendrite interfaces. When the solidification temperature approaches the eutectic temperature, the Si particles precipitate, leading to a local concentration of Cu in the remaining area.

The presence of both strontium and magnesium can lead to the segregation of the copper phase to areas free of eutectic silicon particles. Due to the segregation, the $CuAl_2$ phase precipitates more often in the block-like form rather than in the fine eutectic form. Compared with the eutectic (Al-$CuAl_2$) phase, the coarser block-like form of the phase is much harder to dissolve in the aluminum matrix. Segregation is also affected by the cooling rate. A high cooling rate is beneficial for reducing the amount of eutectic phase precipitation in the grain boundaries.

From the study of Li,[2,37] the mechanism for the dissolution of the $CuAl_2$ phase during solution heat treatment can be proposed as follows (Figure 2.6):

i. separation of the $CuAl_2$ particles from the $\beta$-$Al_5FeSi$ platelets;
ii. necking of the $CuAl_2$ particles followed by spheroidization;
iii. dissolution of the spheroidized particles by radial diffusion of Cu atoms into the surrounding aluminum matrix.

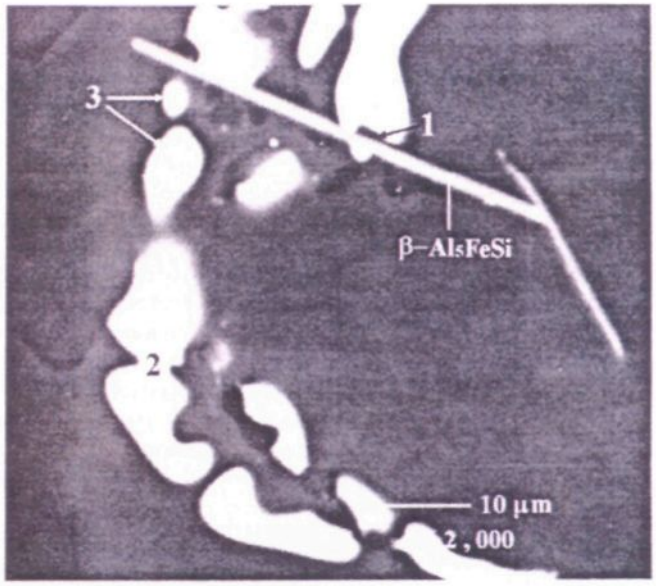


**Figure 2.6** Backscattered image showing the dissolution process of $CuAl_2$ particles in 319 alloy after 8h solution heat treatment at 505°C: (i) separation of the $CuAl_2$ particles from the $\beta$-$Al_5FeSi$ platelets, (ii) necking of the $CuAl_2$ particles, (iii) spheroidization of $CuAl_2$ and reduction in the size of $CuAl_2$ fragments.[2]

During solution heat treatment, melting of the $CuAl_2$ phase may occur if the alloys are subjected to a rather high solution temperature, resulting in a structureless form of the phase upon cooling and porosity formation, which can deteriorate the mechanical properties.

### 2.5.2 Iron Intermetallic Phases

As mentioned previously, during the solidification of Al-Si base alloys, iron, together with other alloying elements such as Cu, Mg, Zn, Mn, Ti, *etc.* partly goes into solid solution in the matrix and partly forms intermetallic compounds, including the plate-like $\beta$-$Al_5FeSi$ phase and the Chinese script–like $\alpha$-$Al_{15}(Mn,Fe)_3Si_2$ phase.[12] Among them,

the β-$Al_5FeSi$ phase platelets, which act as stress raisers, make iron the most deleterious impurity element in cast aluminum alloys. These platelets (which appear as needles in the microstructure) also prevent the flow of liquid metal during the solidification process, restricting the feedability and causing porosity formation and unsoundness in the casting. On the other hand, the *β*-$Al_5FeSi$ plate-like phase also acts as a nucleant for the $CuAl_2$ phase, which helps to reduce the $CuAl_2$ segregation.

The β-$Al_5FeSi$ platelets are light grey in color when observed under the optical microscope. They grow in a lateral or faceted growth mode, and are bounded by slowly growing planes of low indices. Their surfaces are relatively smooth on the atomic scale, so atoms from the liquid can find few possibilities to attach themselves at the interface. Thus, their growth is restricted and slow. This type of growth occurs at low driving forces or slow cooling rates, *i.e.*, at low degrees of undercooling, ΔT.

Mondolfo[38] has summarized the main factors that contribute to the formation of the β-iron $Al_5FeSi$ phase: a) an Fe/Si ratio close to unity, b) a low cooling rate ~ 0.8°C/s, and c) a low Mn and Cr concentration. The cooling rate has a direct impact on the equilibrium kinetics and quantities of iron present in the microstructure. A low cooling rate favors the precipitation of the β-iron $Al_5FeSi$ phase, while rapid solidification favors the crystallization of the iron compound as the α-iron phase.

This other iron intermetallic phase is the Chinese script–like α-$Al_{15}(Mn,Fe)_3Si_2$ phase, also light grey in color, and appearing in script form when observed in the optical microscope. It grows in an irregular, curved mode. Its form is controlled by the temperature gradient and by the diffusion of atoms in the liquid melt. During crystallization, atoms can

attach themselves to the solidified part of the α-iron phase particles when they arrive at the solid/liquid interface. This type of growth occurs at high driving forces of solidification or rapid cooling rates, *i.e.*, at high undercooling, ΔT. The α-iron phase, due to its compact morphology, is less detrimental to mechanical properties compared to the β-iron phase.

## 2.6 HEAT TREATMENT OF AL-SI-CU ALLOYS

Al-Si-Cu alloys are heat-treatable alloys, which means that their mechanical properties can be enhanced though heat treatment. The heat treatment consists of solution heat treatment, quenching, and a combination of natural and artificial aging processes. The improvement in properties is mainly due to the precipitation of $CuAl_2$ within the alloy matrix during the aging process. The morphology changes of silicon during the solution treatment also contribute to the improvement in the properties. Solution heat treatment can also minimize the harmful effect of the β-iron phase. Upon solution heat treatment, the β-iron intermetallics undergo dissolution and fragmentation, which leads to an improvement in the mechanical properties.

### 2.6.1 Solution Heat Treatment

Solution heat treatment is achieved by heating the alloy to a suitable temperature, holding at this temperature long enough to allow the constituents to become supersaturated in solid solution, and cooling rapidly enough not to make the excess solute precipitate. The purpose of solution heat treatment is to put the maximum amount of hardening solutes such as Cu and Mg into solid solution in the aluminum matrix. Solution heat treatment in Al-Si-Cu-Mg alloys is used to homogenize the alloy, change the morphology of the interdendritic

phases and dissolve precipitation-hardening constituents, such as $CuAl_2$, AlMgCu, and $Mg_2Si$.[39] During the solution heat treatment, the morphology of the eutectic Si particles changes with time, though fragmentation, spheroidization, and coarsening of the particles. The spheroidization rate increases with the Sr concentration of the alloy.

In order to dissolve the maximum amount of hardening solutes into solid solution, the temperature of solution heat treatment must be as close as possible to the eutectic temperature, but, at the same time, this temperature should be limited to a safe level below the maximum to avoid overheating and partial melting. Solution temperature and solution time are the two important factors in solution heat treatment. The dissolution rate of intermetallic compounds is temperature sensitive and even a 10°C increase in temperature can have an appreciable effect on the optimum solution time and mechanical properties.

During solution heat treatment, incipient melting of the $CuAl_2$ phase can occur when the composition exceeds the critical composition and the 319 alloy is annealed at a temperature higher than the melting point of eutectic (Al-$CuAl_2$). This results in the formation of a structureless form of the $CuAl_2$ phase and related porosity on quenching, and a consequent deterioration of the tensile properties.

The results of Gauthier *et al.*[40, 41] show that the best combination of tensile strength and ductility is obtained when the as-cast material is solution-heat-treated at 515°C for 8 to 16 h, followed by quenching in warm water at 60°C. A higher solution temperature results in the partial melting of the copper phase at the grain boundaries.

Crowell and Shivkumar[31] stated that the blocky Cu phase in Al-Si-Cu alloys dissolves with increasing solution time at the recommended solution temperature of 495°C.

The rate of dissolution increases with Sr concentration. In their studies on the solution heat treatment of 319 alloy containing ~0.5wt% Mg, de la Sablonnière and Samuel [3] reported the appearance of dark spots on the fracture surface of solution heat treated bars. The size and percentage of the defective test bars obtained increased with increase in solution temperature.

The solution heat treatment process can be carried out in either a single step or in multiple steps. Single-step treatment is normally limited to about 495°C, because higher temperatures lead to the incipient melting of the copper phase. Unfortunately, heat treatment at temperatures of 495°C or less is not capable of maximizing the dissolution of the copper-rich phases, nor is it able to sufficiently modify the silicon particle morphology.

A two-step solution treatment (conventional solution treatment followed by a high-temperature solution treatment) suggested by Sokolowski *et al.*[1] is reported to significantly reduce the amount of the copper-rich phase in 319 alloys, giving rise to better homogenization prior to aging, and thus improving the mechanical properties. The holding time of the first stage and the solution temperature of the second stage are very important parameters in this context. The second-stage solution temperature cannot be higher than 520°C since this may cause the incipient melting of the copper eutectic phase.

Sokolowski *et al.*[30] studied the improvement of 319 aluminium alloy casting durability by high temperature solution treatment. Their results showed that a two-step solution treatment (495°C/2h followed by 515°C/4h) produced the optimum combination of strength and ductility compared to the traditional single-step solution treatment (495°C/8h). In both cases, the solution heat treatment was followed by quenching (in hot water at 74°C) and

artificial aging (250°C/3h). This improvement in the mechanical properties was mainly due to the improvement in homogeneity, as shown in Figure 2.7. Optical micrographs taken from both eutectic Si regions and those containing the Cu-phase revealed the improvement in homogeneity on going from the as-cast to solution heat-treated conditions. As Figure 2.7(b) shows, the as-cast microstructure displayed significant copper segregation. While the single-step solution treatment (495°C/8h) improved the homogeneity to a considerable extent, Figure 2.7(d), some copper phase regions still remained in the matrix. The two-step solution treatment (second step at 515°C), however, brought about a far greater improvement in homogeneity, i.e. only a small amount of the copper-rich phase was presented, as shown in Figure 2.7(f).

The improvement in the Si particle morphology with the solution heat treatment (Figure 2.7(c, e)) is also evident, compared to the as-cast condition (Figure 2.7(a)).

### 2.6.2 Quenching

Quenching is in many ways the most critical step in the sequence of heat treatment operations. The objective of quenching is to preserve the solid solution formed at the solution heat-treating temperature, by rapidly cooling to some lower temperature, which is usually near room temperature. This operation is applied not only to retain solute atoms in solution, but also to maintain a certain minimum number of vacant lattice sites to assist in promoting the low temperature diffusion required for zone formation. The highest strengths attainable and the best combinations of strength and toughness are those associated with the most rapid quenching rates.[42]

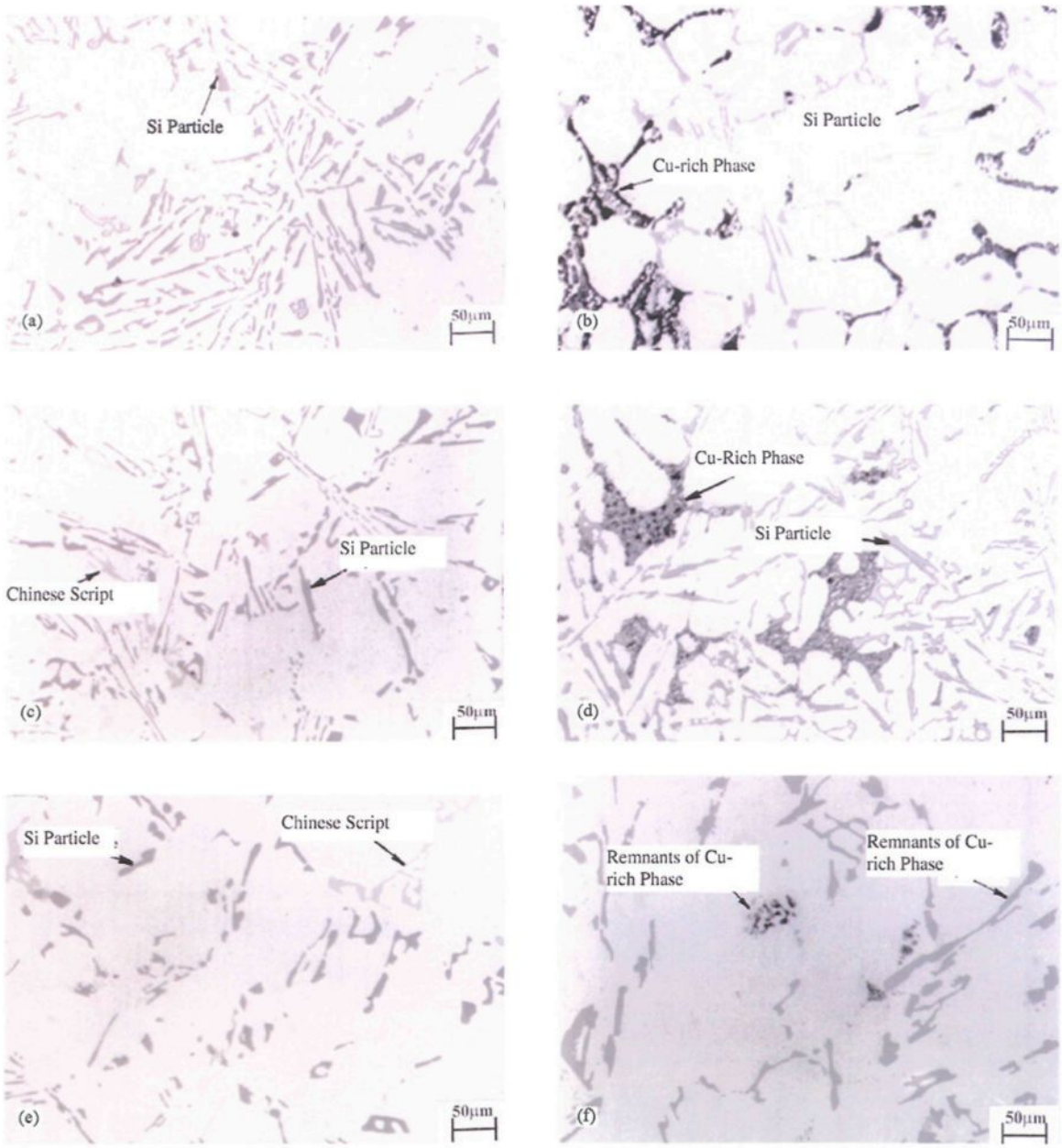


**Figure 2.7** Micrographs taken from a 319 alloy automotive component showing: (a) Si particles, and (b) Cu-rich phase segregation in the as-cast condition; (c) Si particles, and (d) Cu-rich phase segregation after single-step solution treatment; and (e) Si particles, and (f) remnants of Cu-rich phases after two-step solution treatment.[30]

### 2.6.3 Precipitation Heat Treatment (Aging)

The effect of precipitation heat treatment on mechanical properties is greatly accelerated by heating the quenched materials in the range 95°C to 205°C. A characteristic feature of elevated-temperature aging (artificial aging) effects on tensile properties is that the increase in yield strength is more pronounced than the increase in tensile strength. The precipitation heat treatment can also reduce the residual stresses developed during quenching from solution heat treatment. The depression is highly dependent on the time and temperature of the precipitation treatment and on the alloy composition.

## 2.7 POROSITY

Porosity is one of the major factors critical to the casting quality. It is detrimental not only to the surface quality after machining but also to the mechanical properties and corrosion resistance.

Porosity in castings occurs because of the rejection of gas from the liquid metal during solidification and/or the inability of the liquid metal to feed through the interdendritic regions to compensate for the volume shrinkage associated with solidification. Hydrogen is the only gas capable of dissolving to a significant extent in molten aluminum, resulting in outgassing, which leads to the formation of porosity and reduced mechanical properties and corrosion resistance.[43]

### 2.6.1. Theory of Porosity Formation

The formation of porosity in solidifying metals is the result of two mechanisms:

i) Shrinkage, resulting from the volume decrease accompanying solidification. This type of porosity can also occur as "microshrinkage" or "microporosity", dispersed in the interstices of dendritic solidification regions, typically found in alloys with a large difference between their solidus and liquidus temperatures. Limited or inadequate liquid metal feeding in the dendrite solidification area gives rise to shrinkage.

ii) Gas porosity, resulting from the decrease in the solubility of hydrogen in aluminum during solidification.

According to Campbell,[44] the growth tendency of pores is described generically by the following equation:

$$P_g + P_s > P_{atm} + P_H + P_{s\text{-}t}$$

where $P_g$ = equilibrium pressure of dissolved gases in the melt;

$P_s$ = pressure drop due to shrinkage;

$P_{atm}$ = pressure of the atmosphere over the system;

$P_H$ = pressure due to the metallostatic head;

$P_{s\text{-}t}$ = pressure due to surface tension at the pore/liquid interface.

The dissolved gas pressure $P_g$ and pressure drop due to shrinkage $P_s$ are the major driving forces in forming porosity. For a particular casting design, $P_{atm}$ and $P_H$ are constant, and a decrease in $P_{s\text{-}t}$, as observed for modifiers like sodium or strontium, can lead to an increased probability of pore formation.

The pore growth process has been depicted schematically by Kubo and Pehlke[45] as shown in Figure 2.8. In (a), the gas porosity nucleates at the base of the dendrite arms. The synergism between the shrinkage and gas porosities overcomes the large negative free energy required to form a gas-metal surface, facilitating the nucleation shown in Figure 2.8(a). As solidification proceeds, the porosity grows due to the higher potential for gas evolution. The radius of the porosity becomes large enough to decrease the contribution of interfacial energies, and the porosity detaches from the dendrites, as shown in (b). At a still further stage of solidification, neighbouring dendrites collide, making interdendritic feeding difficult. At this stage, the porosity is thought to grow to compensate for solidification shrinkage, as shown in Figure 2.8(c).

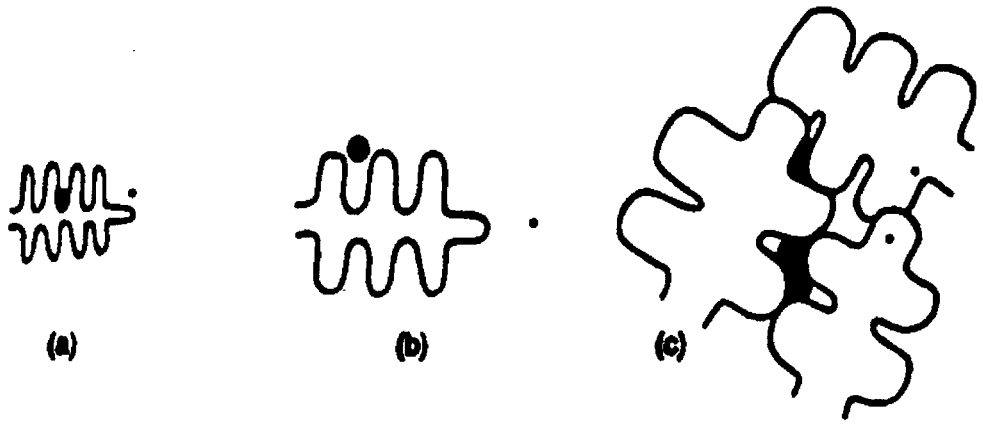


**Figure 2.8** The growth process of porosity formation.[45]

## 2.8 TENSILE PROPERTIES

The tensile properties of an alloy are evaluated in terms of the yield strength (YS), ultimate tensile strength (UTS), and percentage elongation (% El). Figure 2.9 show the

engineering stress-strain curve.[46] The stress, or the average longitudinal stress, in the tensile specimen can be obtained by dividing the load by the original area of cross section of the specimen:

$$S = P / A_0$$

where S stands for stress, P is the original load (zero stress) on the specimen of original cross-section area $A_0$.

Percentage elongation (%El) can be obtained by dividing the elongation of the gage length of the specimen by its original length.

$$\%El = \sigma / L_0 = (L-L_0)/L_0$$

where L is the specimen length at a given load and $L_0$ is the original length of the specimen.

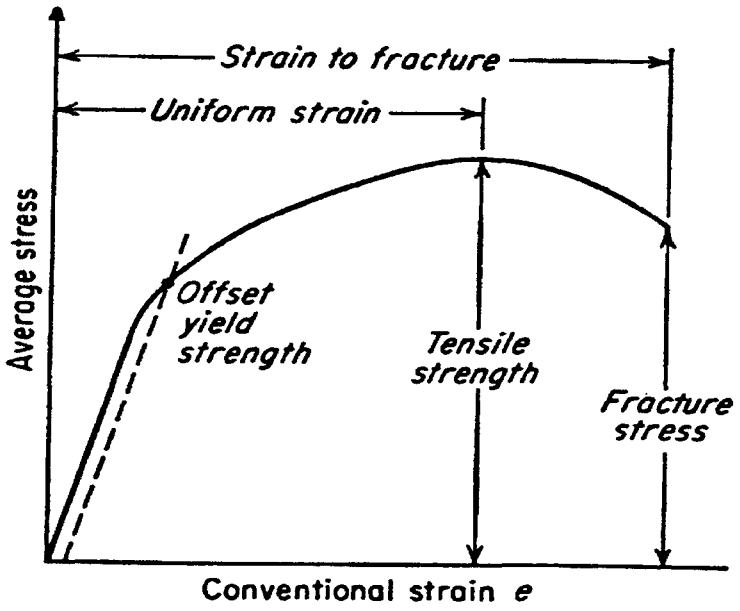


**Figure 2.9** The engineering stress-strain curve.[46]

### 2.8.1 Effect of Alloying Composition

In Al-Si-Cu-Mg alloys, both Cu and Mg act as a hardening element. The addition of Mg will increase the strength during ageing due to the precipitation of submicroscopic and metastable phases containing Mg and Si which provide excellent obstacles for dislocation movement. This phase will act together with the copper phase ($CuAl_2$) to provide precipitation hardening.

Samuel[4] studied the incipient melting of $Al_5Mg_8Si_6Cu_2$ and $Al_2Cu$ intermetallics in unmodified and Sr-modified 319 alloys during solution heat treatment, and observed that magnesium up to 0.5 wt pct contributes to both strength parameters, *i.e.* YS and UTS by about 75% and alloy ductility by about 15%.

The percentage of Si, and its shape and distribution, also play an important role in determining the mechanical properties. The higher the Si content, the harder the alloy. The Sr-modified alloys show a significant improvement in the ultimate tensile strength and a substantial increase in elongation.

### 2.8.2 Effect of Heat Treatment

Gauthier *et al.*[40] studied the effect of solution time and temperature on the room temperature tensile properties of 319.2 alloys. They found that the yield stress remained almost unchanged with solution temperature and time, while the UTS increased greatly (compared with the as-cast value), as the solution temperature increased from 490°C to 515°C, due to the progressive dissolution of copper in the aluminum matrix. The alloy obtained its maximum attainable strength after 8 hours in this temperature range, and no

improvement was observed with further increase in solution time. The use of a temperature higher than 515°C may accelerate partial melting of $Al_2Cu$ which can cause shrinkage porosity and the formation of a structureless phase upon quenching.

Gauthier *et al.*[41] also studied the aging behavior of 319.2 alloy in the temperature range 155°C-220°C. They found that peak aging was achieved after 24 h at 155°C or 5 h at 180°C. Inclusions and oxides had a marginal effect on the yield strength while they deteriorated both UTS and % elongation to levels below those obtained in the as-cast condition.

Li[2] studied the parameters controlling the precipitation and dissolution of $CuAl_2$ phase in 319 alloys and their influence on the alloy performance. The results showed that compared with the T5 condition, the UTS, YS, and %El increase significantly in the T6 condition, since the T6 heat treatment assists in homogenizing the alloys, changing the morphology of the interdendritic phases, and dissolving precipitation-hardening constituents such as $CuAl_2$.

## 2.9 INCIPIENT MELTING

In Al-Si-Cu alloys which contain major alloying elements such as Si, Cu and Mg and impurity elements such as Fe, Mn, Ni and Cr, several brittle intermetallic compounds may form in addition to the Al-Si eutectic. Among them, the Cu intermetallic phase is considered to be more detrimental to mechanical properties due to its formation along the interdendritic and grain boundaries. During solution heat treatment, incipient melting of the $CuAl_2$ phase can occur when the composition exceeds the critical composition and the 319

alloy is annealed at a temperature higher than the melting point of eutectic (Al-$CuAl_2$). This results in the formation of a structureless form of the $CuAl_2$ phase and related porosity on quenching, and a consequent deterioration of the tensile properties.

### 2.9.1 Proposed Heat Treatments for Al-Si-Cu Alloys

Al-Si-Cu alloys are heat treated to obtain an optimum combination of strength and ductility. The conventional heat treatment consists of solution heat treatment, quenching, and a combination of natural and artificial aging. In order to dissolve the maximum amount of hardening solutes into solid solution, the temperature of solution heat treatment must be as close as possible to the eutectic temperature, but, at the same time, this temperature should be limited to a safe level below the maximum to avoid the consequences of overheating and partial melting. In the case of 319 alloys, the solution temperature is often limited to 495°C which is the Cu binary eutectic reaction temperature. Otherwise, the copper phase may cause grain boundary melting and incipient melting.

It has been reported that the final solidification temperature for unmodified 319 alloy containing 0.06 wt% Mg is about 498°C. The results of Gauthier *et al.*[40] on 319.2 alloy containing 0.06 wt% Mg show, however, that the best combination of tensile strength and ductility is obtained when the as-cast material is solution-heat-treated at 515°C for 8 to 16 hours, followed by quenching in warm water at 60°C. A higher solution temperature results in the partial melting of the copper phase at the grain boundaries.

On the other hand, heat treatment at temperatures of 495°C or less is not capable of maximizing the dissolution of the copper-rich phases, nor is it able to sufficiently modify

the silicon particle morphology. To overcome this, a two-step solution treatment was developed, where the conventional solution treatment was followed by a second solution treatment at a temperature above 495°C.

The two-step solution treatment suggested by Sokolowski *et al.*[1, 30] is reported to significantly reduce the amount of the copper-rich phase in 319 alloys, giving rise to better homogenization prior to aging, and thus improving the mechanical properties. Their results show that two-step solution treatment produces the optimum combination of strength and ductility compared to the single-step treatment. This improvement in mechanical properties is mainly due to the improvement in homogeneity through the dissolution of the copper-rich phases.

In the case of Sr-modified alloys, the presence of strontium can lead to the segregation of the copper phase to areas free of eutectic silicon particles. Due to the segregation, the $CuAl_2$ phase precipitates more often in the block-like form rather than in the fine eutectic form. Compared with the eutectic (Al-$CuAl_2$) phase, the blocky phase has a higher nucleation temperature (525°C), so that the characteristic temperature pertaining to the copper-rich eutectic reaction is raised by the addition of strontium.

Sokolowski *et al.*[1] have suggested that it is likely that in higher Sr-containing alloys, a higher temperature two-step solution treatment would be required to optimize the mechanical properties. The holding time of the first stage and the solution temperature of the second stage are very important parameters in this context. The second-stage solution temperature cannot be higher than 520°C since this may cause the incipient melting of the copper eutectic phase.

As seen in Figure 2.10, a two-stage solution treatment with the second-stage at temperatures below 525°C gives both an increase in strength and elongation (ductility) compared to the conventional single-stage solution treatment at 495°C. This improvement in mechanical properties is due to better dissolution of the Cu-rich phase and subsequent precipitation of hardening phases on artificial aging. Any large Cu-rich phase segregation regions remaining after solution treatment weaken the alloy and reduce the ductility because of their brittle nature. The reduction in strength and ductility observed for second-stage solution treatments at temperatures above 525°C is attributed to the incipient melting of the copper eutectic phase.

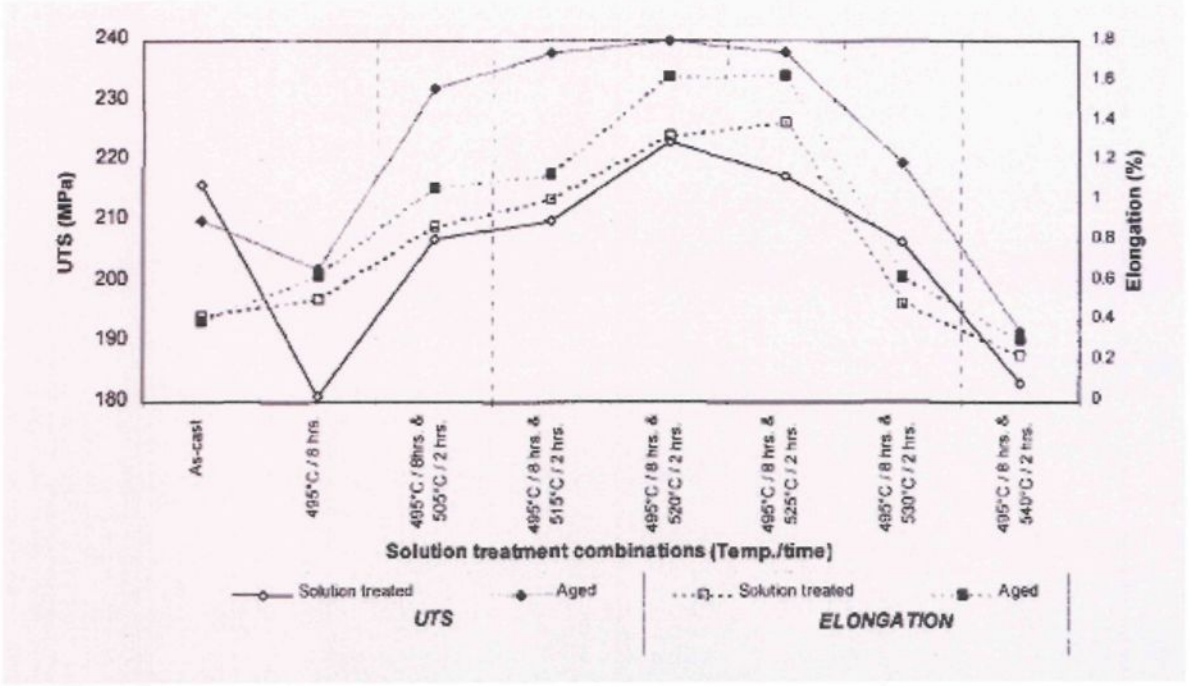


**Figure 2.10** Effect of solution heat treatment conditions and artificial aging on the UTS and Elongation (%) of cast 319 alloy.[1]

Fuoco and Corrêa[47] studied the incipient melting during solution heat treatment of Al-Si-Mg and Al-Si-Cu-Mg alloys. Their results show that iron content has a very small effect on the temperature range of formation of complex eutectics in 319 Al-Si-Cu-Mg alloys (with silicon content around 7%). They also reported that in the case of conventional solution heat treatment, the maximum safe solution temperature for Al-Si-Cu-Mg alloys is 500°C, which is lower than the temperature recommended in the literature. They also found that compared with conventional solution heat treatment (4 h at 485°C), two-step solution heat treatment (2 h at 485°C followed by 2 h at 500°C) improved the mechanical properties greatly: the ultimate tensile strength was improved from 296 MPa to 345 MPa, and the percent elongation increased from 1.9% (conventional solution treatment) to 2.4% with the two-step solution heat treatment.

Figure 2.11(a) presents a light truck brake master cylinder, made from Al-Si-Cu-Mg alloy, which failed in service. The failure of this component was the result of incipient melting during solution heat treatment (at 525°C). The microstructure corresponding to the cracked region shown in Figure 2.11(a) is displayed in Figure 2.11(b). The arrows point to the regions where incipient melting occurred.

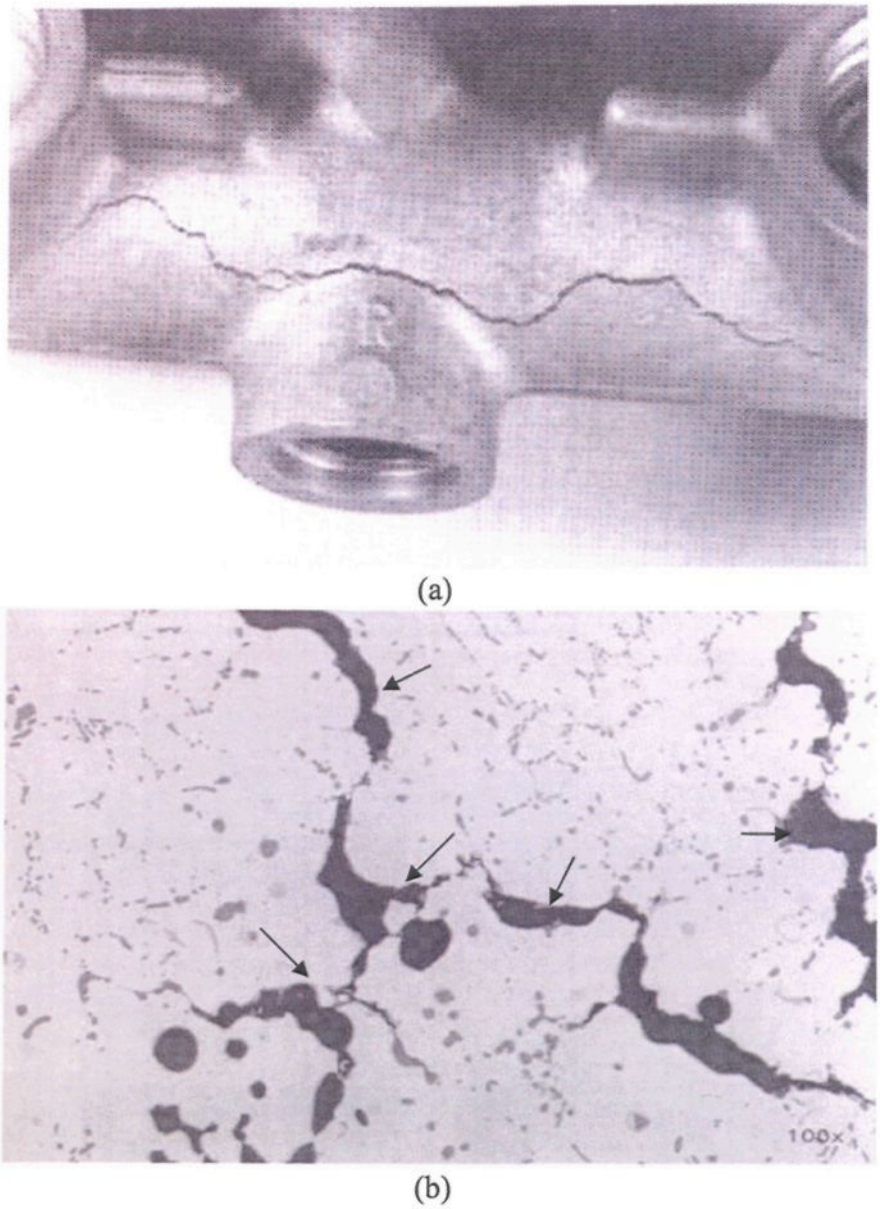


(a)

(b)

**Figure 2.11** Brake master cylinder component made from Al-Si-Cu-Mg alloy, showing: (a) failure (cracking) after solution heat treatment at 525°C, and (b) corresponding microstructure of part of the cracked region.[47]

Lasa and Rodriguez-Ibabe[48] monitored the dissolution of the $Al_2Cu$ phase in two Al-Si-Cu-Mg casting alloys using calorimetry, with the aim of investigating the possibility of using DSC analysis to optimize solution heat treatment in high Cu-content Al-Si-Cu-Mg

alloy. The two alloys, of similar compositions (containing ~4.4 wt% Cu), but prepared using gravity casting (alloy A) and thixoforming (alloy B), respectively, displayed different microstructures.

The solution heat treatment were carried out in a salt bath at 500°C ± 2°C for solution times of 0.5, 1, 2, 3, 5, 7, 12 and 24 h, followed by water quenching to room temperature. They analyzed the dissolution of the $CuAl_2$ phase by relating the energy variation of the first endothermic peak obtained during the DSC runs, corresponding to the reaction

$$Al + Si + CuAl_2 + Al_5Mg_8Cu_2Si_6 \rightarrow \text{Liquid}$$

The mount of the $CuAl_2$ dissolved was calculated from the loss of energy of the peak compared to that obtained for the alloys in the as-received condition (taken to be 100%).

The heating rate is also an important factor with respect to the dissolution of the copper phase. It must be high enough to avoid dissolution of the copper phase during heating.

Lasa and Rodriguez-Ibabe[48] found that below 10°C/min, a large amount of $CuAl_2$ was dissolved during heating. On the other hand, at higher heating rates (above 10°C/min), overlap of different eutectic reactions made it difficult to measure the peak energy accurately. As 10°C/min heating rate still allowed for partial dissolution of the $CuAl_2$ phase, they proposed an different heating schedule, as shown in Figure 2.12(b), compared to that used for the solution treatments carried out in the DSC apparatus (Figure 2.12(a)).

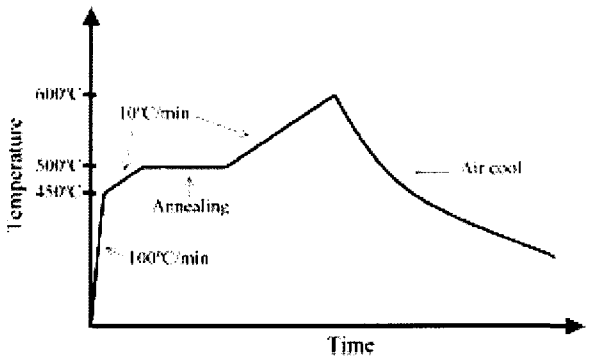


(a)

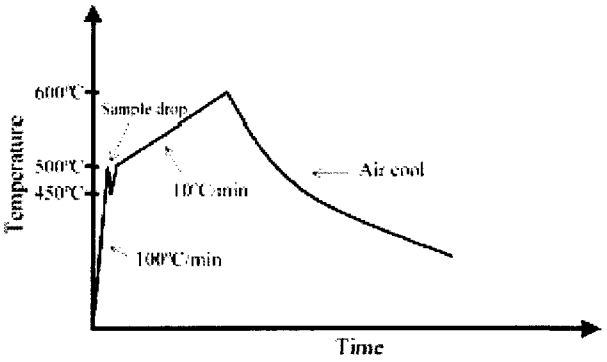


(b)

**Figure 2.12** Heating cycles used to measure the peak energy of the two Al-Si-Cu-Mg alloys: (a) in the DSC apparatus, (b) in an alternative heating schedule.[48]

The peak energy obtained with the alternate schedule was higher (than when heating from 450°C to 500°C at 10°C/min.), minimizing the dissolution of $CuAl_2$ and improving the accuracy of the DSC peak measurement.

The results obtained using DSC analysis were found to agree well with those obtained from SEM metallographic analysis. Figure 2.13 compares the results obtained for the two alloys.

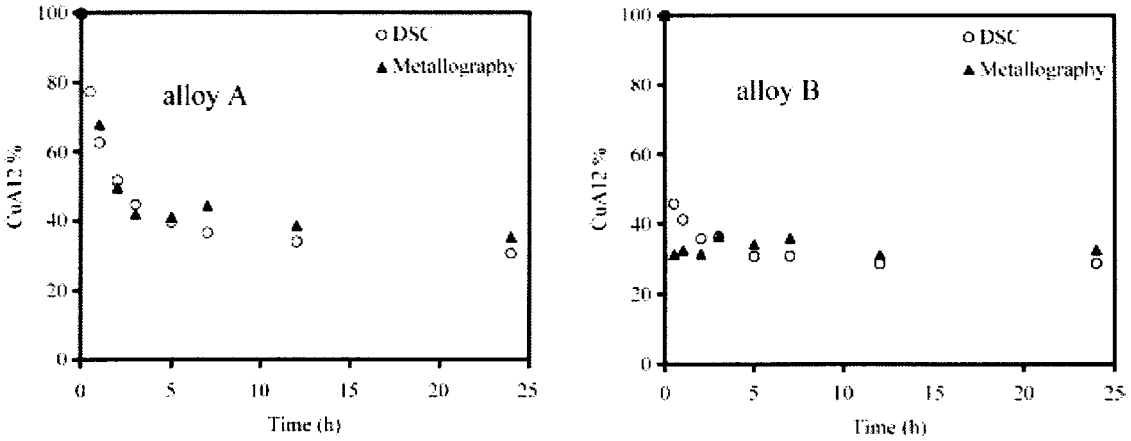


(a) (b)

**Figure 2.13** Percentage of $CuAl_2$ phase obtained as a function of solution treatment time at 500°C for alloys A and B, using both DSC and metallographic analyses.[47]

In was also found that the dissolution rate of the copper phase during isothermal heating depended on the alloy microstructure. In the gravity cast alloy A, a solution time of at lease 2 h was needed to reach equilibrium dissolution of $CuAl_2$ phase, whereas in the thixoformed alloy B, only about 0.5 h was enough. Lasa and Rodriguez-Ibabe[48] attributed this to the fine size and high aspect ratio of the $CuAl_2$ phase particles in the latter.

### 2.9.2 Role of Magnesium

The role of magnesium addition to Al-Si-Cu alloys has already been discussed in Section 2.4. In the context of incipient melting, the addition of Mg can cause the segregation of the $CuAl_2$ phase so that it becomes more difficult to dissolve during solution heat treatment. The addition of Mg in quantities up to 0.5 wt% leads to a significant increase in the volume fraction of the Cu-containing phase with a clear tendency to segregation in localized areas, leading to the formation of the block-like rather than the fine eutectic-like $CuAl_2$ phase.[3] It is important to avoid segregation of the copper phases in

order to prevent the occurrence of incipient melting, and ensure that the alloy properties and castings remain sound.

De la Sablonnière and Samuel[3] found that "burn spots" resulting from the burning of the molten copper phase in 319 alloy test bars containing a high Mg level can occur when the test bars are solution heat treated at a temperature higher than 520°C. They also showed that increasing the Mg content to ~0.5 wt% led to a significant decrease in the eutectic silicon temperature. This temperature determines the maximum temperature that 319 alloy can be exposed to during heat treatment without incurring incipient melting.

# CHAPTER 3

# EXPERIMENTAL PROCEDURES

# CHAPTER 3

# EXPERIMENTAL PROCEDURES

## 3.1 PREPARATION OF ALLOYS AND MELTING PROCEDURE

Both industrial (commercial) and experimental 319 alloys were used in the present study. The industrial B319 alloy was received in the form of 12.5 Kg ingots, the chemical composition of which is show in Table 3.1.

**Table 3.1** Chemical composition of the B319 commercial alloy used in the present work

| Alloy | Element (wt%) | | | | | | | |
|---|---|---|---|---|---|---|---|---|
| | Si | Cu | Mg | Fe | Mn | Zn | Ni | Al |
| B319 | 6.75 | 3.082 | 0.2945 | 0.3003 | 0.2471 | 0.1126 | 0.0386 | bal. |

The magnesium level of the alloy was increased by adding pure Mg to the 319 alloy melt, to achieve a Mg level of 0.6 wt% in order to investigate the effect of Mg on the incipient melting in the alloy, as well as compare the porosity levels obtained at the two different Mg levels. These two alloys were respectively coded I3 and I6 (see Table 3.2).

Measured quantities of pure aluminum, silicon, copper and magnesium were used to prepare the experimental 319 (Al-7%Si-3.5%Cu-Mg) alloy. The base experimental alloy was coded E0 (see Table 3.2). Five other experimental alloys were prepared from the base

**Table 3.2** List of the alloys used in the present work and their respective codes

| Alloy Type | Alloy Code | Nominal Composition |
|---|---|---|
| Experimental Alloy | E0 | Al-7%Si-3.5%Cu (Base Alloy) |
| | E1 | Base Alloy + 0.1 wt% Mg |
| | E2 | Base Alloy + 0.2 wt% Mg |
| | E3 | Base Alloy + 0.3 wt% Mg |
| | E4 | Base Alloy + 0.4 wt% Mg |
| | E6 | Base Alloy + 0.6 wt% Mg |
| Industrial Alloy | I3 | B319 Alloy |
| | I6 | B319 Alloy + 0.3 wt% Mg |

E0 alloy, with Mg levels of 0.1, 0.2, 0.3, 0.4, and 0.6 wt%, respectively. Table 3.2 lists these experimental alloys and their respective codes.

The experimental alloys were prepared using a large 150 Kg-capacity crucible electrical resistance furnace as shown in Figure 3.1. About 100 Kg of each alloy was prepared. The melting temperature was kept at 725°C ± 5°C. Samplings for chemical analysis were taken from each experimental alloy melt that was prepared. The melts were poured into ingots which were then kept aside for further use. The actual chemical compositions of these and the two industrial alloys used are shown in Table 3.3.

**Figure 3.1** Furnace used for preparing experimental alloys.

**Table 3.3** Average chemical compositions (wt%) of the experimental alloys and industrial alloys studied

| Alloy code | Element Concentration (wt %) | | | | | | | |
|---|---|---|---|---|---|---|---|---|
| | Si | Fe | Cu | Mn | Mg | Zn | Ni | Al |
| Alloy E0 | 6.91 | 0.161 | 3.314 | 0.0008 | 0.0017 | <0.0017 | 0.0529 | Bal. |
| Alloy E1 | 6.5 | 0.1726 | 3.561 | <0.0005 | 0.0793 | <0.0017 | 0.0074 | Bal. |
| Alloy E2 | 6.787 | 0.1529 | 3.396 | <0.0005 | 0.1683 | <0.0017 | 0.0050 | Bal. |
| Alloy E3 | 6.61 | 0.1409 | 3.248 | <0.0005 | 0.2675 | <0.0017 | 0.0042 | Bal. |
| Alloy E4 | 6.55 | 0.1464 | 3.337 | <0.0005 | 0.3412 | <0.0017 | 0.0045 | Bal. |
| Alloy E6 | 7.66 | 0.1635 | 3.703 | 0.0018 | 0.588 | <0.0017 | 0.0028 | Bal. |
| Alloy I3 | 6.75 | 0.3003 | 3.082 | 0.2471 | 0.2945 | 0.1126 | 0.0386 | Bal. |
| Alloy I6 | 6.81 | 0.2953 | 3.357 | 0.2411 | 0.6 | 0.1132 | 0.0388 | Bal. |

E=experimental, I=industrial

## 3.2 CASTING PROCEDURES

The various 319 alloys were used to prepare castings from which test bars were obtained for tensile testing purposes. Figure 3.2 shows the ASTM B-108 type permanent mold that was used to prepare the castings, where each casting provided two test bars. The mold was preheated at 450°C to ensure that no moisture was present and for obtaining good castability.

**Figure 3.2** The permanent mold used for preparing the tensile test bars.

In each case, the alloy ingots were cut into small pieces, cleaned, dried and melted in a 40 kg capacity SiC crucible, using an electrical resistance furnace. The melting temperature was kept at 750°C ± 5°C. Degassing of the melt was carried out using pure, dry argon, injected into the melt by means of a graphite rotary impeller. The degassing time/speed was kept constant at 30min/150rpm. Two samplings for chemical analysis were

taken from each melt before the start of casting and at the end of casting, after the required number of test bars has been obtained. Four melts were prepared for each alloy, using charges of 36 Kg each. Each melt provided 20 castings (i.e., 40 test bars). Thus, a total of 80 castings were prepared, giving 160 test bars per alloy.

Thermal analysis also was carried out for each alloy by pouring the molten metal into a 600°C preheated cylindrical graphite crucible (length: 10cm, diameter: 6cm). The preheating of the mold provided close-to-equilibrium cooling conditions and allowed enough time for solidification and growth of the precipitating phases to facilitate identification when examined under an electron microscope/microprobe. The temperature-time data obtained from the thermal analysis was analyzed to determine the reactions that took place during solidification in each case.

### 3.2.1 Thermal Analysis

Thermal analysis is used mainly to estimate the grain size and degree of modification of Al-Si melts prior to pouring. This melt control method involves obtaining the temperature-time or cooling curve of a solidifying alloy and analyzing the various inflection points on the curve. Major phase changes are usually obvious on a cooling curve, but depending on the composition, some of the minor reactions can only be detected clearly by employing a derivative curve in which the slope of the cooling curve (dT/dt) is plotted as a function of time. In the case of 319 alloy, the main microstructural constituents observed include formation of the $\alpha$-aluminum dendritic network, solidification of the main

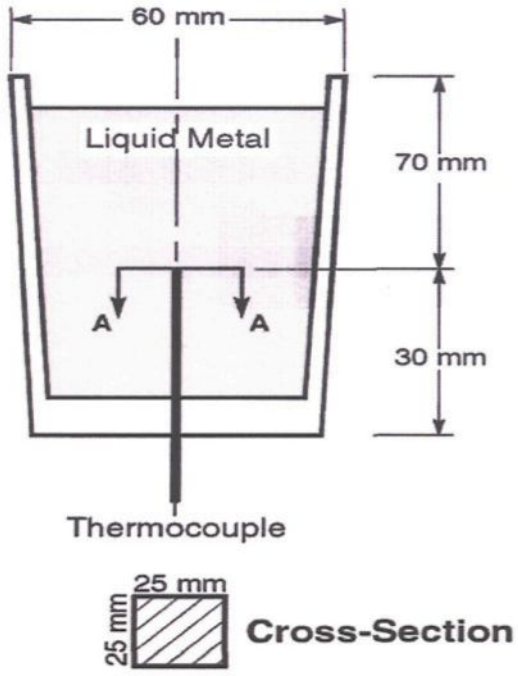


**Figure 3.3** Schematic diagram of graphite mold and set-up used for thermal analysis.

Al-Si eutectic, formation of secondary eutectic phases ($Mg_2Si$, $CuAl_2$) and other more complex intermetallics due to the impurities and other trace elements present in the alloy.

For the thermal analysis experiments, about 1 Kg of the alloy was melted in a 2-Kg capacity SiC crucible, using a small electrical resistance furnace. The melting temperature was kept at 750° ± 5°C. The melt was poured into a cylindrical graphite mold preheated at 600°C to obtain close-to-equilibrium cooling conditions. Thermal analysis was performed by passing a K-type thermocouple (chromel-alumel) vertically through the hole at the bottom of the mold, reaching to a height of ~30 mm within the mold cavity. The set-up used for thermal analysis is shown above in the schematic diagram of Figure 3.3, where A-

A denotes the position at which the sample for microstructural analysis was sectioned from each graphite mold casting. The temperature-time data was collected by using a high speed data acquisition system linked to the computer with an acquisition rate of 5 readings/sec. From the thermal analysis data, the cooling curves and their first derivatives were plotted using Microsoft Excel software.

## 3.3 SOLUTION HEAT TREATMENT AND AGING

The test bars obtained from the various alloy castings were subjected to a single or two-step solution heat treatment as follows.

Single-step solution treatment

Test bars corresponding to all alloys listed in Table 3.3 were solution heat treated at temperatures of 490°C, 495°C, 500°C, 505°C, 510°C, 515°C, 520°C, 525°C, 530°C, 535°C, and 540°C for 8 h each, then quenched in warm water (at 60°C), followed by aging at 155°C for 5 h.

Two-step solution treatment

In this case, test bars corresponding to alloys E0, E3, E6, I3 and I6 were used. The test bars were solution heat treated at 505°C for 8 h, followed by a second solution treatment at 520°C or 530°C for 2 h, followed by quenching in warm water (at 60°C) and aging at 155°C for 5 h, as above.

## 3.4 TENSILE TESTING

Tensile testing was carried out on as-cast and heat-treated test bars of the various alloys, using an MTS Servohydraulic mechanical testing machine, as shown in Figure 3.4. The tests were conducted at room temperature at a strain rate of $2 \times 10^{-4}$ $s^{-1}$. Tensile properties measured included ultimate tensile strength (UTS), the 0.2% offset yield strength (YS), and percentage elongation (%EL). The aim of the tensile tests was to determine how Mg addition and the type of heat treatment used would affect the alloy tensile properties.

**Figure 3.4** MTS Servohydraulic mechanical testing machine.

## 3.5 METALLOGRAPHY

Samples for metallography were sectioned from the tensile-tested bars, about 3mm below the fracture surface, mounted in bakelite and polished to a fine finish (1 μm diamond suspension).

The polished samples were examined using optical microscopy (Olympus BH-UMA microscope). Quantitative measurements of porosity were carried out using a Leco 2001 image analyzer in conjunction with the optical microscope. The optical microscope-image analyzer system used is shown in Figure 3.5.

**Figure 3.5** Optical microscope-image analyzer system used for quantitative metallography measurements.

For porosity measurements, the sample surfaces were examined at a magnification of 100X. Forty fields were measured such that the entire sample surface was traversed in a regular, systematic manner. The percentage porosity and pore characteristics (area, length

and aspect ratio) were determined in each case (field), and the average value and standard deviation obtained for each sample.

### 3.5.1 Electron Probe Microanalysis

Phase identification was carried out using the graphite mold-cast samples, employing electron probe microanalysis (EPMA), coupled with energy dispersive X-ray (EDX) and wavelength dispersion spectroscopic (WDS) analyses. Figure 3.6 shows the Jeol WD/ED combined microanalyzer (McGill Microprobe Laboratory) that was employed for this purpose (model JXA-8900R, operating at 20 kV and 30 nA, with an electron beam size of ~ 1μm).

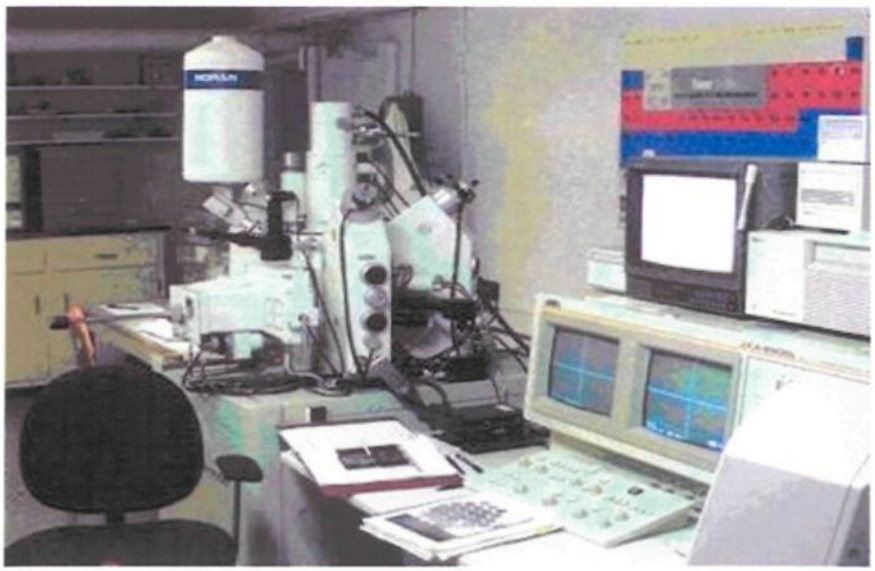

**Figure 3.6** Electron probe microanalyzer used in the present work.

# CHAPTER 4

# THERMAL ANALYSIS AND TENSILE PROPERTIES

# CHAPTER 4

# THERMAL ANALYSIS AND TENSILE PROPERTIES

## 4.1 INTRODUCTION

In this part of the work, the alloys with different Mg contents were melted and poured into a graphite mold (preheated at 600°C) in order to determine the possible reactions that could take place during solidification under conditions close to equilibrium. The effect of Mg addition on the Al-Si eutectic was also studied. The temperature-time data obtained from the thermal analysis results were analyzed and interpreted in terms of the microstructural characteristics of the corresponding castings.

Thermal analysis is used mainly to estimate the grain size and degree of modification of Al-Si melts prior to pouring. This melt control method involves obtaining the temperature-time or cooling curve of a solidifying alloy and analyzing the various inflection points on the curve. Major phase changes are usually obvious on a cooling curve, but depending on the composition, some of the minor reactions can only be detected clearly by employing a derivative curve in which the slope of the cooling curve (dT/dt) is plotted as a function of time. In the case of 319 alloy, the main microstructural constituents observed include formation of the $\alpha$-aluminum dendritic network, solidification of the main

Al-Si eutectic, formation of secondary eutectic phases ($Mg_2Si$, $CuAl_2$) and other more complex intermetallics due to the impurities and other trace elements present in the alloy.

It has been reported that the addition of Mg affects the eutectic temperature in that the eutectic temperature decreases with increasing Mg content. The addition of magnesium refines the Si eutectic structure, and the depression of the eutectic temperature depends very much on the Mg content.[49, 3, 29, 34]

Addition of magnesium is also seen to result in an increase in the volume fraction of Cu-containing phases, with a clear tendency for segregation in localized areas, leading to the formation of the block-like, rather than the fine eutectic-like, $CuAl_2$ phase. This makes it more difficult to dissolve the $CuAl_2$ phase during solution heat treatment. It is important to avoid such segregation which can lead to the occurrence of incipient melting.

The effect of various solution heat treatments and Mg content on the alloy tensile properties was also investigated. This chapter presents the results of the tensile tests that were carried out for the single-stage and two-stage solution heat-treated specimens of all the alloys studied. The tensile properties (UTS, YS and %El) were measured using an MTS Servohydraulic Mechanical Testing machine. The details of the sample preparation and testing procedures have been provided in Chapter 3. Microstructures of the tensile bars corresponding to the different solution treatments, *i.e.*, heat treated at 505°C, 530°C, 505°C followed by 520°C, and 505°C followed by 530°C are also presented in this chapter.

## 4.2 RESULTS AND DISCUSSION

### 4.2.1 Thermal Analysis

From the thermal analysis data, the cooling curve and the first derivative curve were plotted for each alloy condition. These are shown in Figure 4.1 through Figure 4.8. The corresponding reactions expected to occur (marked A through D in the figures) are given in Table 4.1, and were identified with reference to the atlas of Bäckerud *et al.*[7] on the solidification of aluminum foundry alloys. The four main reactions observed correspond to the formation of the α-Al dendrite network (peak A), followed by the precipitation of the Al-Si eutectic (peak B), and the precipitation of the copper intermetallics (peaks C and D). The precipitation temperatures of the copper phases (eutectic Al-$CuAl_2$ and $Al_5Mg_8Cu_2Si_6$) for these alloys are listed in Table 4.2, and show a clear tendency to decrease as the Mg addition is increased up to 0.4% (*i.e.* from 516.7 °C in alloy E0 to 501.3 °C in alloy E4), then remain almost stable with further Mg addition. These observations are in accordance with those of other investigators.[49, 3, 29] The precipitation temperatures of the Al-$CuAl_2$ eutectic in the industrial and experimental alloys are somewhat different at 0.3 wt% Mg level (506.4°C and 504.2°C, respectively), but remain the same at 0.6 wt% Mg content.

Addition of Mg also led to the precipitation of the $Al_5Mg_8Cu_2Si_6$ phase, and to the splitting of the copper phase formation temperature range into two explicit peaks representing the precipitation of $CuAl_2$ and $Al_5Mg_8Cu_2Si_6$ phases. Figure 4.9 compares the cooling curves of all the alloys studied. Comparatively speaking, one can say that in the

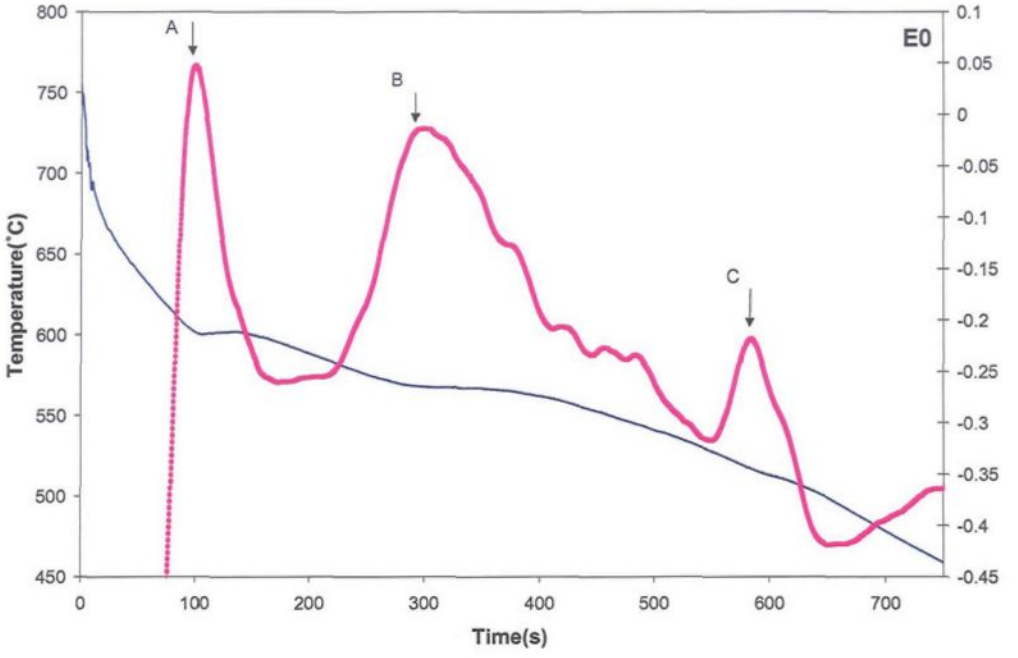


**Figure 4.1** Cooling curve and first derivative obtained from 319 alloy E0 (0% Mg).

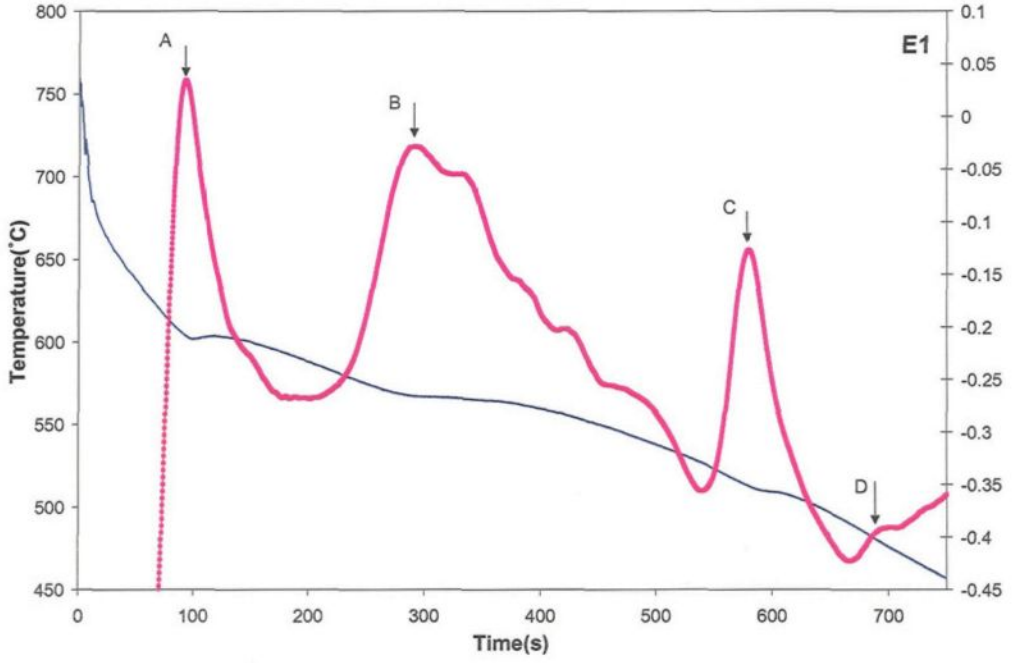


**Figure 4.2** Cooling curve and first derivative obtained from 319 alloy E1 (0.1% Mg).

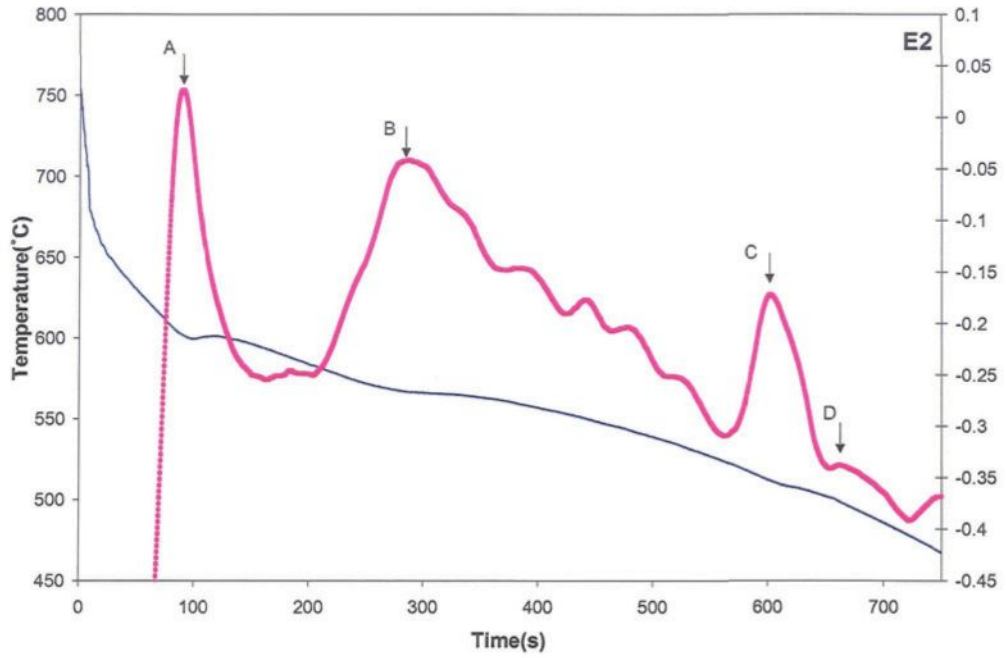


**Figure 4.3** Cooling curve and first derivative obtained from 319 alloy E2 (0.2% Mg).

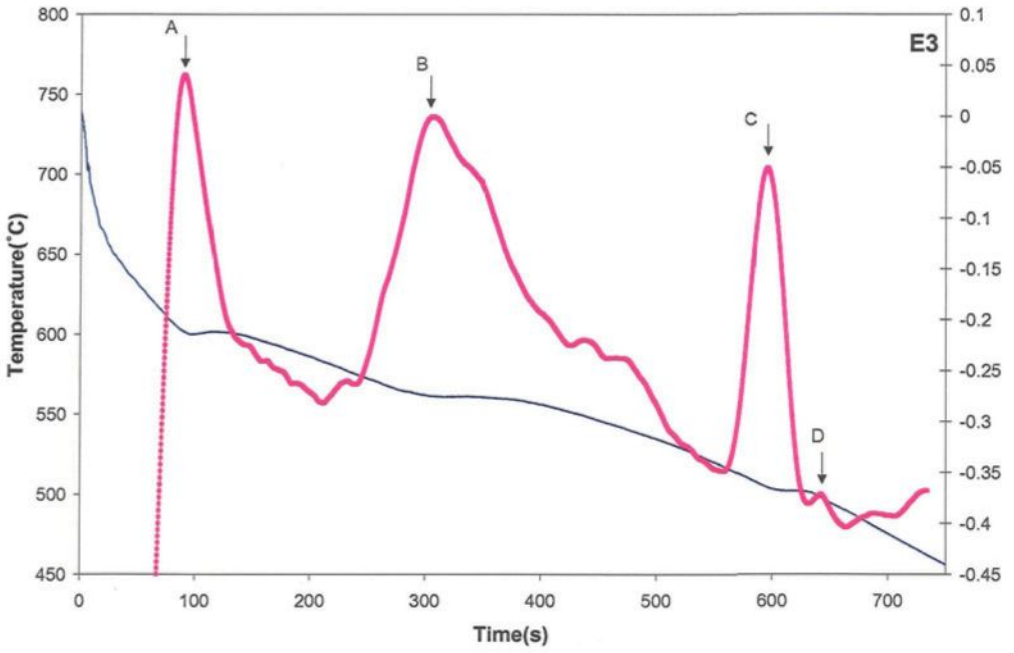


**Figure 4.4** Cooling curve and first derivative obtained from 319 alloy E3 (0.3% Mg).

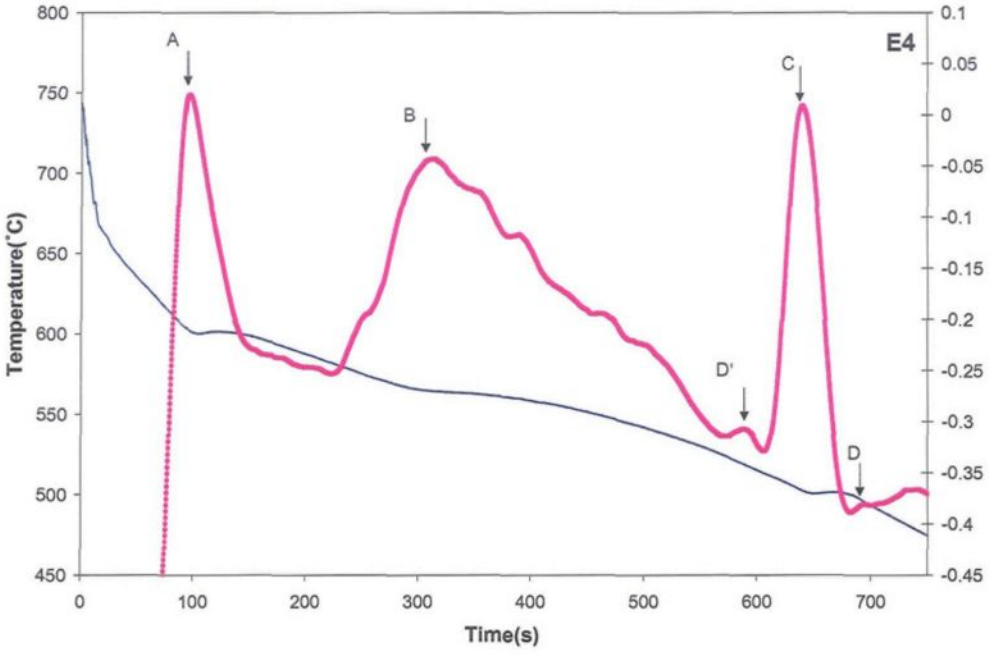


**Figure 4.5** Cooling curve and first derivative obtained from 319 alloy E4 (0.4% Mg).

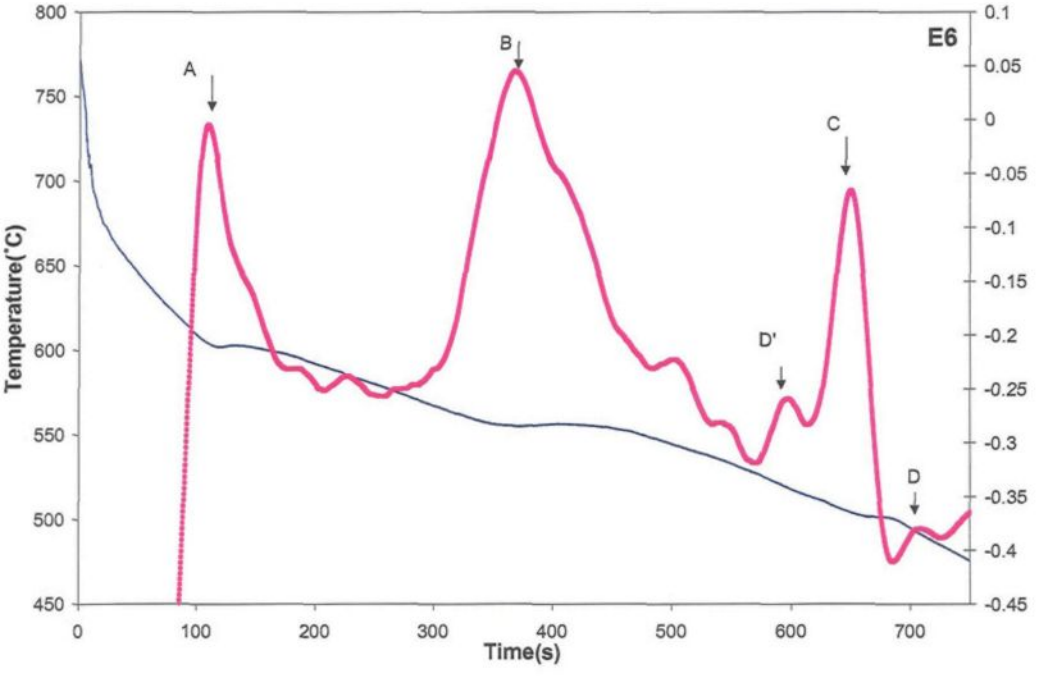


**Figure 4.6** Cooling curve and first derivative obtained from 319 alloy E6 (0.6% Mg).

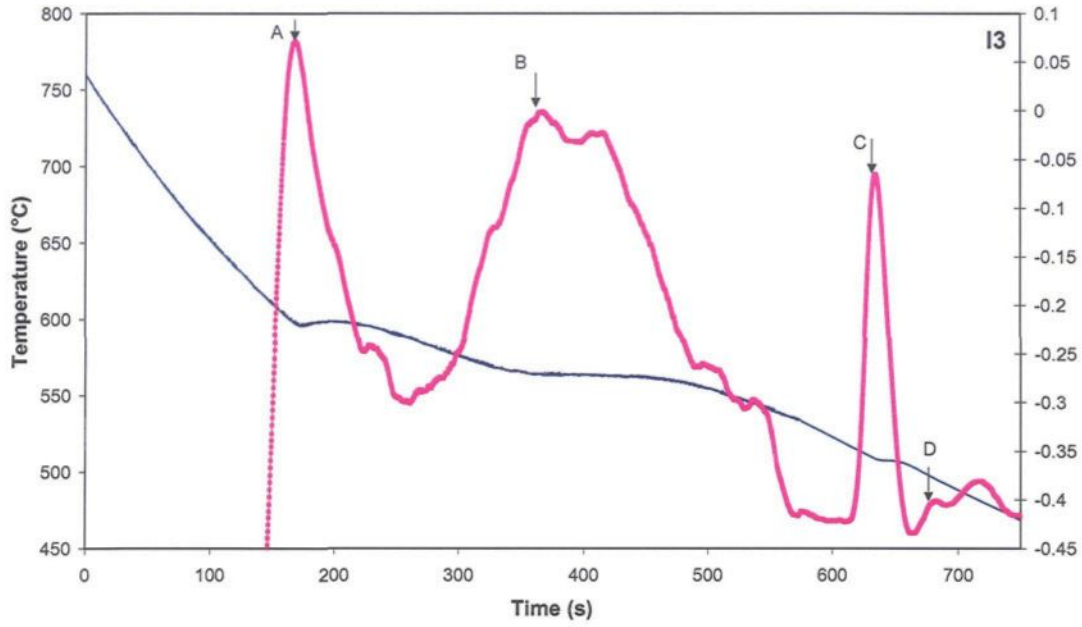


**Figure 4.7** Cooling curve and first derivative obtained from 319 alloy I3 (0.3% Mg).

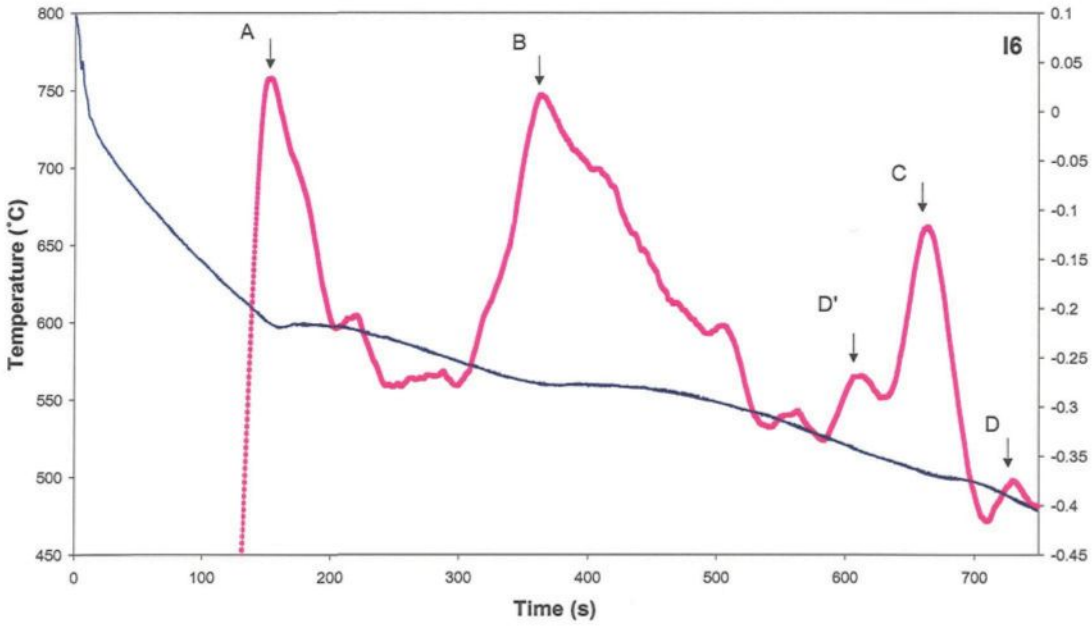


**Figure 4.8** Cooling curve and first derivative obtained from 319 alloy I6 (0.6% Mg).

**Table 4.1** Expected reactions[7] in the 319 alloys studied

| Alloy | Peak | Temperature (°C) | Reaction |
|---|---|---|---|
| E0 (0 wt% Mg) | A | 601.3 | Precipitation of α-Al dendrite network |
| | B | 567.6 | Al-Si eutectic reaction |
| | C | 516.7 | Al-$CuAl_2$ eutectic reaction |
| E1 (0.1 wt% Mg) | A | 604.0 | Precipitation of α-Al dendrite network |
| | B | 567.0 | Al-Si eutectic reaction |
| | C | 513.9 | Al-$CuAl_2$ eutectic reaction |
| | D | 478.0 | Precipitation of $Al_5Mg_8Cu_2Si_6$ |
| E2 (0.2 wt% Mg) | A | 601.8 | Precipitation of α-Al dendrite network |
| | B | 566.6 | Al-Si eutectic reaction |
| | C | 511.9 | Al-$CuAl_2$ eutectic reaction |
| | D | 498.8 | Precipitation of $Al_5Mg_8Cu_2Si_6$ |
| E3 (0.3 wt% Mg) | A | 602.1 | Precipitation of α-Al dendrite network |
| | B | 561.2 | Al-Si eutectic reaction |
| | C | 504.2 | Al-$CuAl_2$ eutectic reaction |
| | D | 498.1 | Precipitation of $Al_5Mg_8Cu_2Si_6$ |
| E4 (0.4 wt% Mg) | A | 601.3 | Precipitation of α-Al dendrite network |
| | B | 564.1 | Al-Si eutectic reaction |
| | C | 501.3 | Al-$CuAl_2$ eutectic reaction |
| | D | 495.4 | Precipitation of $Al_5Mg_8Cu_2Si_6$* |
| E6 (0.6 wt% Mg) | A | 604.2 | Precipitation of α-Al dendrite network |
| | B | 555.4 | Al-Si eutectic reaction |
| | C | 501.4 | Al-$CuAl_2$ eutectic reaction |
| | D | 491.3 | Precipitation of $Al_5Mg_8Cu_2Si_6$* |
| I3 (0.3 wt% Mg) | A | 598.4 | Precipitation of α-Al dendrite network |
| | B | 564.4 | Al-Si eutectic reaction |
| | C | 506.4 | Al-$CuAl_2$ eutectic reaction |
| | D | 495.4 | Precipitation of $Al_5Mg_8Cu_2Si_6$ |
| I6 (0.6 wt% Mg) | A | 599.4 | Precipitation of α-Al dendrite network |
| | B | 559.4 | Al-Si eutectic reaction |
| | C | 501.7 | Al-$CuAl_2$ eutectic reaction |
| | D | 486.4 | Precipitation of $Al_5Mg_8Cu_2Si_6$* |

* Precipitation of $Al_5Mg_8Cu_2Si_6$ also observed prior to Al-$CuAl_2$ eutectic reaction (see peak D') in alloys E4, E6 and I6.

**Table 4.2** Precipitation temperatures (°C) of Al-$CuAl_2$ eutectic and $Al_5Mg_8Cu_2Si_6$ phases in the alloys studied

| Alloy Code | Al-$CuAl_2$ eutectic | $Al_5Mg_8Cu_2Si_6$ |
|---|---|---|
| E0 | 516.7 | |
| E1 | 513.9 | 478.0 |
| E2 | 511.9 | 498.8 |
| E3 | 504.2 | 498.1 |
| E4 | 501.3 | 495.4 |
| E6 | 501.4 | 491.3 |
| I3 | 506.4 | 495.4 |
| I6 | 501.7 | 486.4 |

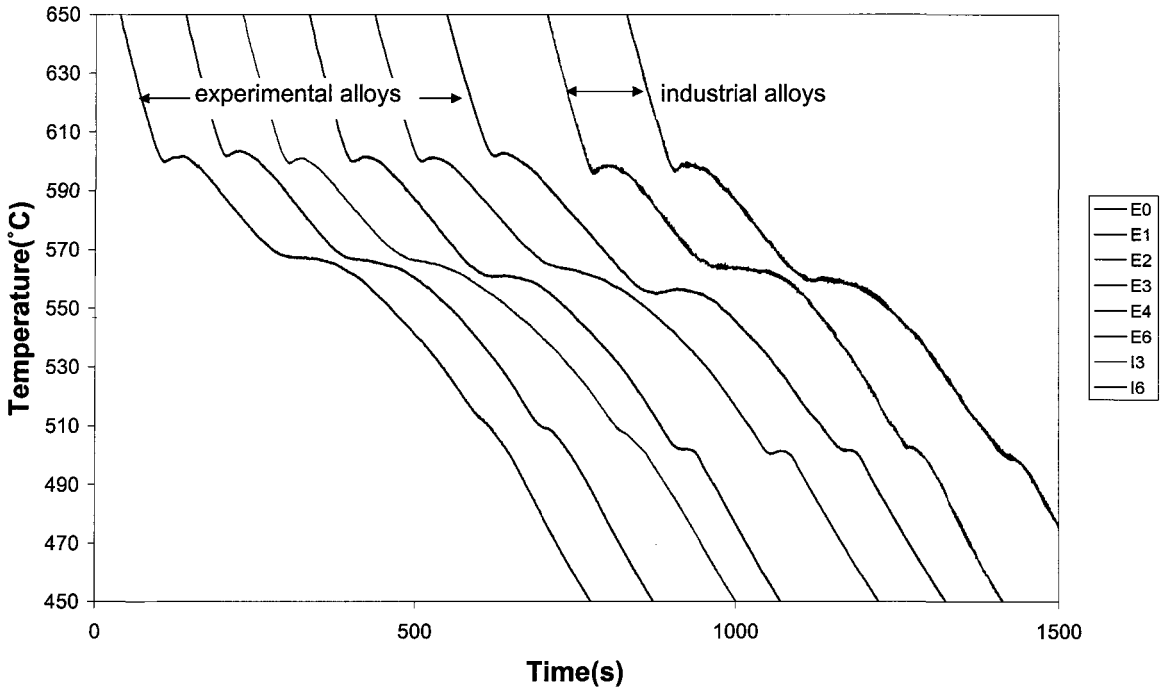


**Figure 4.9** Cooling curves for all the 319 alloys studied.

case of the experimental alloys, the addition of Mg does not affect the precipitation temperature of the α-Al dendrite network overall, but it does decrease the Al-Si eutectic reaction temperature, indicating that Mg act as a "modifier". Similar observations are noted in the case of the industrial alloys (see Table 4.1). It should be pointed out that the Al-Si eutectic temperature dropped slightly with Mg addition up to 0.4 wt% (from 567.6°C to 564.1°C), then at 0.6 wt% Mg addition, it decreased sharply to 555.4 °C. It is expected that at low cooling rate, the modification effect of Mg may not be very obvious at low Mg additions. This was also evidenced from an examination of the corresponding microstructures.

### 4.2.2 Microstructural Analysis

Samples for microstructural analysis were obtained from the corresponding graphite mold castings poured for conducting the thermal analysis experiments. Each sample was sectioned at the position A-A, as shown in Figure 3.3 in Chapter 3. Figure 4.10 shows the Si particle morphology obtained in as-cast samples of alloys E0, E3 and E6. Figure 4.10(a) shows the presence of large, coarse lamellar Si particles in the base alloy (without Mg). At 0.3 wt% Mg addition, Figure 4.10(b), the Al-Si eutectic exhibits a somewhat refined eutectic structure. At 0.6 wt% Mg addition, however, the eutectic is clearly refined, as shown in Figure 4.10(c), indicating clearly that Mg also has a modification effect on the eutectic silicon. Similar observations were noted in the case of the industrial alloys in that addition of Mg changed the Si morphology from lamellar in alloy I3 (Figure 4.11(a)) to an acicular form in alloy I6 (Figure 4.11(b)).

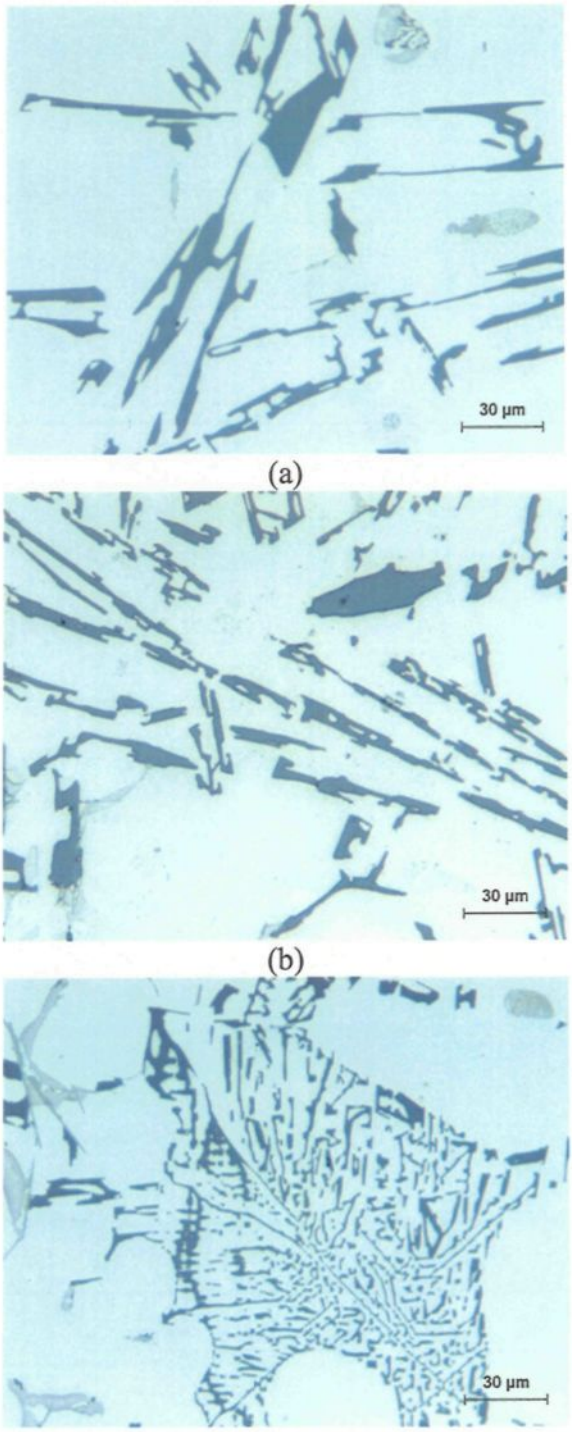


**Figure 4.10** Optical micrographs showing the Si particle morphology obtained in as-cast samples of (a) E0, (b) E3 and (c) E6 experimental 319 alloys.

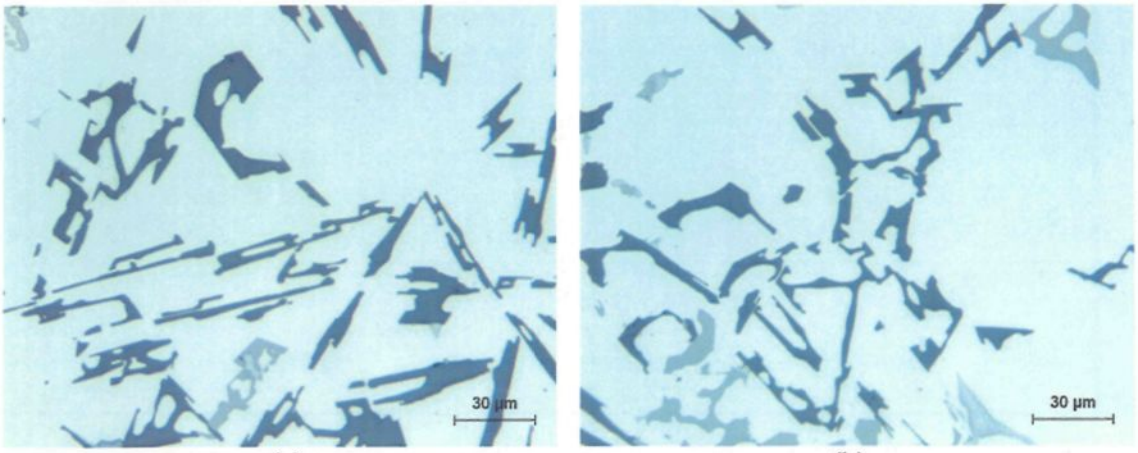


(a) (b)

**Figure 4.11** Optical micrographs showing the Si particle morphology obtained in as-cast samples of (a) I3 and (b) I6 industrial 319 alloys.

From the results of thermal analysis, the depression in the Al-Si eutectic temperature in alloy E3 was 6°C compared with that of alloy E0, while in the case of alloy E6, the depression in the eutectic temperature reached 12°C. Coupled with the Si particle morphology shown in Figure 4.10, these depressions in temperature can be used as an indicator of the extent of the Si structure modification in the casting: the lower the eutectic temperature, the greater the modification effect.

Figure 4.12(a) shows another example of the as-cast microstructure of alloy E0, in which the copper phase is seen mainly as fine eutectic Al-$CuAl_2$, nucleating on the coarse Si particles. When magnesium is added to the alloy, there is a clear tendency for segregation of the copper phase in localized areas, leading to the formation of the block-like, rather than the fine eutectic-like $CuAl_2$ phase. Figure 4.12(b) and (c) shows the microstructure of alloys E3 and E6, where the $CuAl_2$ phase appears in the blocky form rather than in the eutectic form due to Mg addition. Along with the $CuAl_2$ phase, the

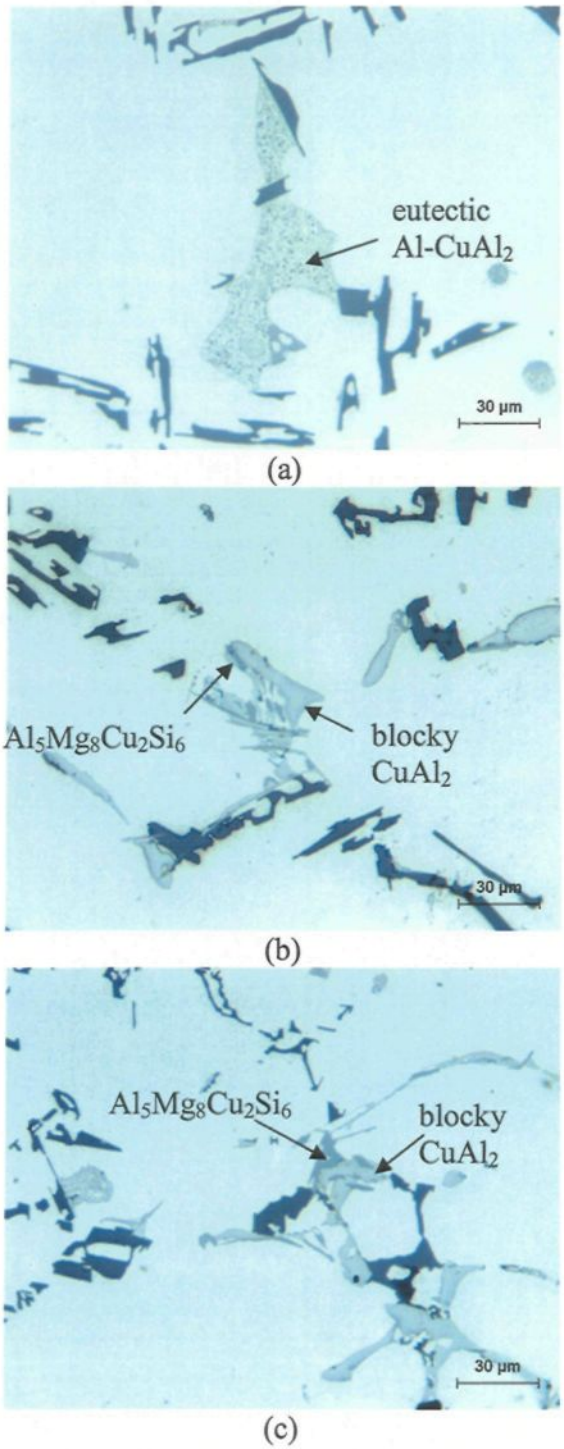


**Figure 4.12** Optical micrographs showing $CuAl_2$ phase obtained in as-cast samples of (a) E0, (b) E3 and (c) E6 experimental 319 alloys.

$Al_5Mg_8Cu_2Si_6$ phase is also present, growing out from the former. Similar observations have been reported by De la Sablonnière and Samuel.[3]

Figure 4.13 shows the microstructures of the industrial alloys I3 and I6. Similar to the case of the experimental alloys, the addition of Mg to the industrial alloy also causes segregation of the copper phase, leading to its precipitation in the blocky form. It is interesting to note that in the case of alloy I6 (Figure 4.13(b)), the $Al_5Mg_8Cu_2Si_6$ phase also precipitates with a different morphology, *viz.*, script–like, rather than the acicular, irregular form usually observed (see Figure 4.13).

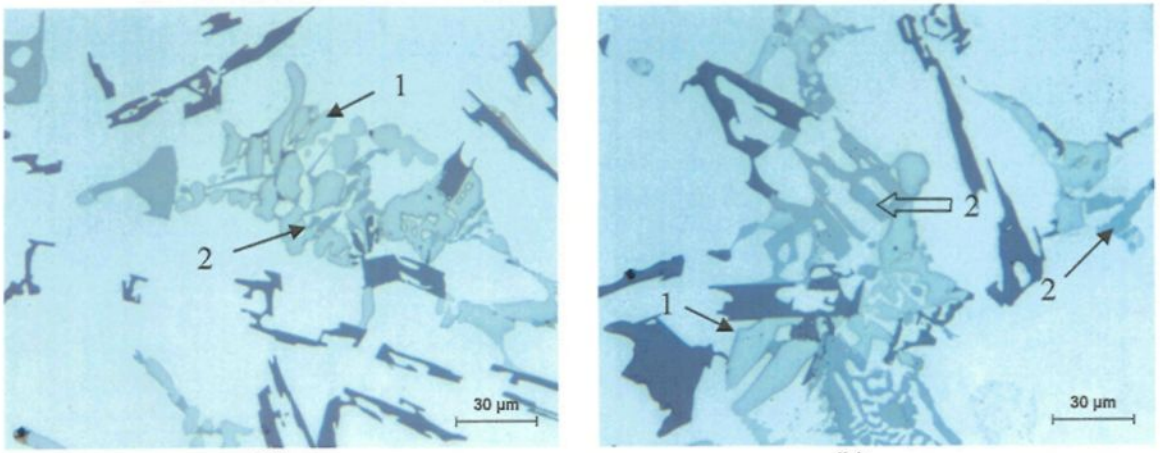


(a) (b)

**Figure 4.13** Optical micrographs showing $CuAl_2$ phase obtained in as-cast samples of (a) I3 and (b) I6 alloys: 1) Blocky $CuAl_2$ phase, 2) $Al_5Mg_8Cu_2Si_6$ phase. Open arrow points to the script-like morphology of the $Al_5Mg_8Cu_2Si_6$ phase.

Figure 4.14 shows examples of the two other phases which precipitated during solidification of alloy I6. During solidification, iron, together with other alloying elements partly goes into solid solution in the matrix and partly forms intermetallic compounds, including the plate-like β-$Al_5FeSi$ phase and the Chinese script–like α-$Al_{15}(Mn,Fe)_3Si_2$

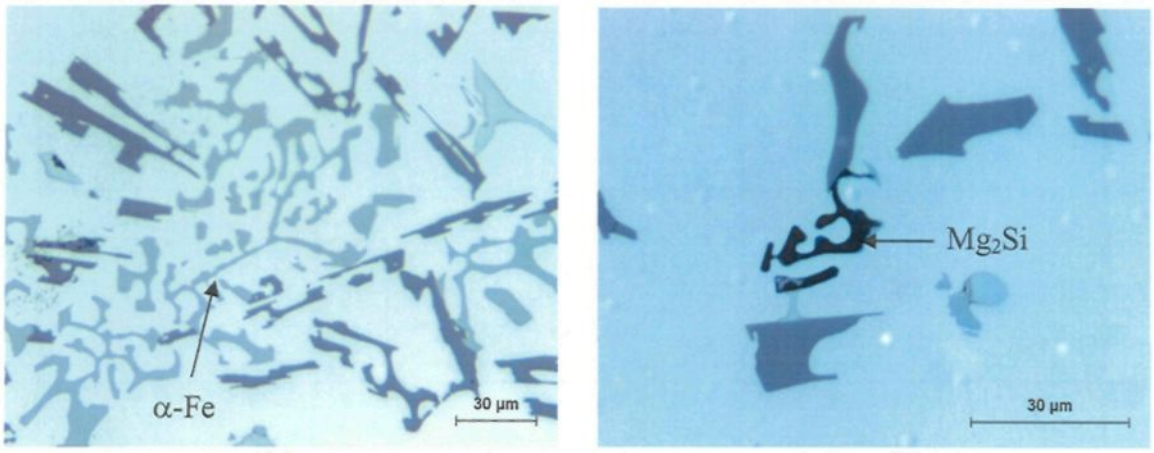


**Figure 4.14** Optical micrographs of as-cast samples obtained from alloy I6 showing (a) α-Fe and (b) $Mg_2Si$ phase.

phase. Figure 4.14(a) shows the Chinese script–like α-$Al_{15}(Mn,Fe)_3Si_2$ phase. The α-Fe intermetallic phase is less detrimental to the mechanical properties due to its compact morphology, compared to the β-iron $Al_5FeSi$ phase. Figure 4.14(b) is a high magnification micrograph showing the presence of the $Mg_2Si$ phase in this alloy. With solution heat treatment, the $Mg_2Si$ will be dissolved into the aluminium matrix, the solubility being dependent on the solution temperature. Quenching thereafter will lock the Mg and Si atoms within the aluminium matrix to form a supersaturated solid solution. The solution temperature is the key factor and must be high enough so that the $Mg_2Si$ can fully dissolve in solution.

### 4.2.3 Electron Probe Microanalysis

The metallographic samples obtained from alloys E6 and I6 were also examined using electron probe microanalysis (EPMA) in order to get a complete assessment of the

intermetallic phases that precipitated during solidification. The backscattered image of the as-cast E6 alloy in Figure 4.15(a) clearly reveals the segregation of the copper phase particles in the interdendritic regions. The high magnification micrograph of Figure 4.15(b) depicts details of the circled area in Figure 4.15(a). The phases numbered 1 and 2 were analyzed using wavelength dispersion spectroscopy (WDS) and the corresponding chemical compositions are listed in Table 4.3, where both the calculated formulae and the phases to which they correspond are shown.

**Table 4.3** Chemical compositions of the copper phases observed in alloy E6, corresponding to Figure 4.15(b)

| Phase | Element | Average wt% | Average at.% | Calculated formula | Suggested formula |
|---|---|---|---|---|---|
| 1 | Al | 49.67 | 68.678 | $CuAl_2$ | $CuAl_2$ |
| | Cu | 50.95 | 29.912 | | |
| | Total | 101.85 | 100 | | |
| 2 | Al | 21.07 | 21.949 | $Al_5Mg_9Cu_2Si_7$ | $Al_5Mg_8Cu_2Si_6$ +$Mg_2Si$ |
| | Si | 29.95 | 29.963 | | |
| | Cu | 19.95 | 8.823 | | |
| | Mg | 33.94 | 39.226 | | |
| | Total | 105 | 100 | | |

Figure 4.16 shows the EDX spectra corresponding to the two phases. These results show that the copper mainly exists in the form of two compounds in the experimental alloy, $CuAl_2$ and $Al_5Mg_8Cu_2Si_6$.

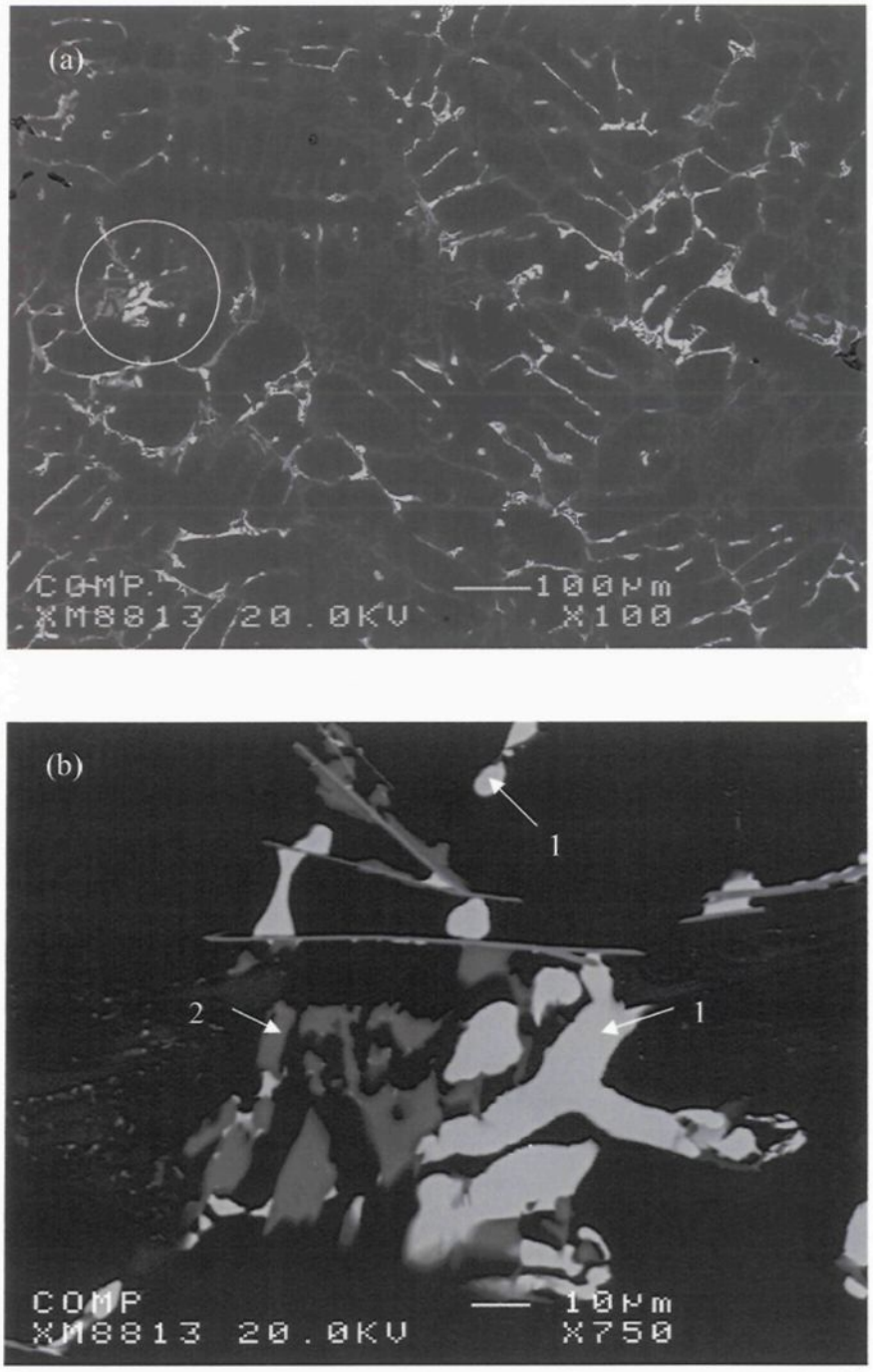


**Figure 4.15** Backscattered images showing (a) $CuAl_2$ phase distribution in as-cast E6 alloy, (b) a high magnification micrograph of the circled area in (a) showing precipitation of 1- block-like $CuAl_2$ and 2- $Al_5Mg_8Cu_2Si_6$.

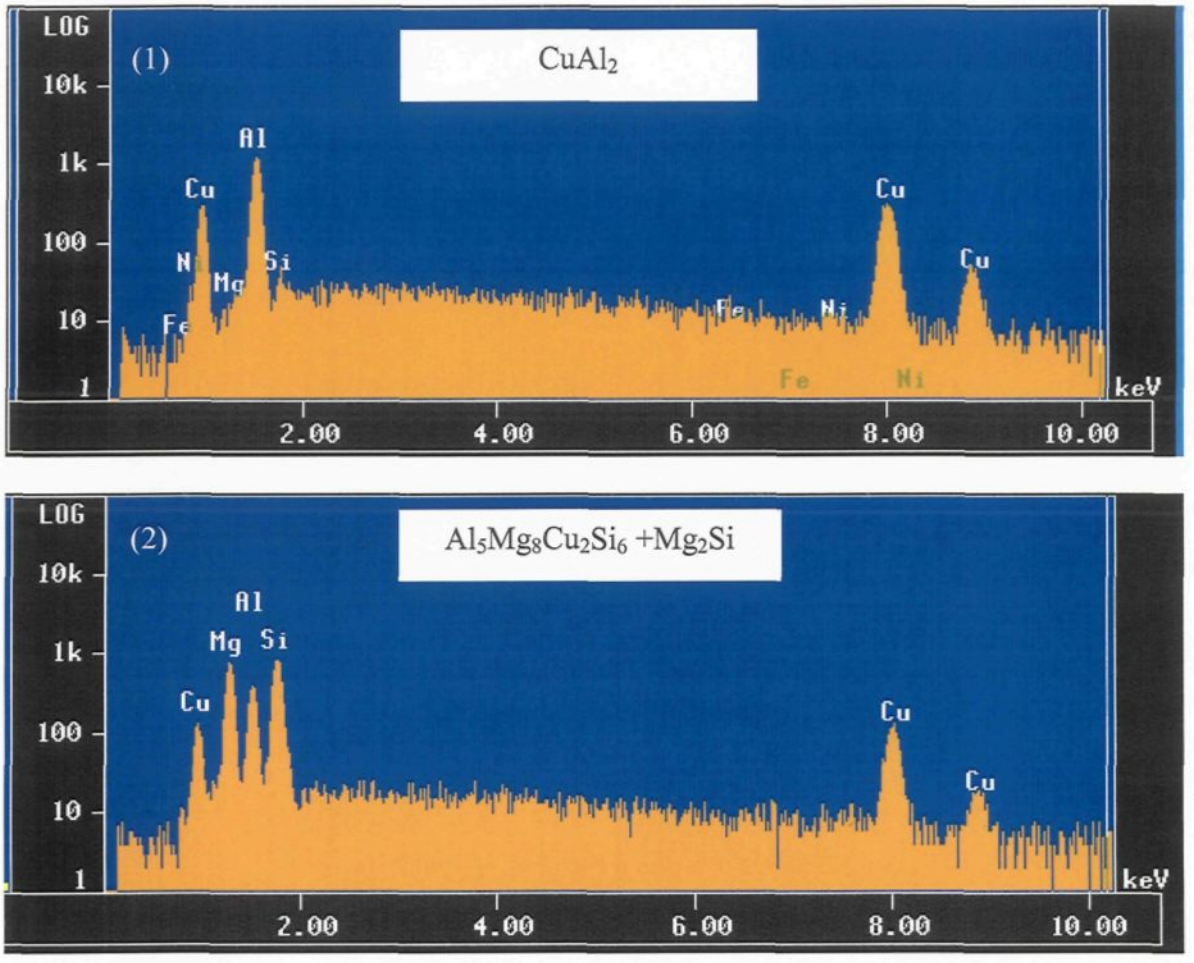


**Figure 4.16** EDX spectra corresponding to the phases shown in Figure 4.15(b) for as-cast E6 alloy: 1) $CuAl_2$ and 2) $Al_5Mg_8Cu_2Si_6$ +$Mg_2Si$.

Figure 4.17 depicts four backscattered (BS) images obtained from alloy I6. The various phases marked 1 through 6 observed in these figures were analyzed using wavelength dispersion spectroscopy (WDS) and the corresponding chemical compositions are listed in Table 4.4. Figure 4.18 shows the EDX spectra corresponding to these phases. The BS images of Figure 4.17 show that the $Al_5Mg_8Cu_2Si_6$ phase precipitates in two different morphologies: the script–like form observed in Figure 4.17(a) (marked 2) and an

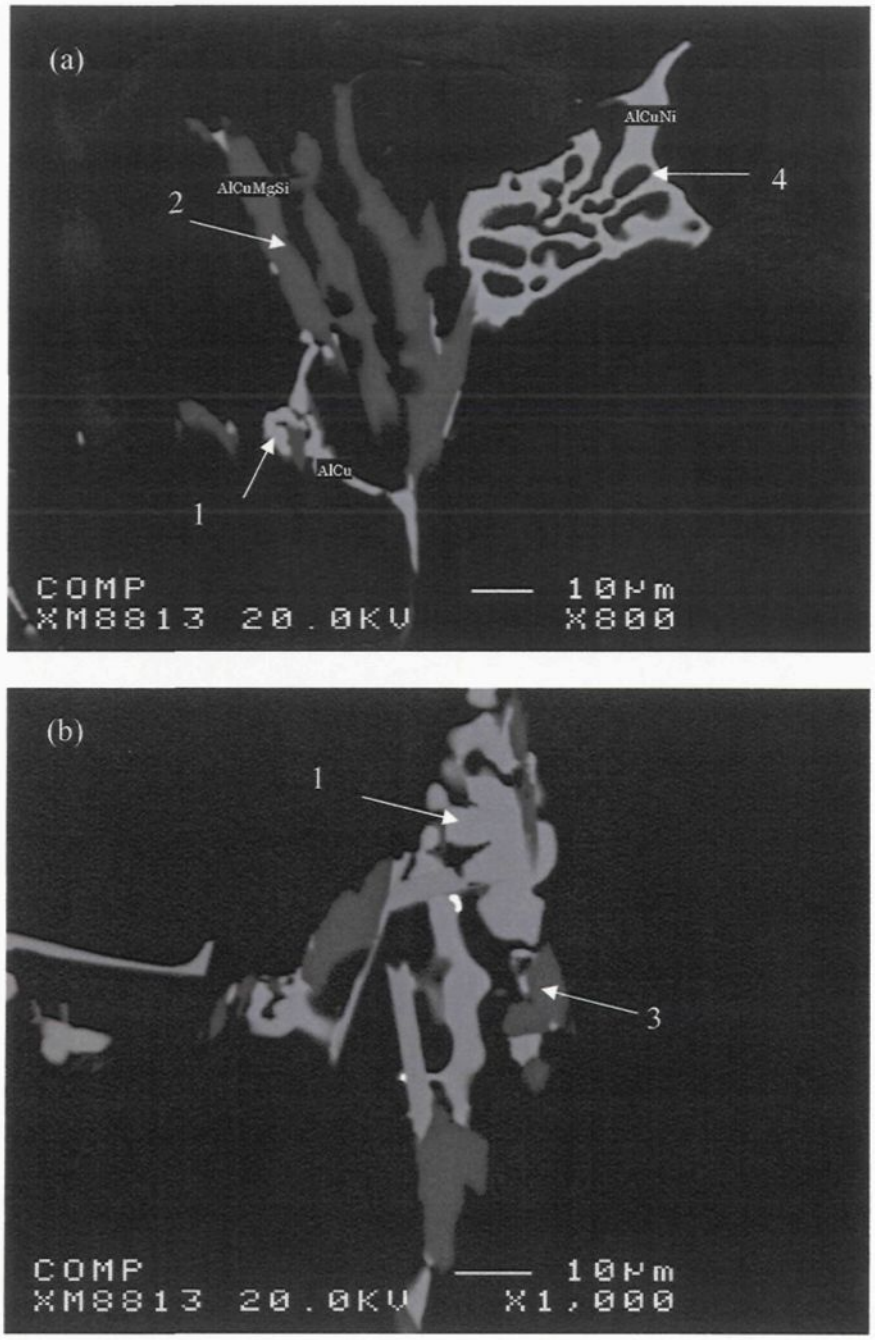


**Figure 4.17** Backscattered images obtained from as-cast alloy I6. The various phases marked 1 to 6 in (a)-(d) correspond to: 1-$CuAl_2$; 2 -script-like $Al_5Mg_8Cu_2Si_6$; 3-irregular shaped $Al_5Mg_8Cu_2Si_6$; 4-$Al_6NiCu_3$; 5-$Al_3$(FeCuNi); 6-$Al_8Mg_3FeSi_6$.

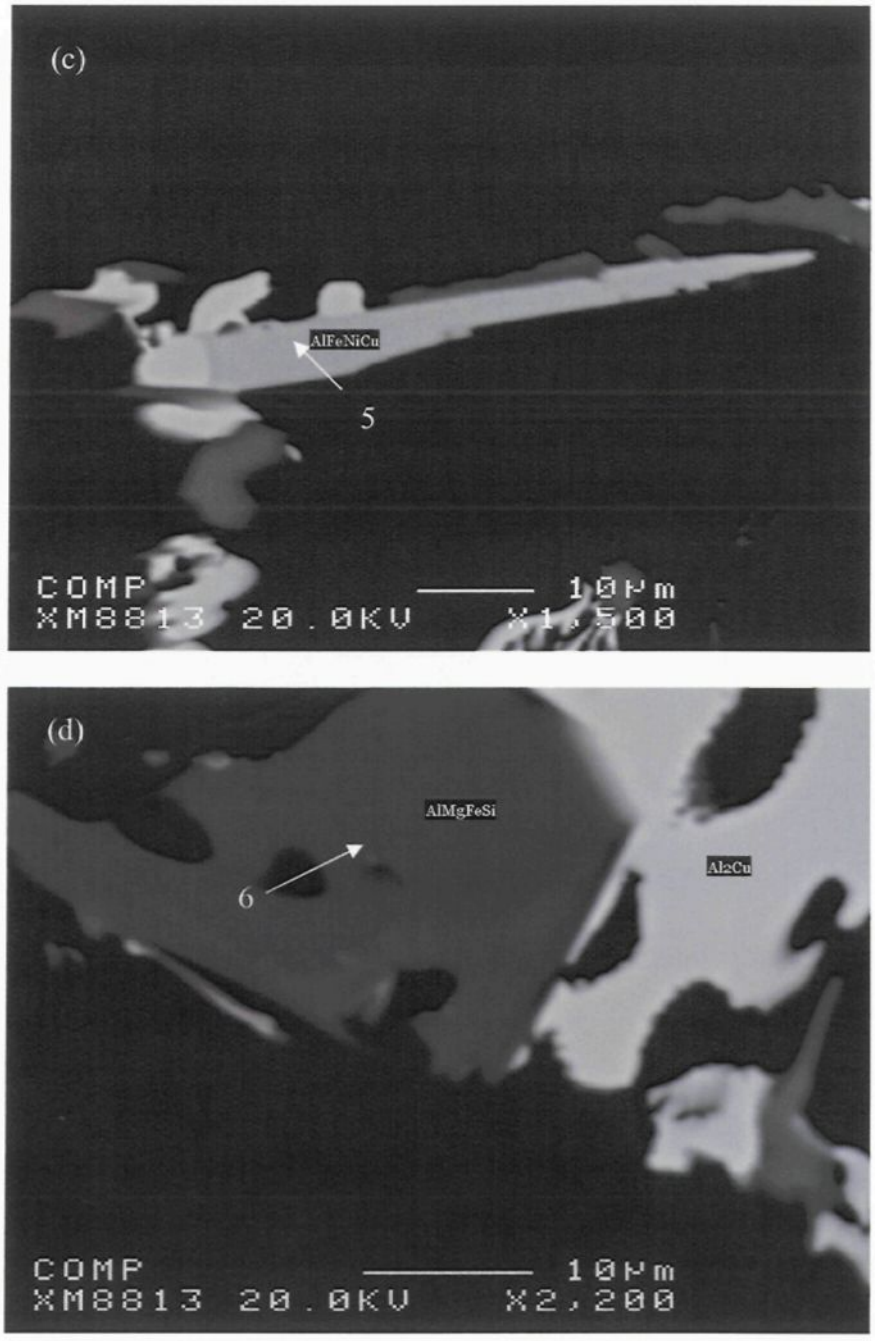


**Figure 4.17** Backscattered images obtained from as-cast alloy I6. The various phases marked 1 to 6 in (a)-(d) correspond to: 1-$CuAl_2$; 2-script-like $Al_5Mg_8Cu_2Si_6$; 3-irregular shaped $Al_5Mg_8Cu_2Si_6$; 4-$Al_6NiCu_3$; 5-$Al_3(FeCuNi)$; 6-$Al_8Mg_3FeSi_6$.

acicular, irregular form seen in Figure 4.17(b) (marked 3). Some other complex intermetallics were also observed due to the trace elements present in the industrial alloy. Ni is observed combined with Cu in the Chinese script-like $Al_6NiCu_3$ phase.

**Table 4.4** Chemical compositions of phases observed in alloy I6, corresponding to Figure 4.17

| Phase | Element | Average wt% | Average at.% | Calculated formula | Suggested formula |
|---|---|---|---|---|---|
| 1 | Al | 49.04 | 68.012 | $CuAl_2$ | $CuAl_2$ |
| | Cu | 51.15 | 30.118 | | |
| | Total | 102.6 | 100 | | |
| 2 | Al | 22.98 | 24.125 | $Al_5Mg_8Cu_2Si_6$ | $Al_5Mg_8Cu_2Si_6$ |
| | Si | 28.76 | 28.998 | | |
| | Cu | 18.73 | 8.348 | | |
| | Mg | 32.83 | 38.25 | | |
| | Total | 103.95 | 100 | | |
| 3 | Al | 22.275 | 22.993 | $Al_5Mg_9Cu_2Si_6$ | $Al_5Mg_8Cu_2Si_6$ |
| | Si | 28.42 | 28.2435 | | |
| | Cu | 19.735 | 8.6655 | | |
| | Mg | 34.705 | 39.841 | | |
| | Total | 105.32 | 100 | | |
| 4 | Al | 43.57 | 62.771 | $Al_7NiCu_3$ | $Al_6NiCu_3$+Al |
| | Cu | 45.89 | 28.072 | | |
| | Ni | 13.18 | 8.728 | | |
| | Total | 103.14 | 100 | | |
| 5 | Al | 54.02 | 69.934 | $Al_{14}FeCu_2Ni_2$ | $Al_3$(Fe,Cu,Ni) |
| | Fe | 7.55 | 4.719 | | |
| | Cu | 19.72 | 10.841 | | |
| | Ni | 14.17 | 8.43 | | |
| | Total | 100.79 | 100 | | |
| 6 | Al | 46.9 | 49.141 | $Al_{13}Mg_5FeSi_7$ | $Al_8Mg_3FeSi_6$+Al |
| | Si | 25.7 | 25.859 | | |
| | Fe | 7.25 | 3.671 | | |
| | Mg | 16.65 | 19.358 | | |
| | Total | 100.67 | 100 | | |

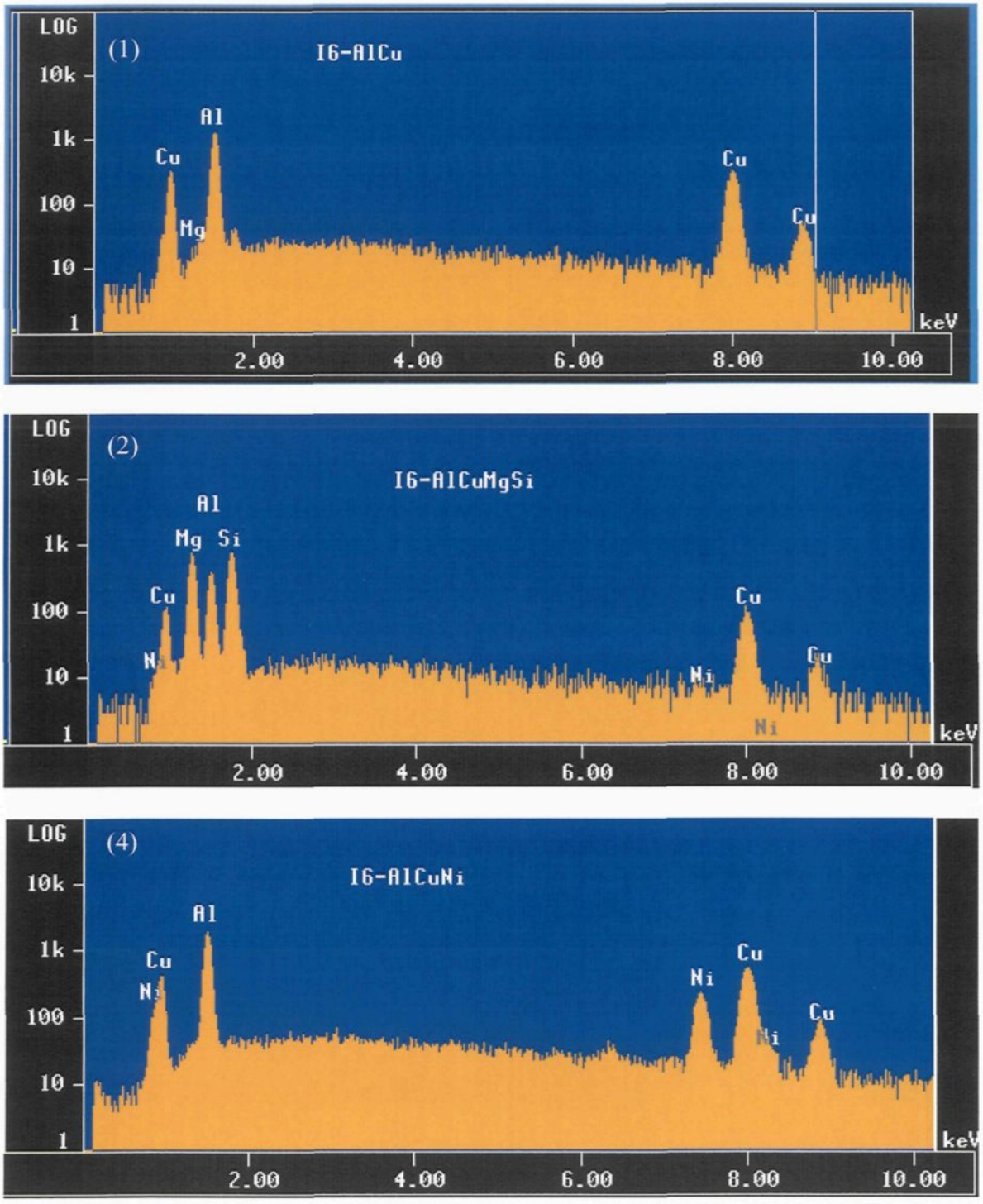


**Figure 4.18** EDX spectra corresponding to the phases in Figure 4.17 observed in I6 alloy: 1-$CuAl_2$; 2-script-like $Al_5Mg_8Cu_2Si_6$; 4-$Al_6NiCu_3$; 5-$Al_3$(Fe,Cu,Ni); 6- $Al_8Mg_3FeSi_6$.

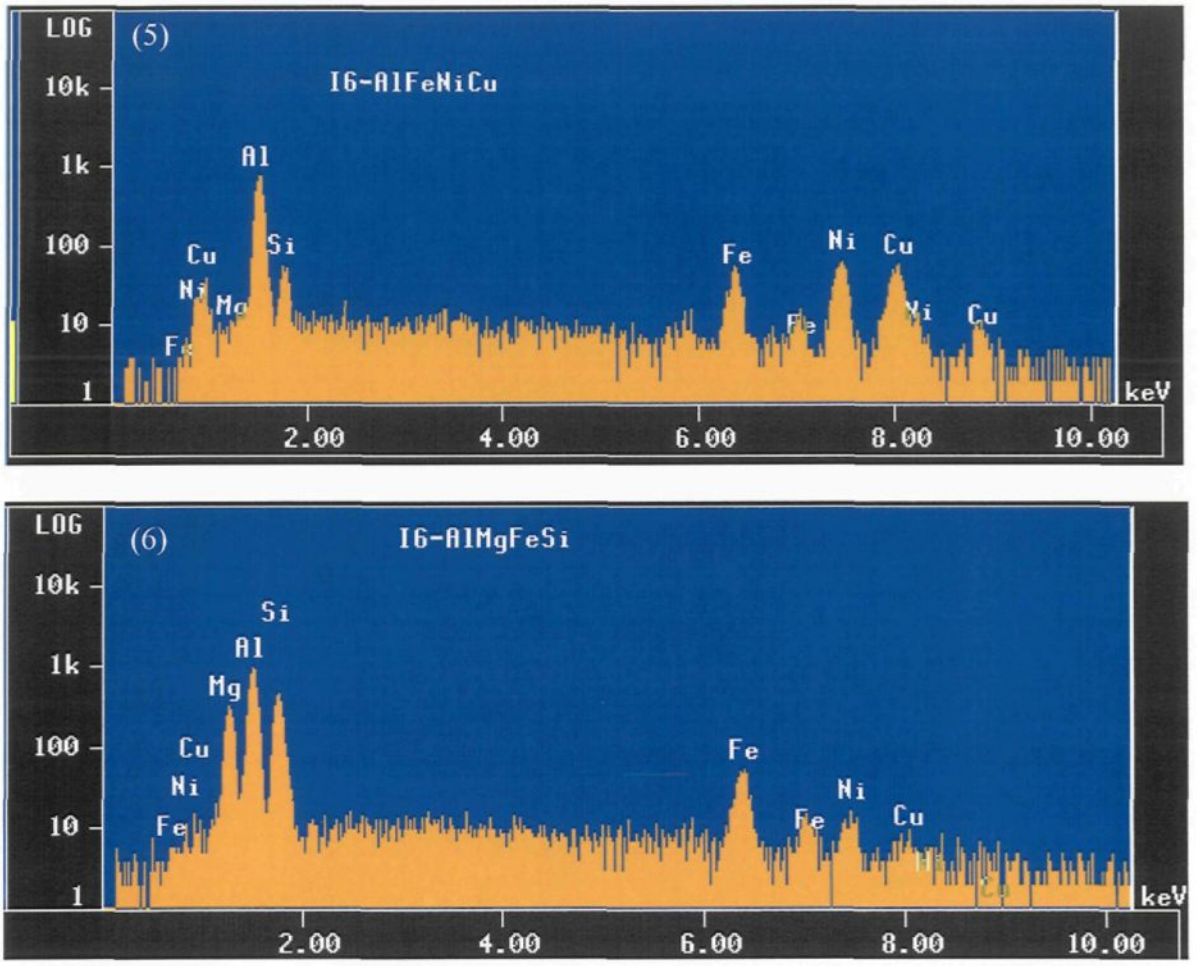


**Figure 4.18** EDX spectra corresponding to the phases in Figure 4.17 observed in I6 alloy: 1- $CuAl_2$; 2- script-like $Al_5Mg_8Cu_2Si_6$; 4- $Al_6NiCu_3$; 5- $Al_3(Fe,Cu,Ni)$; 6- $Al_8Mg_3FeSi_6$.

### 4.2.4 Tensile Properties

The mechanical properties of 319 type alloys are mainly controlled by the secondary dendrite arm spacing (SDAS), eutectic Si particle characteristics, alloying element additions (Mg, Fe, and others), and the presence of casting defects such as porosity and inclusions. In addition, the effects of modification and solution heat treatment can also

control the tensile properties of the alloy through the changes brought about in the eutectic Si particle characteristics. However, when the solution temperature exceeds the melting point of the $CuAl_2$ phase, incipient melting can occur at the grain boundaries, resulting in the formation of a structureless form of the $CuAl_2$ phase and related porosity on quenching, and a consequent deterioration of the tensile properties.

#### 4.2.4.1 Single stage solution heat treatment

The ultimate tensile strength (UTS) values of the experimental 319 alloys as a function of solution heat treatment temperature are shown in Figure 4.19. In the as-cast condition, it is expected that the UTS will increase with increasing Mg level of the alloy due to the combined effects of modification and natural age hardening. The higher the Mg content, the more the age hardening expected to be achieved. However, as Figure 4.19 shows, the UTS remains more or less the same in the as-cast condition, ranging from 273 to 280 MPa for the four alloys studied (E1 through E4). Nevertheless, there is still an increase of about 22% in the UTS compared with that of the base alloy E0 without any Mg addition (230 MPa). Compared to the as-cast condition, the strength increases after solution heat treatment due to the changes in the eutectic Si particle size and shape that occur during the treatment, as well as the precipitation of submicroscopic and metastable phases containing Mg and Si which act as obstacles for dislocation movement, leading to precipitation hardening, in addition to that provided by Cu and Al.

As Figure 4.19 shows, after a critical temperature, the UTS drop sharply, due to the melting of the copper phase and the related porosity formed upon quenching. The addition

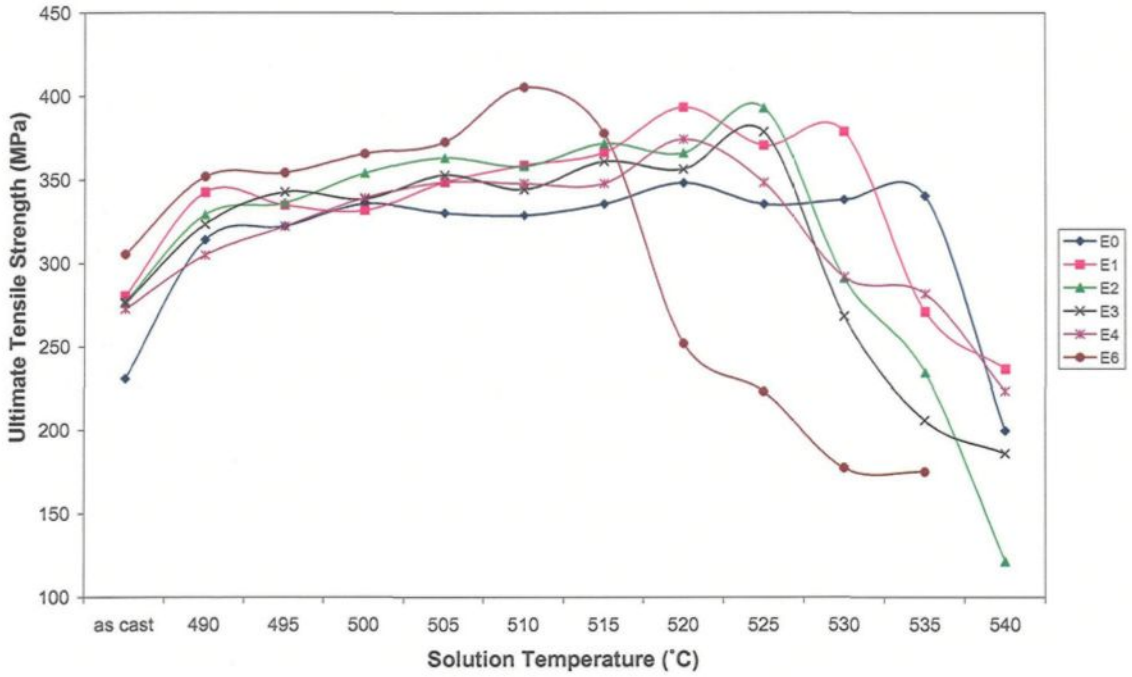


**Figure 4.19** UTS of experimental 319 alloys as a function of solution heat treatment temperature.

of Mg leads to a significant increase in the volume fraction of the Cu-containing phase, with a clear tendency to segregation in localized areas, leading to the formation of the block-like $CuAl_2$ phase. Compared with the fine eutectic $CuAl_2$ phase, the block-like phase is more difficult to dissolve during solution heat treatment. That is why the onset temperature of incipient melting of a high Mg-containing alloy is lower than that of an alloy with low Mg addition.

Figure 4.20 show the UTS of the industrial 319 alloys as a function of solution heat treatment temperature. Compared with the as-cast case, solution heat treatment at 490°C increases the UTS by about 40% (*i.e.* from 240 to 337 MPa in the case of I6 alloy, and from

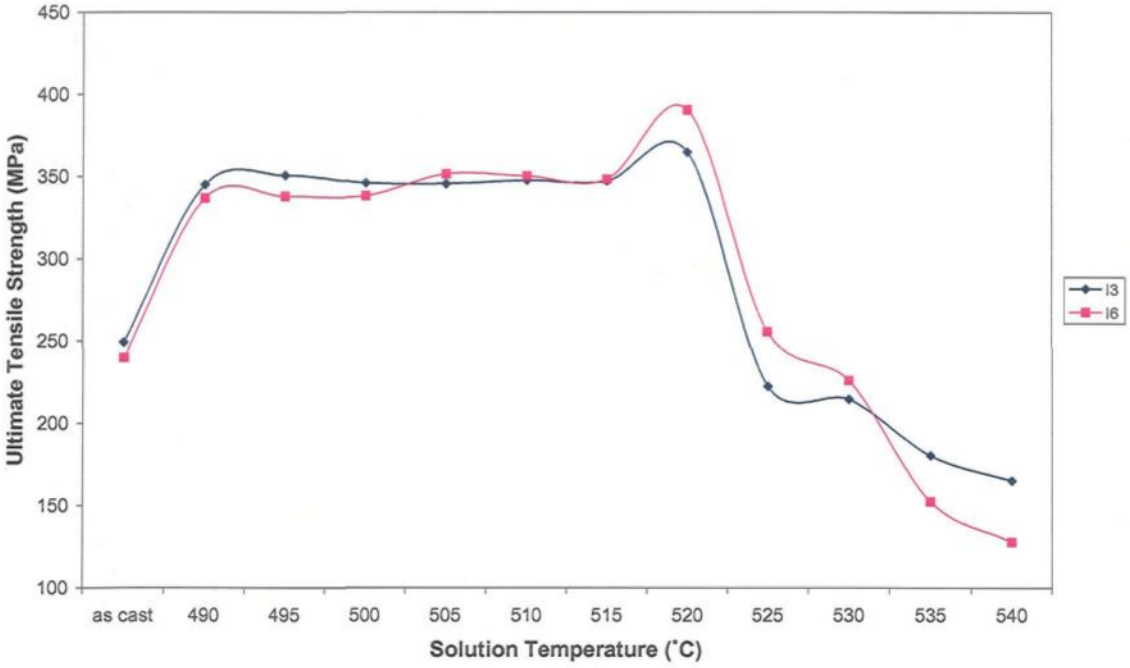


**Figure 4.20** UTS of industrial 319 alloys as a function of solution heat treatment temperature.

249 to 345 MPa in the case of I3 alloy). This may be due to the progressive dissolution of copper in the aluminum matrix. Thereafter, the UTS of both alloys remains more or less the same with further increase in solution temperature up to 515°C. At 520°C, which is high enough to maximize the dissolution of the copper-rich phases and to sufficiently modify the silicon particle morphology, the UTS values reach their maximum. At temperatures higher than 520°C, incipient melting occurs, lowering the ultimate tensile strength.

According to Shivkumar *et al.*,[50] yield strength is essentially determined by the Mg content and the aging condition rather than the eutectic Si particle characteristics. Increase in Mg content up to 0.7% in 356 alloys has been reported to result in higher yield strength or lower ductility and fracture toughness.[51] This is also observed in the experimental results

of the present work. As shown in Figure 4.21, the yield strength increases with increasing Mg concentration in the experimental alloys. As observed in the case of ultimate tensile strength, the yield strength for all alloys drops sharply after exceeding a critical solution temperature. In the case of the industrial alloys, Figure 4.22, solution heat treatment in the range 490°C to 520°C does not produce any significant change in the yield strength, which varies, for example, between 257 and 282 MPa in the I6 alloy.

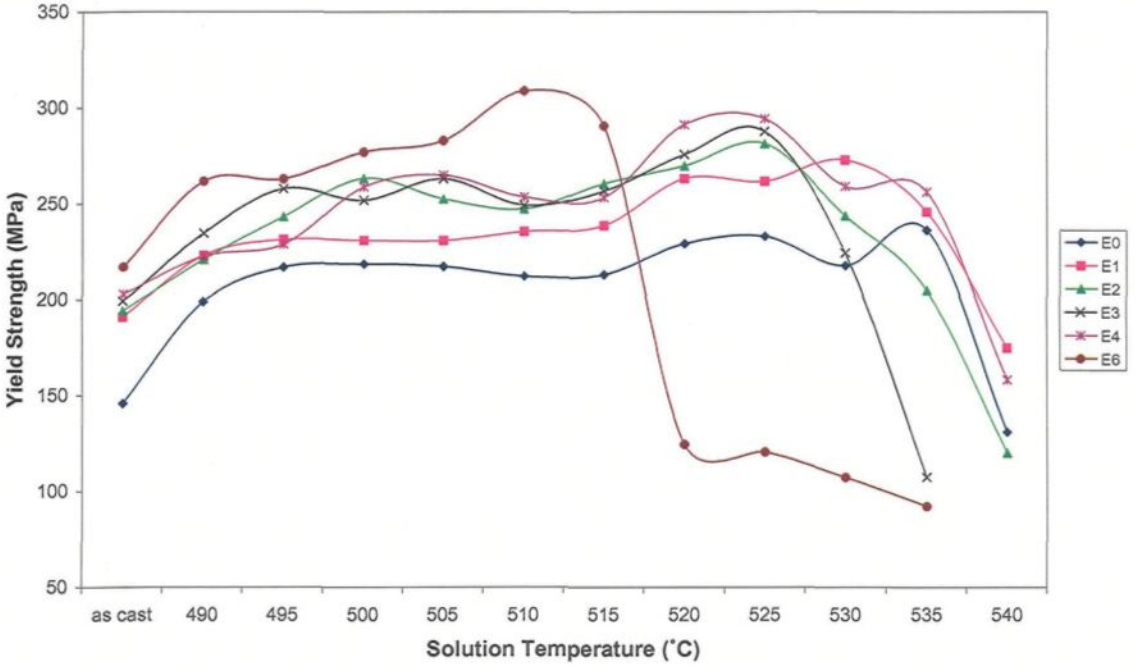


**Figure 4.21** YS of experimental 319 alloys as a function of solution heat treatment temperature.

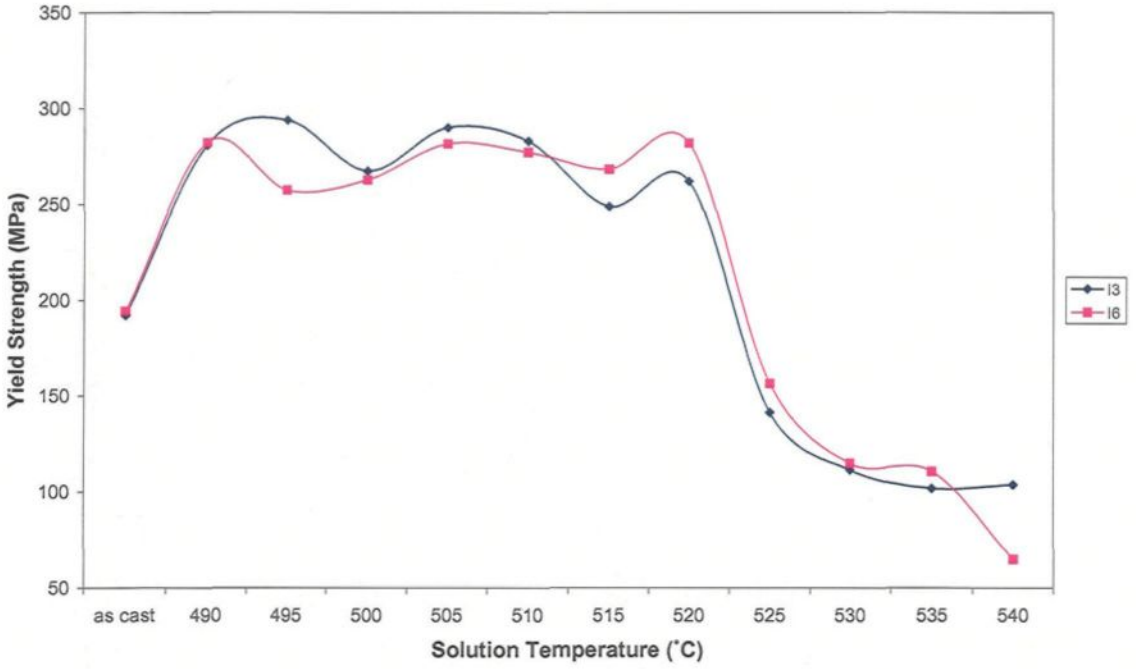


**Figure 4.22** YS of industrial 319 alloys as a function of solution heat treatment temperature.

The percentage elongations obtained from the experimental alloys and industrial alloys as a function of solution treatment temperature are shown in Figure 4.23 and Figure 4.24, respectively. The higher the Mg content of the alloy, the greater the volume fraction of intermetallics expected to precipitate and thus reduce the elongation in the as-cast condition. The ductility can be enhanced by changing the morphology of the eutectic silicon particles from their normally acicular brittle form to a more fibrous and rounded form. Solution heat treatment causes the fragmentation and spheroidization of the Si particles. Consequently, with respect to the as-cast condition, the elongation improves with solution treatment, increasing to a maximum at a solution temperature of 520°C or 525°C.

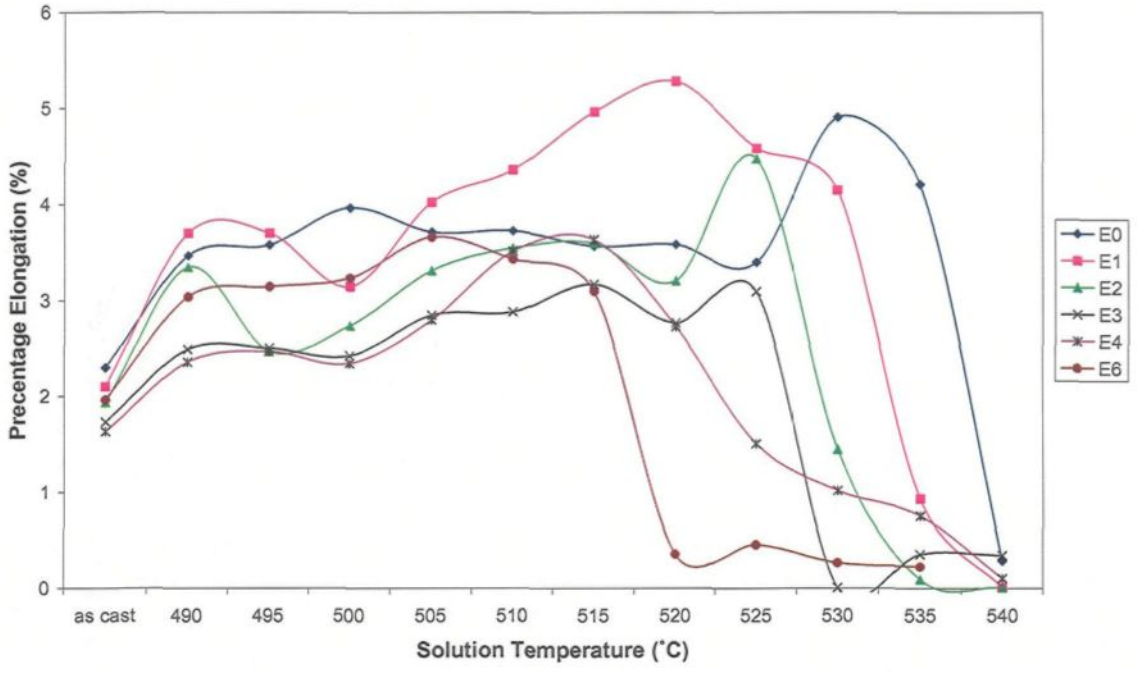


**Figure 4.23** Percentage elongation of experimental 319 alloys as a function of solution heat treatment temperature.

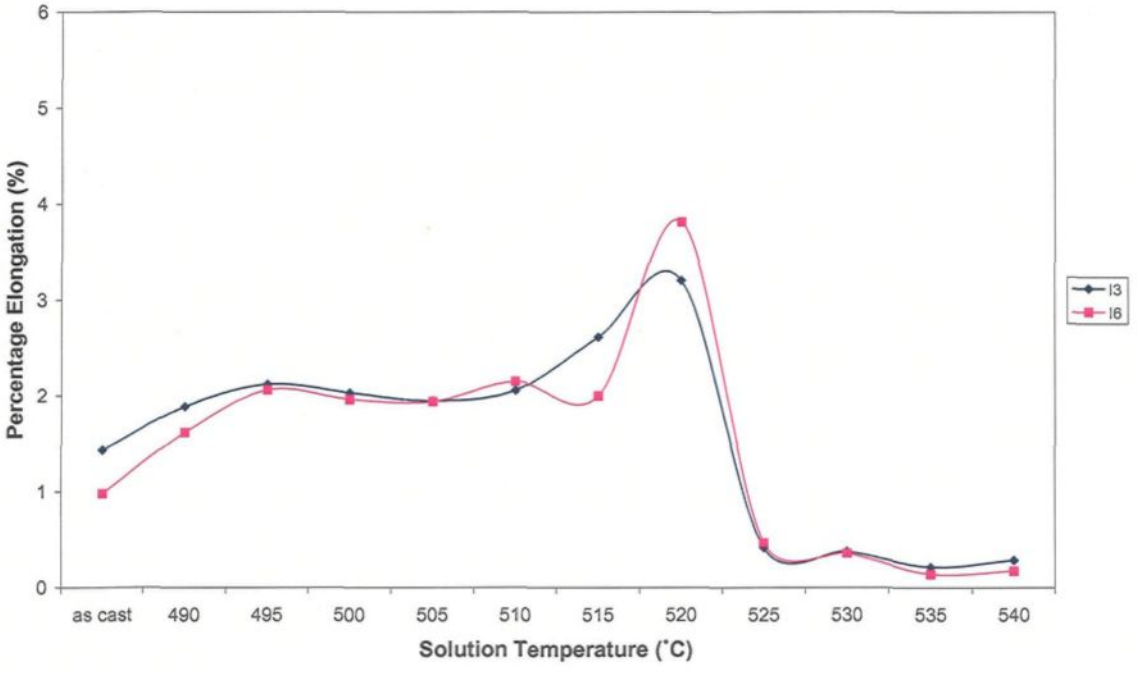


**Figure 4.24** Percentage elongation of industrial 319 alloys as a function of solution heat treatment temperature.

Higher solution temperatures result in the partial melting of the copper phase at the grain boundaries, and lower the elongation to a practically negligible value (less than 0.5%).

Based on the above results, the tensile curves could be divided into four regions across the range of solution temperatures used. This is shown schematically in Figure 4.25. Region I corresponds to the change in tensile properties of the alloy on going from the as-cast to the solution heat-treated condition. Region II represents the recommended solution treatment temperature range. Region III represents a continuation of region II until peak properties are reached, following which incipient melting begins to occur, while Region IV corresponds directly to the progress of incipient melting with the increase in solution temperature.

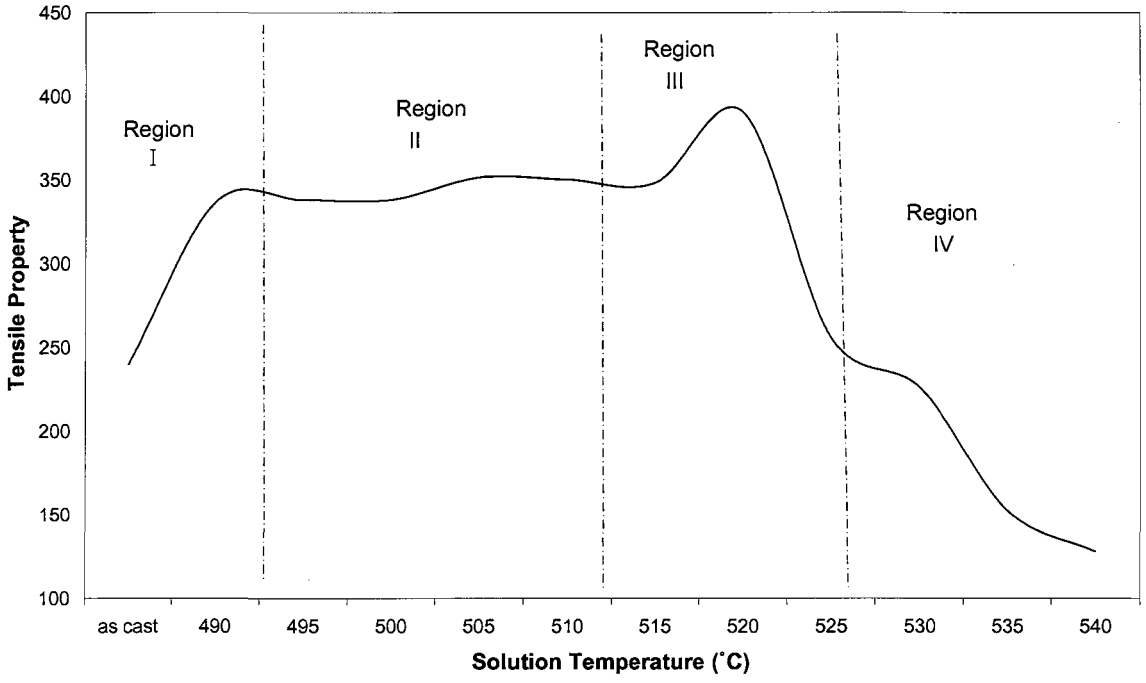


**Figure 4.25** Schematic diagram showing the progress of a tensile property curve as a function of solution treatment temperature.

Compared with the E6 alloy, the onset temperature of melting of the copper phase is about 10°C higher in I6 alloy. The main difference in the chemical compositions of these two alloys lies in the trace concentrations of Fe, Mn, Zn and Ni elements found in the commercial alloy. It is expected that the formation of intermetallic phases like $Al_6NiCu_3$, $Al_{11}(MnFeNiCu)_4Si$ and $\beta$-$Al_5FeSi$ would delay the occurrence of incipient melting in the high-Mg-containing I6 alloy.

Several reactions take place during solution heat treatment: for example, the change in the Si particle morphology and the dissolution of the precipitation-hardening constituents, $CuAl_2$ and $Mg_2Si$, which contribute to the improvement in the properties. On the other hand, a higher solution temperature results in the partial melting of the copper phase at the grain boundaries which can reduce the mechanical properties. This would explain the presence of a maximum peak in each curve of the tensile properties. Before this peak, the hardening effect is predominant. After a certain temperature, however, the detrimental effect due to the melting of the copper phase is much greater than the hardening effect, leading to a drop in the mechanical properties.

Based on the results of the tensile property measurements, a maximum solution temperature for each alloy is suggested, as shown in Table 4.5. Solution heat treating above this temperature will cause degradation of the mechanical properties.

**Table 4.5** Maximum solution temperatures suggested for the 319 alloys studied, based on the tensile test data obtained

| Alloy Code | E0 | E1 | E2 | E3 | E4 | E6 | I3 | I6 |
|---|---|---|---|---|---|---|---|---|
| Temperature (°C) | 535 | 530 | 525 | 525 | 520 | 510 | 520 | 520 |

The degradation in mechanical properties is mainly due to the melting of the $CuAl_2$ phase, since the $Al_5Mg_8Cu_2Si_6$ phase is insoluble up to temperatures as high as 530°C (to be discussed later on, in Section 4.2.5). Comparing Table 4.5 with Table 4.2, we can see that the characteristic temperatures of the copper phases recorded from the cooling curves (thermal analysis results, Table 4.2) are approximately 15°C lower than the temperatures obtained from tensile test data. This may be attributed to thermal hysteresis, which would explain why the temperatures of the onset of incipient melting estimated from the tensile property curves are higher than those measured from the cooling curves.

Similar observations were reported by Samuel *et al.*[52] In their work, they studied the dissolution and melting of the $CuAl_2$ phase in 319 alloy using differential scanning calorimetry (DSC). Figure 4.26 shows the results of a DSC run carried out on a powdered sample of their experimental 319 alloy (containing 0.003 wt% Mg and 0.15 wt% Fe), where the fusion temperature of the $CuAl_2$ phase in the heating curve is observed to be 18°C higher than that observed from the cooling curve.

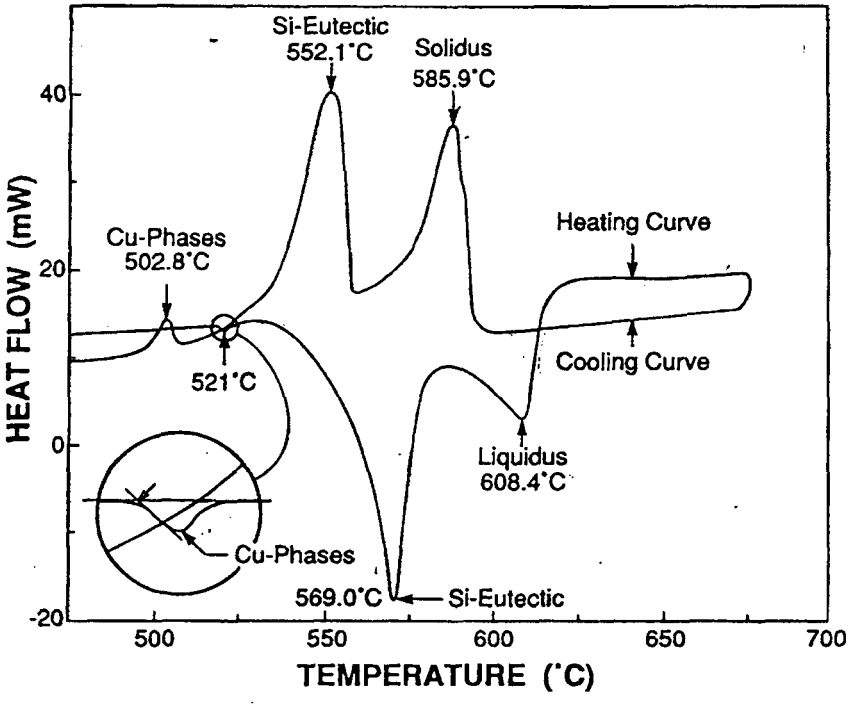


**Figure 4.26** DSC run for a powdered sample obtained from experiment 319 alloy solidified at 10°C /s. The arrow in the enlarged circled area indicates the onset of melting of the $CuAl_2$ phase.[52]

#### 4.2.4.2 Two-stage solution heat treatment

The tensile properties of alloys E0, E3, E6, I3 and I6 are presented in Figure 4.27. Compared with the single-step solution treatment at 505°C, the two-stage solution treatment (505°C/8 h followed by 530°C/2 h) increases the ultimate tensile strength by about 29 MPa in alloy E0, Figure 4.27(a), with a slight increase in yield strength and percentage elongation, probably due to maximum dissolution of the copper phase. In Figure 4.27(b), after a two-stage solution heat treatment (with 520°C as the second stage solution temperature), the E3 alloy shows 10-13% higher UTS and YS values compared to the

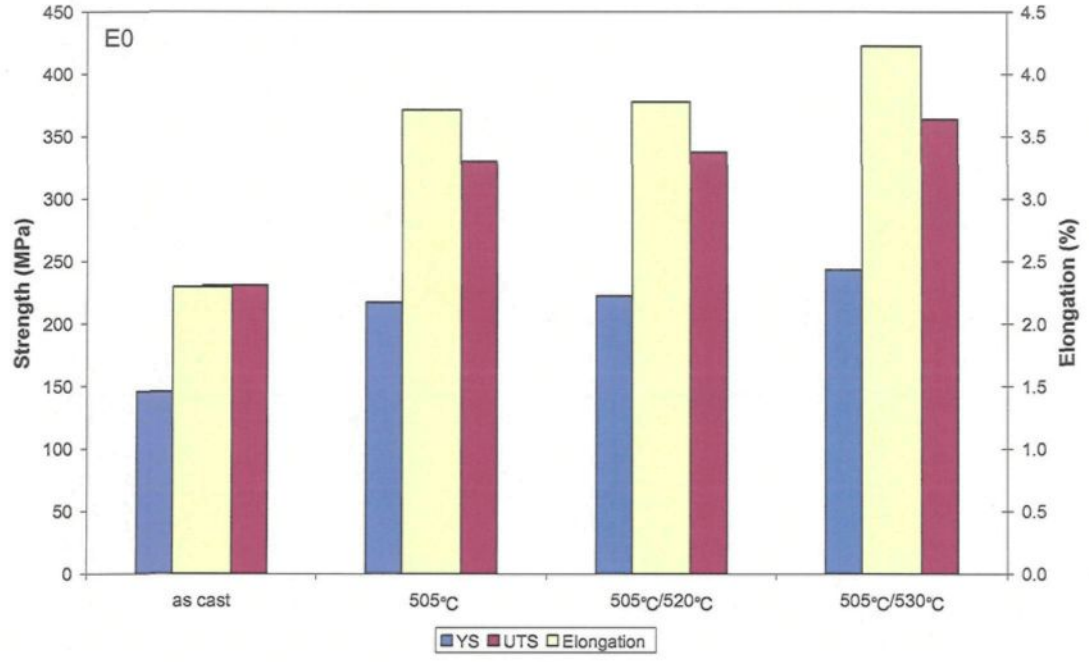


(a)

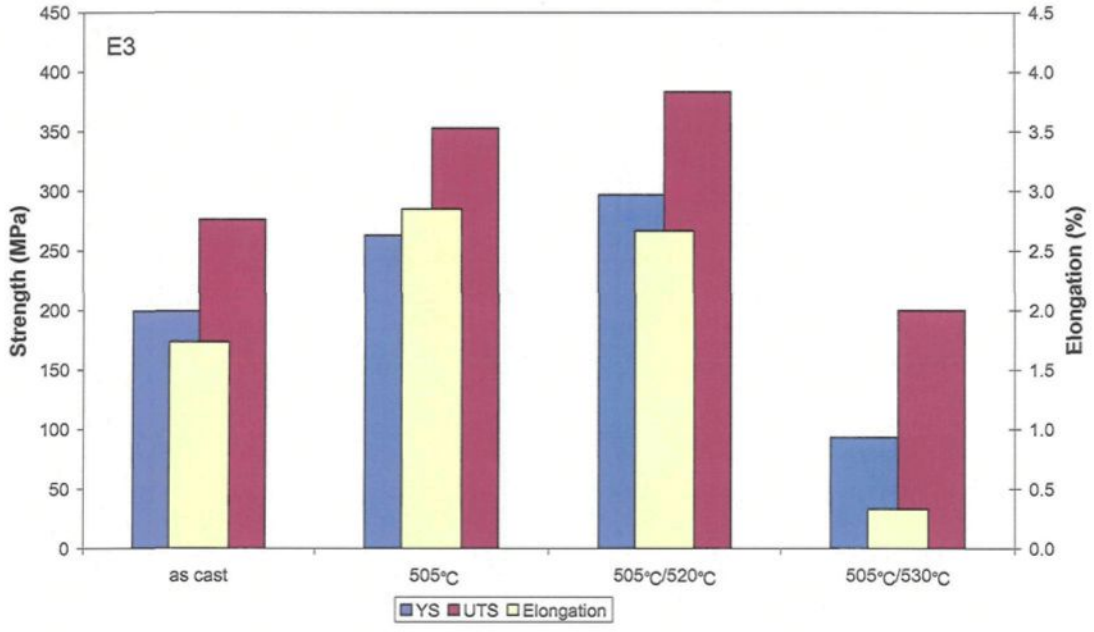


(b)

**Figure 4.27** Tensile properties of as-cast, single-stage solution heat-treated and two-stage solution heat-treated 319 alloys: (a) E0, (b) E3, (c) E6, (d) I3 and (e) I6.

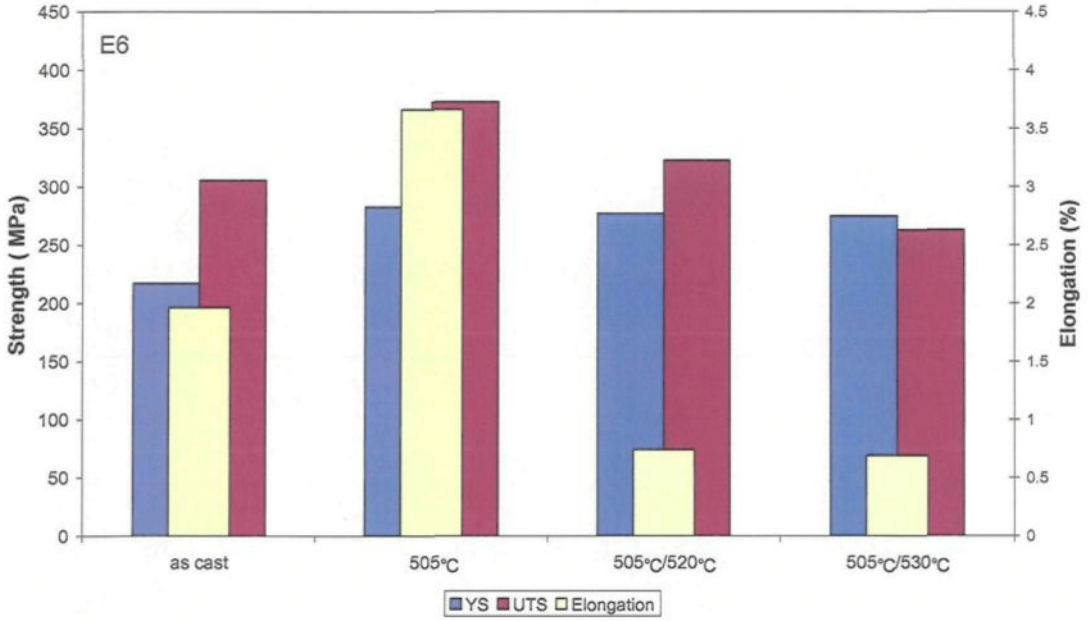


(c)

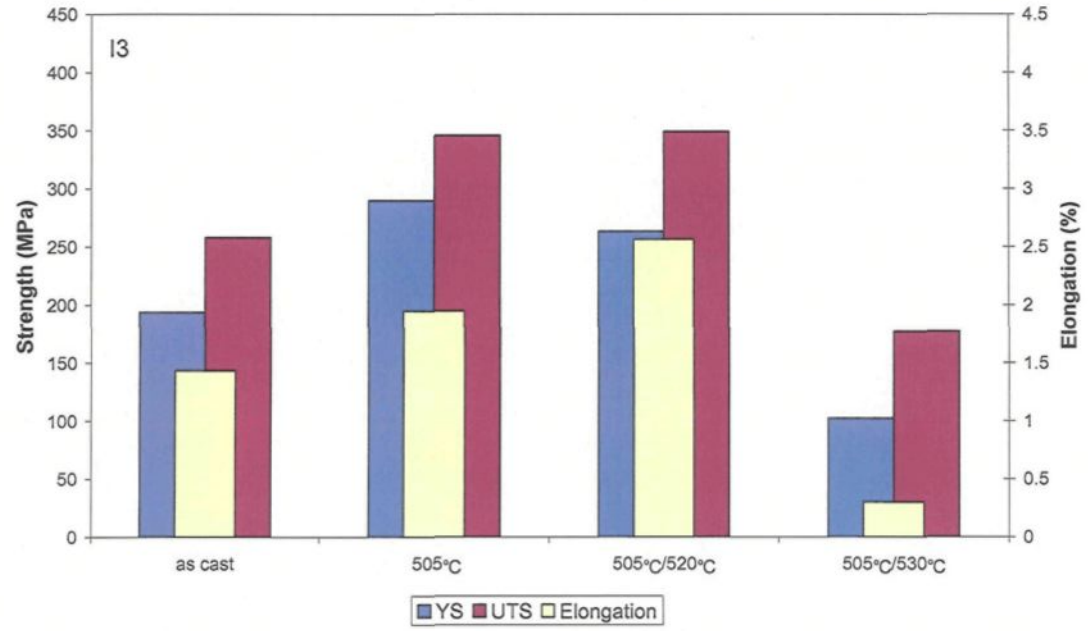


(d)

**Figure 4.27** Tensile properties of as-cast, single-stage solution heat-treated and two-stage solution heat-treated 319 alloys: (a) E0, (b) E3, (c) E6, (d) I3 and (e) I6.

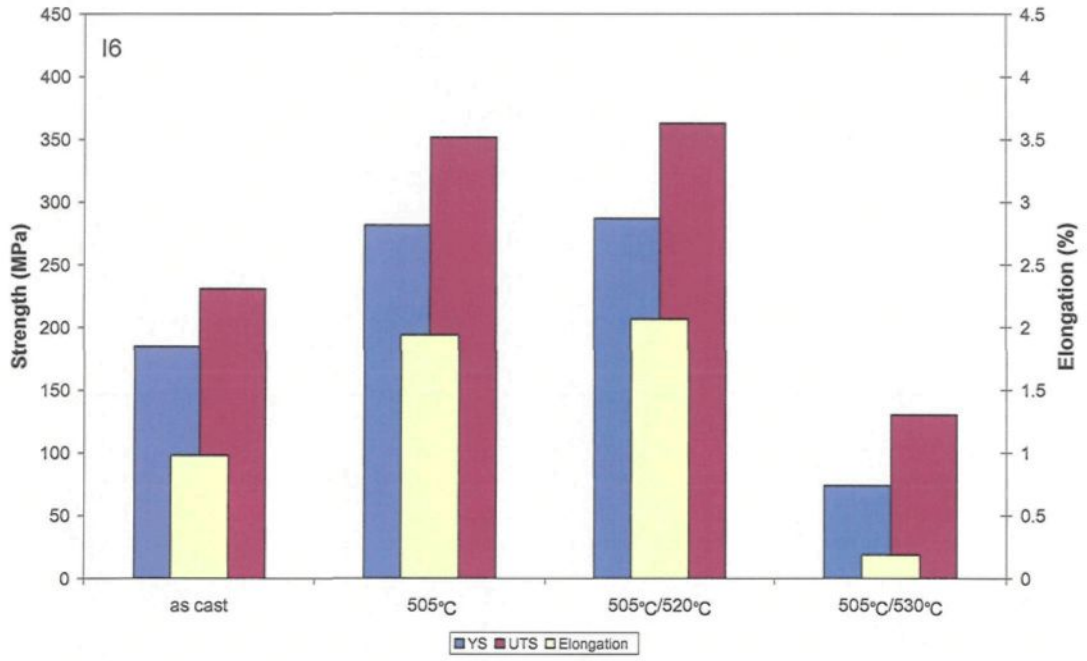


(e)

**Figure 4.27** Tensile properties of as-cast, single-stage solution heat-treated and two-stage solution heat-treated 319 alloys: (a) E0, (b) E3, (c) E6, (d) I3 and (e) I6.

single-stage solution treated sample, while the elongation decreases very slightly. This improvement in mechanical properties is mainly attributed to the improvement in homogeneity through the dissolution of the copper phase. Heating at a higher second-stage solution temperature (530°C) causes incipient melting of the copper phase, reducing the mechanical properties significantly. As Figure 4.27(c) shows, in the case of E6 alloy, the best tensile properties are achieved with the single-stage solution treatment. In comparison, the two-stage solution treatments deteriorate the mechanical properties. Increasing the second-stage solution temperature from 520°C to 530°C mostly affects the UTS, whereas the YS and percentage elongation values remain the same.

In the case of the industrial alloys, as can be seen from Figure 4.27(d) and Figure 4.27(e), the tensile properties are not significantly affected by the type of solution treatment used, *viz.*, one stage or two-stage. This is particularly so in the case of the I6 alloy, while some improvement in elongation (about 0.5%) is noted for the I3 alloy. However, on changing the second stage solution temperature from 520°C to 530°C, the properties are reduced significantly.

From an analysis of Figure 4.27, the following may be summarized:

1. Both the source (experimental *vs.* industrial) and the Mg level of the alloy determine which heat treatment will provide the best tensile properties.
2. With respect to the two-stage solution treatment, the second stage solution temperature should not exceed 520°C, particularly at Mg levels of 0.6%.
3. Choice of the heat treatment will also depend upon the strength-ductility combination required of the cast component.

### 4.2.5 Microstructural Analysis

Samples for microstructural analysis were sectioned from the tensile-tested bars corresponding to the various solution treatment conditions. Figure 4.28 shows the microstructures of as-cast E6 alloy and alloys E0, E3, E6, I3 and I6 after solution heat treatment at 505°C, while those corresponding to the alloys submitted to 530°C solution treatment are given in Figure 4.29.

Figure 4.28(a) shows the morphology of the Si particles in the as-cast E0 alloy, while Figure 4.28(b) through (f) shows the spheroidization of the Si particles, resulting

from the solution heat treatment. Fragmentation and necking of the Si particles were also observed (see Figure 4.28(c) and (f)). Due to the change in the Si particle morphology, the alloy properties are improved. Whereas the coarse acicular silicon platelets act as internal stress raisers in the microstructure and provide easy paths for fracture, the modified Si fibers are able to bend and curve easily during solidification, giving the alloy somewhat higher values of ultimate tensile strength and greatly increased values of ductility.[53,54]

Compared with the eutectic $CuAl_2$ phase observed in Figure 4.28(a), together with very fine Si particles (dark points) interspersed within, dissolution of the copper phase was evidenced by the fine (darker) Si particles remaining behind in the aluminium matrix (see rectangular areas in (b)). These observations are in keeping with those of Samuel *et al.*[52] Although the precipitation temperature of the $Al_5Mg_8Cu_2Si_6$ phase is less than that of the $CuAl_2$ phase (see Table 4.1), it can still be observed after solution heat treatment at 505 °C (see Figure 4.28(d) and (e)), its insolubility probably being due to its large number of atoms. Some researchers have reported that $Al_5Mg_8Cu_2Si_6$ phase is insoluble as high as 530°C in Al-Si-Cu-Mg alloys with relatively low silicon contents. [55]

Generally speaking, 505°C is a safe temperature, as no evidence of the occurrence of incipient melting was found in all the alloys investigated. Solution treatment at 530°C, however, caused melting of the copper phase, irrespective of the alloy source (experimental or industrial) or its Mg content (see Figure 4.29). Figure 4.29(a) shows an example of the melted form of the copper phase upon quenching. The unmelted part of the $CuAl_2$ phase can be seen wedged between the melted regions on either side. It should be pointed out that

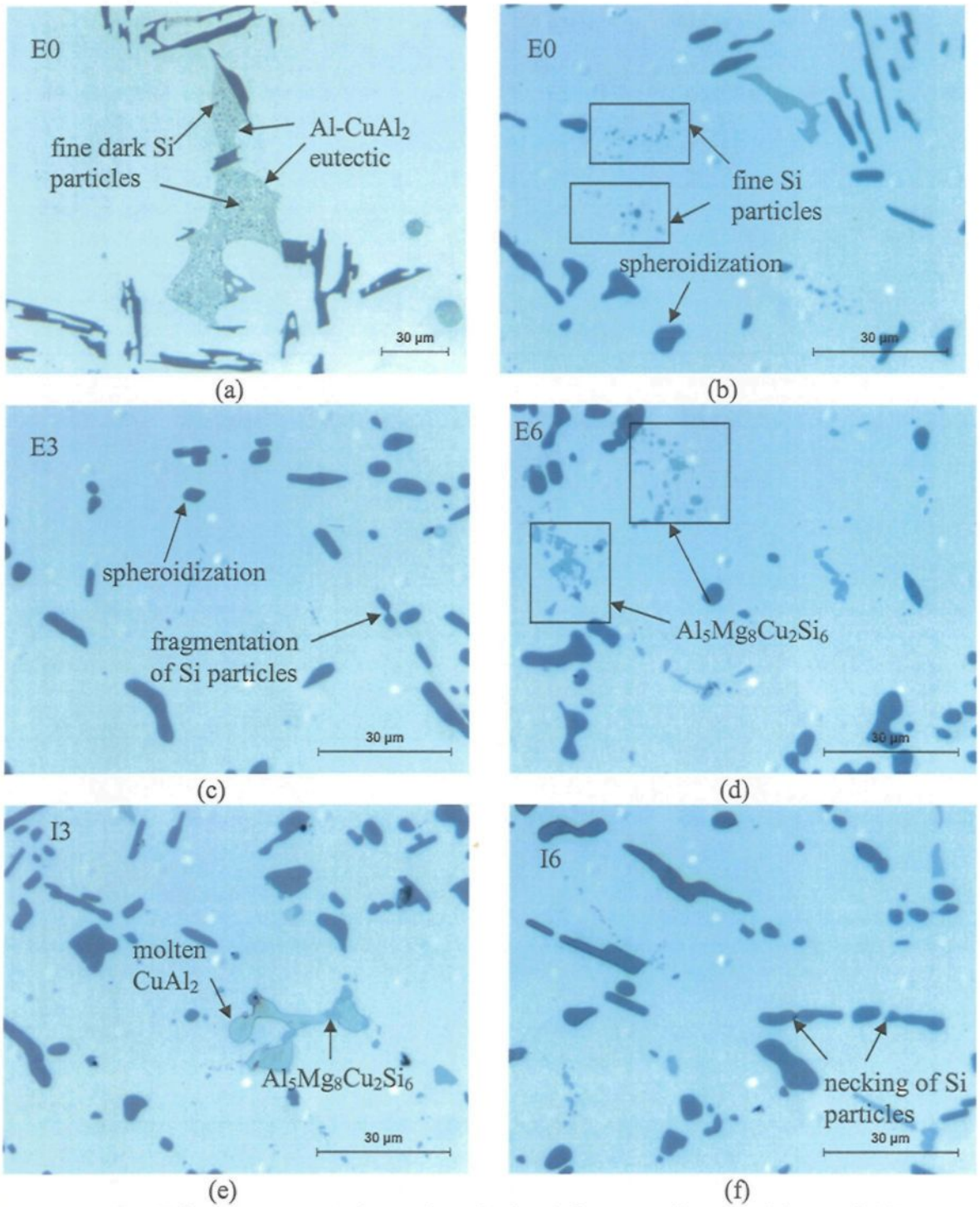


**Figure 4.28** Microstructures of samples obtained from tensile-tested bars of (a) as-cast E0 and (b) E0, (c) E3, (d) E6, (e) I3, (f) I6 alloys submitted to solution heat treatment at 505°C.

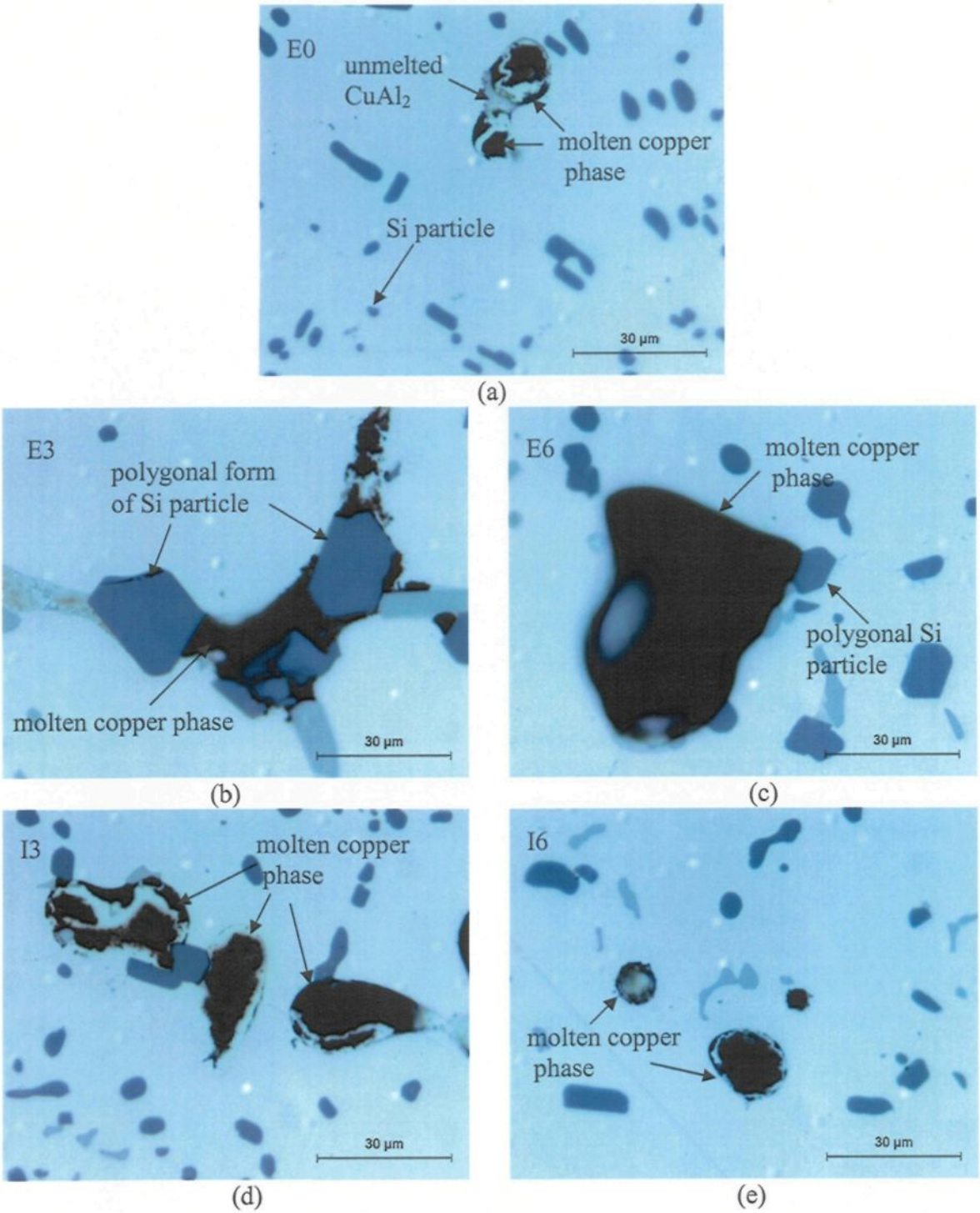


**Figure 4.29** Microstructures of samples obtained from tensile-tested bars of (a) E0, (b) E3, (c) E6, (d) I3 and (e) I6 alloys submitted to solution heat treatment at 530°C.

the tensile properties still remain high at this temperature, indicating that the melting of the copper phase has already occurred before the tensile properties reach their maximum value. This could be interpreted in terms of the competition between the dissolution of copper in the matrix (causing precipitation hardening upon aging) and the melting of the $CuAl_2$ phase. It is interesting to note the presence of polygonal Si particles in Figure 4.29(b) in the vicinity of the molten copper phase (at 530°C), different from the spheroidized form of the Si particles observed elsewhere in the matrix after solution heat treatment.

Figure 4.30 and Figure 4.31 show the microstructures of alloys E0, E3, E6, I3 and I6 after solution heat treatment at 505°C followed by second stage solution treatment at 520°C or 530°C. From Figure 4.30, we can see that in the alloys containing less than 0.3 wt% Mg, the microstructure remains sound after solution heat treatment at 505°C/520°C, while higher Mg additions lower the melting point of the copper phase which causes incipient melting. Increasing the second stage solution temperature to 530°C causes copper melting even in the low-Mg-containing alloys (see Figure 4.31(b) and (d)). These observations are in keeping with the results on the tensile properties.

Comparing the optical micrographs obtained from the experimental and industrial alloys for the same Mg addition and after two-stage solution heat treatment, it can be seen that the melted area in the industrial alloy sample is less than that observed in the experimental alloy (see, for example, Figure 4.31(b) and (d)). This was also confirmed by the porosity measurements. It is expected that the reaction between Cu and trace elements such as Fe and Ni present in the industrial alloy would lead to an increase in the incipient melting temperature of the copper phase in the industrial alloy.

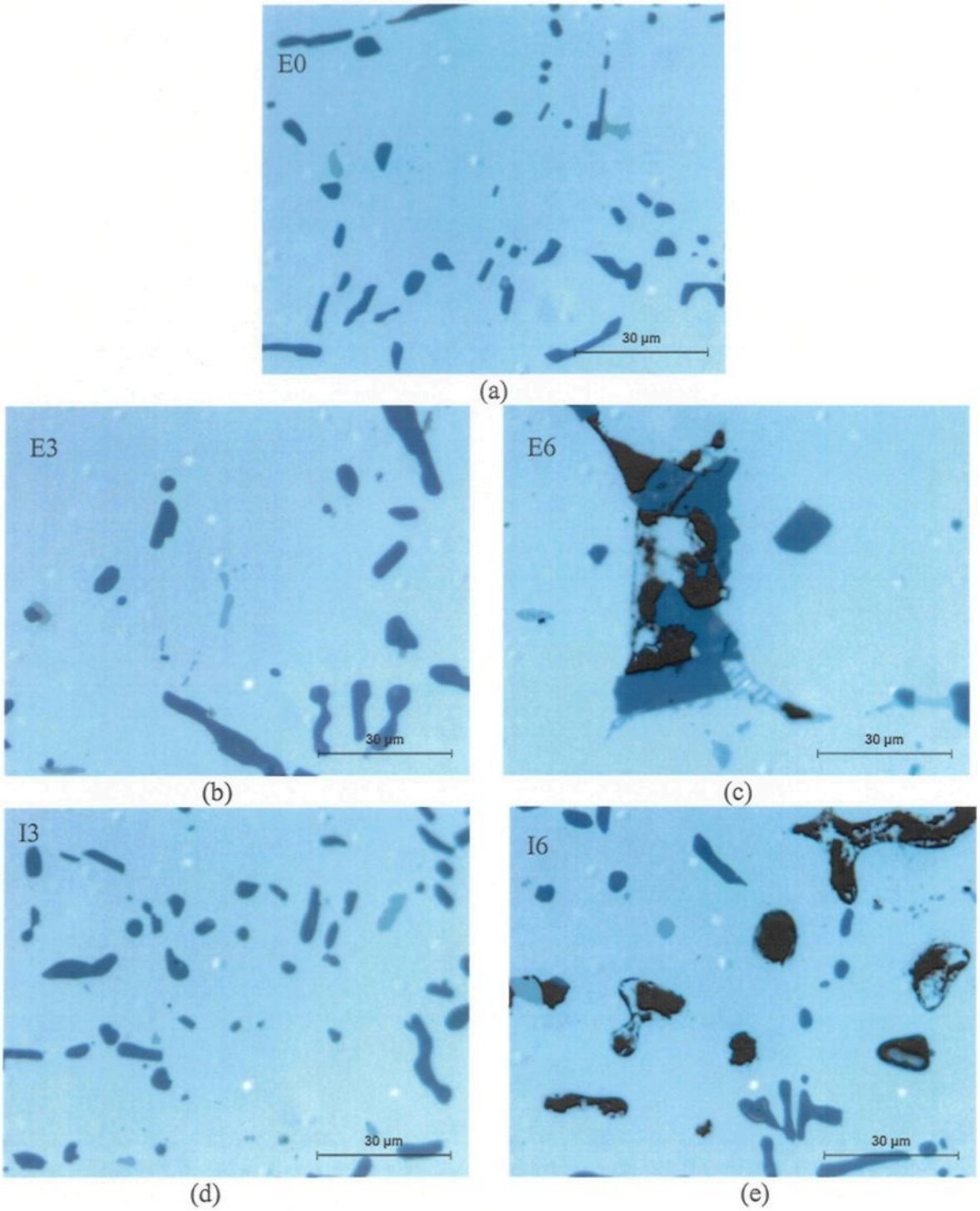


**Figure 4.30** Microstructures of samples obtained from tensile-tested bars of (a) E0, (b) E3, (c) E6, (d) I3 and (e) I6 alloys submitted to the 505°C/520°C two-stage solution heat treatment.

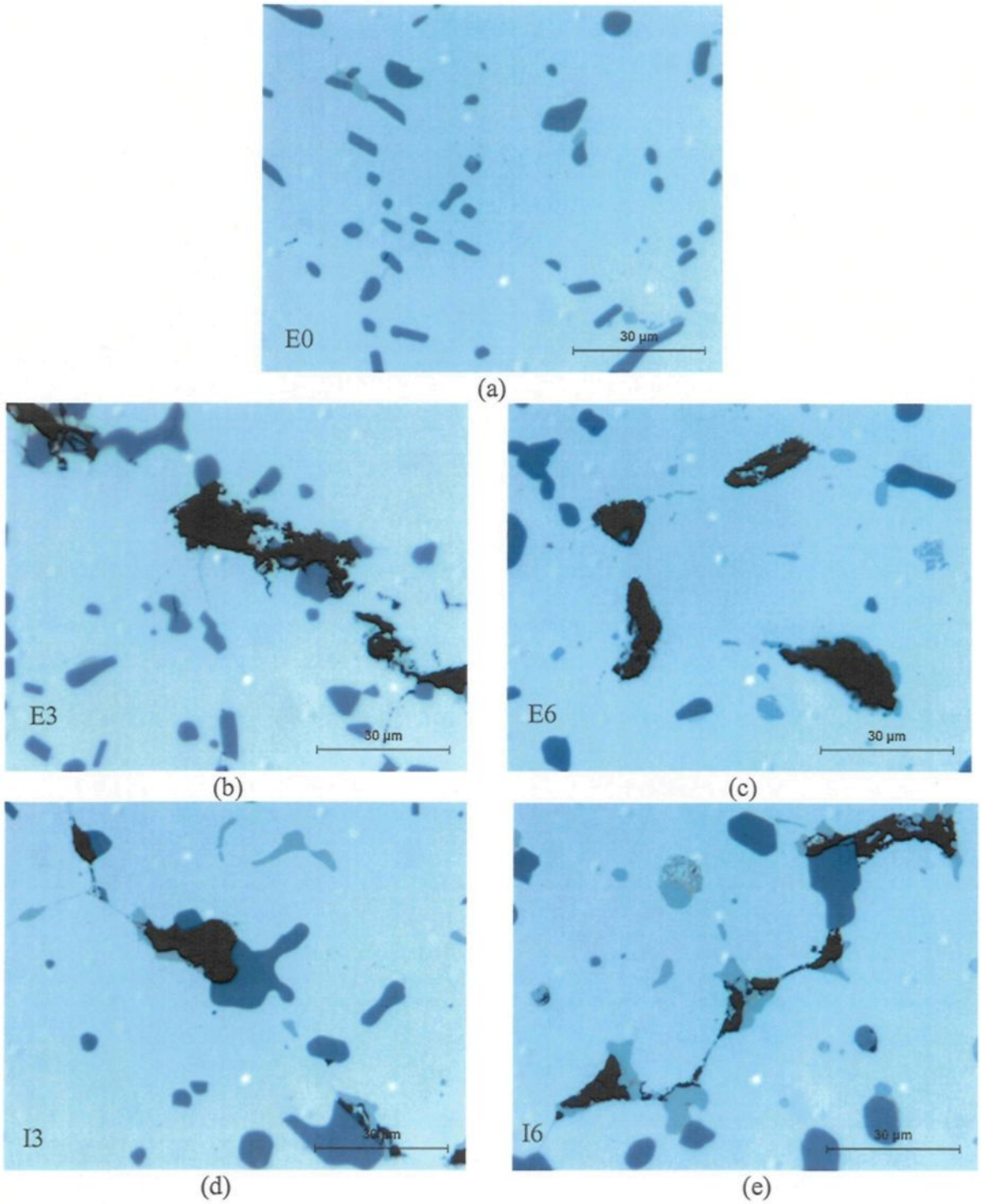


**Figure 4.31** Microstructures of samples obtained from tensile-tested bars of (a) E0, (b) E3, (c) E6, (d) I3 and (e) I6 alloys submitted to the 505°C/530°C two-stage solution heat treatment.

# CHAPTER 5

# DEFECTS RELATED TO INCIPIENT MELTING

# CHAPTER 5

# DEFECTS RELATED TO INCIPIENT MELTING

## 5.1 INTRODUCTION

The occurrence of incipient melting in 319 type alloys has posed serious problems to castings producers of engine blocks and cylinder heads. It is important to guard against its occurrence by careful selection of the alloy composition and heat treatment parameters to maintain casting quality and performance.

In this chapter, some of the defects resulting from the occurrence of incipient melting in the experimental and industrial 319 alloys studied will be elaborated upon, in particular those related to the dimensional changes, macrocracking and porosity formation.

## 5.2 DIMENSIONAL CHANGES

In the production of 319 aluminum alloy castings, one of the important factors to consider is the dimensional stability of the cast part. This is particularly crucial in the case of critical components. Dimensional changes in heat-treated aluminum alloys are of a metallurgical nature, which arise from the introduction and relaxation of stresses, recrystallization, and solution or precipitation of alloying elements. Apart from the reversible, simple temperature and thermal expansion coefficient-related dimensional

changes that take place, expansions and contractions of a more permanent type can occur during heat treatment.[56]

The substitutional solid solution-forming elements that are major alloying components of heat-treatable aluminum alloys (including 319 alloys) exhibit limited temperature-dependent solubility in the solid state. Their atomic sizes relative to that of the solvent aluminum atoms and valence factors determine their effect on the atomic lattice in the solid solution. Due to the fact that certain elements expand the lattice and others contract it, these effects can vary considerably with the composition of the commercial alloy being used.[8] Among the elements most commonly present in aluminum alloys, only Mg in solid solution expands the lattice. Most elements decrease the lattice spacing in solid solution. This causes contractions during dissolution, whereas precipitation causes the opposite effect.

Ouellet *et al.*[57] have reported the effect of Mg content on the dimensional stability and tensile properties of heat-treated Al-Si-Cu (319) type alloys. Their study showed that the addition of 0.45 wt% led to almost 1.5% increase in the sample length. Modification of high Mg-containing alloys with Sr resulted in an additional increase in the alloy dimensions, producing an overall expansion of ~2.15%.

In heat treating at high temperatures, changes can result from plastic deformation (creep) induced by gravitational forces. In Figure 5.1, an as-cast E6 alloy bar (marked B) is compared with those obtained from the 540°C solution heat-treated E6 alloy (experimental alloy with 0.6 wt% Mg). As can be seen, serious deformation occurs in these high-Mg


**Figure 5.1** Comparison between an as-cast bar (marked B) and 540°C solution heat-treated bars of E6 alloy (containing 0.6 wt% Mg).

containing alloy bars after heat treatment at such high temperature. Due to the effect of gravity, the bars exhibit buckling in the gage section.

These results emphasize the fact that selection of the correct solution treatment temperature is extremely important to maintain all the quality aspects of 319 alloy castings including their dimensional stability. As the present study shows, this temperature should obviously be kept much below 540°C, in fact, around or below 530°C as the tensile property results presented in Chapter 4 reveal.

## 5.3 MACROCRACKING

Figure 5.2 shows the presence of the macrocracks observed in bars of E1 alloy (experimental alloy with 0.1 wt% Mg) after solution heat treatment at 540°C. This may due to the severity of the incipient melting. Quenching may also cause localized plastic deformation due to the transient temperature differences within the bar, establishing a system of residual stresses simultaneously.

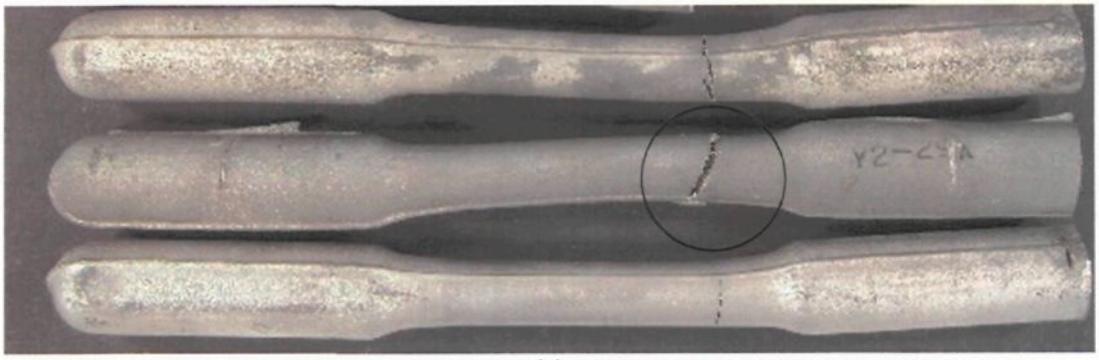

(a)

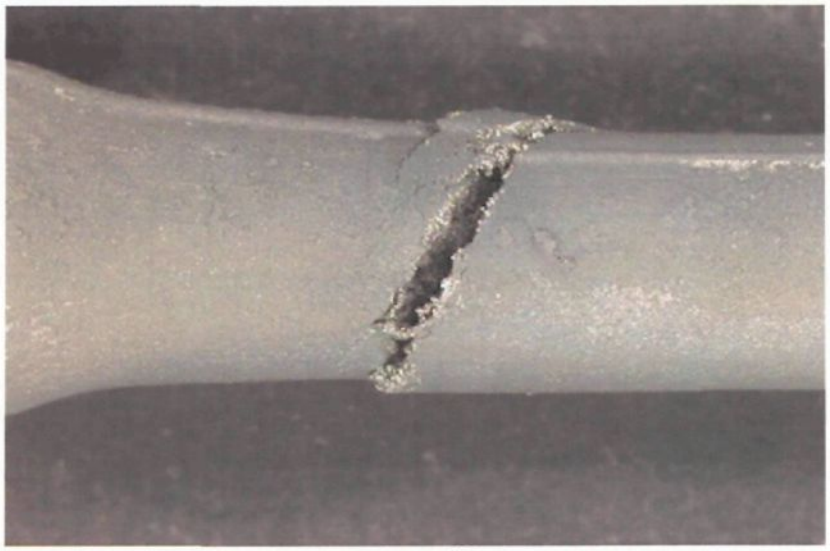

(b)

**Figure 5.2** (a) Macrocracking observed in E1 alloy after solution heat treatment at 540°C, and (b) an enlarged view of the circled area in (a).

## 5.4 POROSITY

Porosity is one of the defects normally present in Al-Si cast alloys. Extensive studies have been conducted to understand the origins and characteristics of porosity formation since the early 1950s.[58] Today, it is well understood that porosity in castings is caused by the combination effects of shrinkage and dissolved gas. With the use of mechanical degassing, it is possible to minimize the gas porosity content, while a well-designed gating/riser system can help to reduce the shrinkage porosity in the casting.

The presence of porosity in a casting deteriorates its mechanical properties, namely, the ductility, fracture toughness, and fatigue life, as well as the surface finish of the casting.[59]

Roy *et al.*[60, 61] reported that the addition of Mg to 319 alloy reduces the percentage porosity without a noticeable change in pore size and shape. They also observed that in materials containing a very low level of hydrogen, shrinkage pores are seen to nucleate at the interface of the blocky $CuAl_2$ particles. According to Edwards *et al.*,[62] the effect of magnesium on microporosity formation in Al-Si-Cu casting alloys is not consistent. However, in most of the alloys, Mg appears to decrease the porosity by amounts ranging from ~0.01% to 0.3%.

A main consequence of incipient melting in Al-Si-Cu alloys is the formation of a structureless form of the $CuAl_2$ phase and related porosity on quenching. In the present study, the only variable factor is the temperature. Hence, any changes in the porosity characteristics could be reasonably assumed to be mainly due to the melting of the copper phase resulting from the changes in the temperature variable. Porosity measurements were

therefore carried out to monitor the incipient melting that resulted in the alloys studied, corresponding to the various solution heat treatments.

The porosity characteristics were analyzed and quantified using a Leco 2001 image analyzer in conjunction with an optical microscope (Olympus BHU-2). The porosity parameters measured were: average area percent porosity (percentage porosity over a constant sample surface area), average pore area and average pore length. The details of the porosity measurements are given in Chapter 3, Section 3.5.

### 5.4.1 Single stage solution heat treatment

The average pore area values obtained for the experimental and industrial alloys as a function of solution treatment temperature are shown in Figure 5.3 and Figure 5.4, respectively. In general, with the increase in the solution temperature, an overall increase in the average pore area is observed, irrespective of the alloy type/source. Apart from the E6 alloy, the average pore area of all alloys does not change much until the temperature reaches 520°C. These observations match the results from tensile testing (see Table 4.5). The addition of Mg leads to a significant increase in the volume fraction of the $CuAl_2$ phase, with a clear tendency to segregation in localized areas, resulting in the formation of the block-like, rather than the fine eutectic-like, $CuAl_2$ phase. Compared with the latter, the block-like $CuAl_2$ phase is more difficult to dissolve during solution heat treatment. This may explain why the average pore size increases with the increase in Mg content.

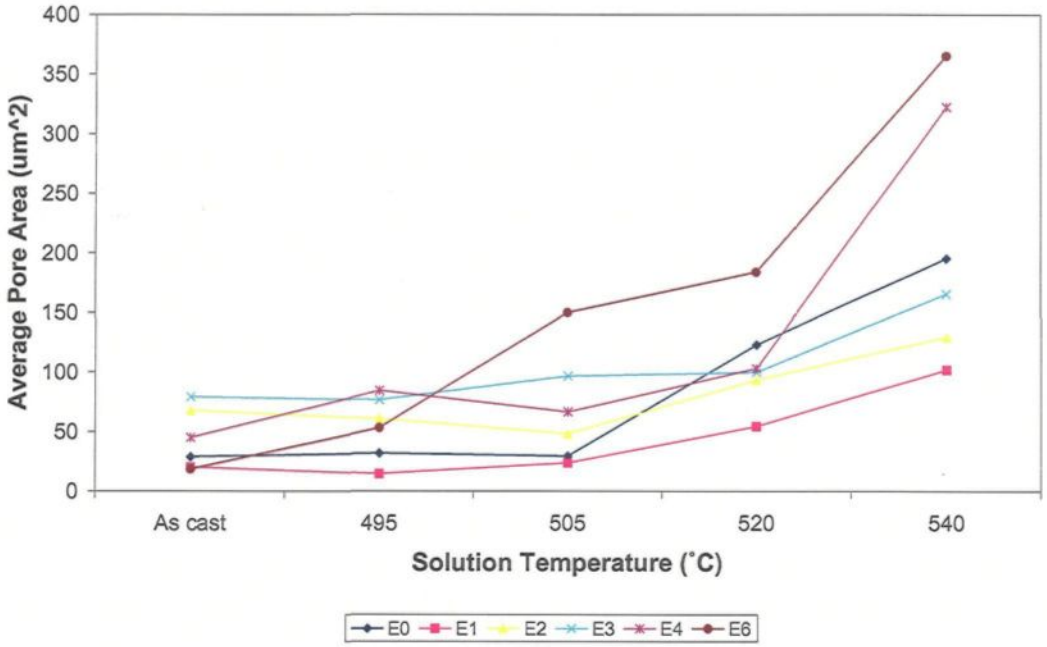


**Figure 5.3** Average pore area of experimental 319 alloys as a function of solution heat treatment temperature.

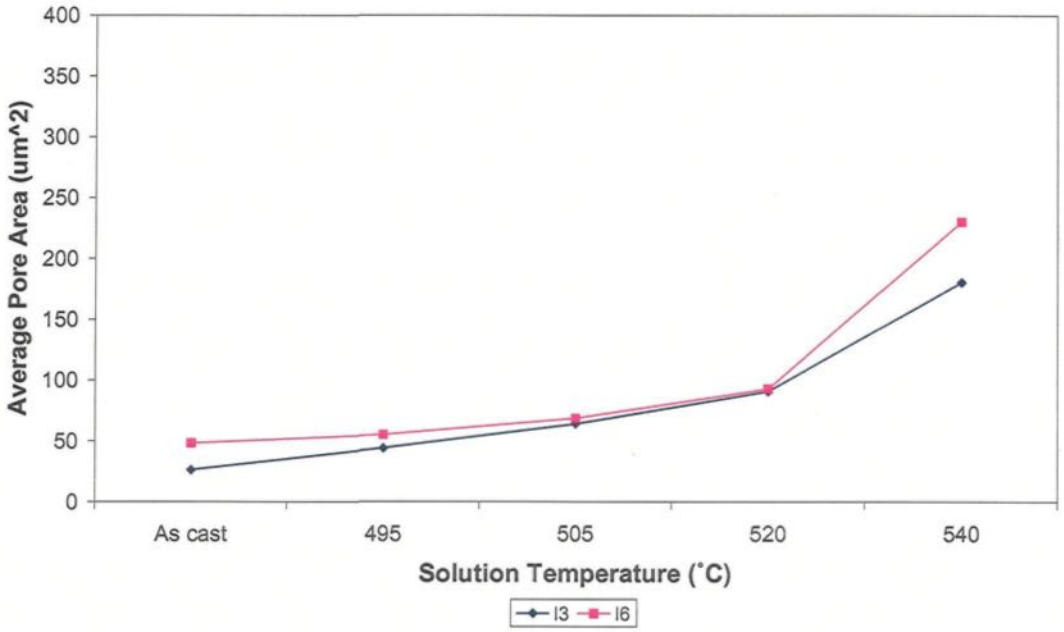


**Figure 5.4** Average pore area of industrial 319 alloys as a function of solution heat treatment temperature.

Figure 5.5 and Figure 5.6 show the plots of the average pore length as a function of solution temperature. The fact that the average pore length increases with increasing solution temperature may be considered as an indication that the incipient melting takes place at the grain boundaries.

The percentage porosity obtained from the experimental alloys and industrial alloys as a function of solution treatment temperature are shown in Figure 5.7 and Figure 5.8, respectively. Similar to the plots of average pore area, only alloy E6 shows evidence of incipient melting at 505°C, while the percentage porosity values of all other alloys remain stable, even up to 520°C temperature. It is interesting to note the sharp increase in percentage porosity of the E6 alloy after solution treatment at 540°C. This gives a clear indication of the severity of the incipient melting that has occurred in the alloy at this temperature. In comparison, the increase in porosity for the I6 alloy is relatively less, indicating a lower degree of incipient melting in this case.

In general, the results of porosity measurement match those of tensile testing. Compared with E6 alloy, the I6 alloy shows better resistance to the melting of the copper phase, as inferred from the corresponding porosity parameter plots.

### 5.4.2 Two-stage solution heat treatment

The porosity parameters obtained for the E0, E3, E6, I3 and I6 alloys are presented in Figure 5.9. Compared with the single-step solution treatment at 505°C, the two-stage solution treatment (505°C/8 h followed by 520°C/2 h) is found to decrease all three parameters, attributed mainly to the improvement in homogeneity with the dissolution

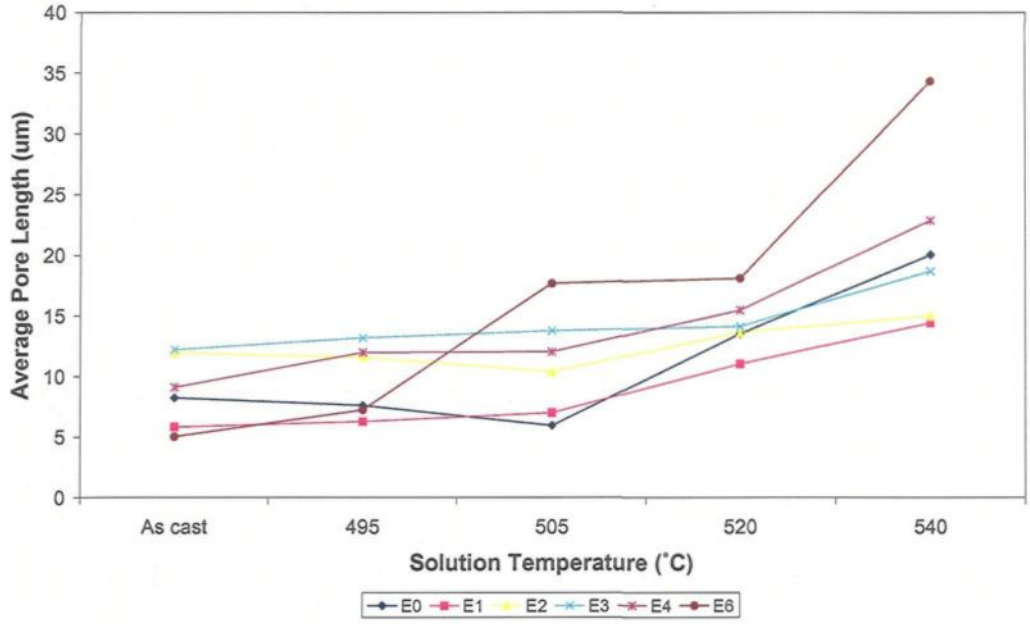


**Figure 5.5** Average pore length of experimental 319 alloys as a function of solution heat treatment temperature.

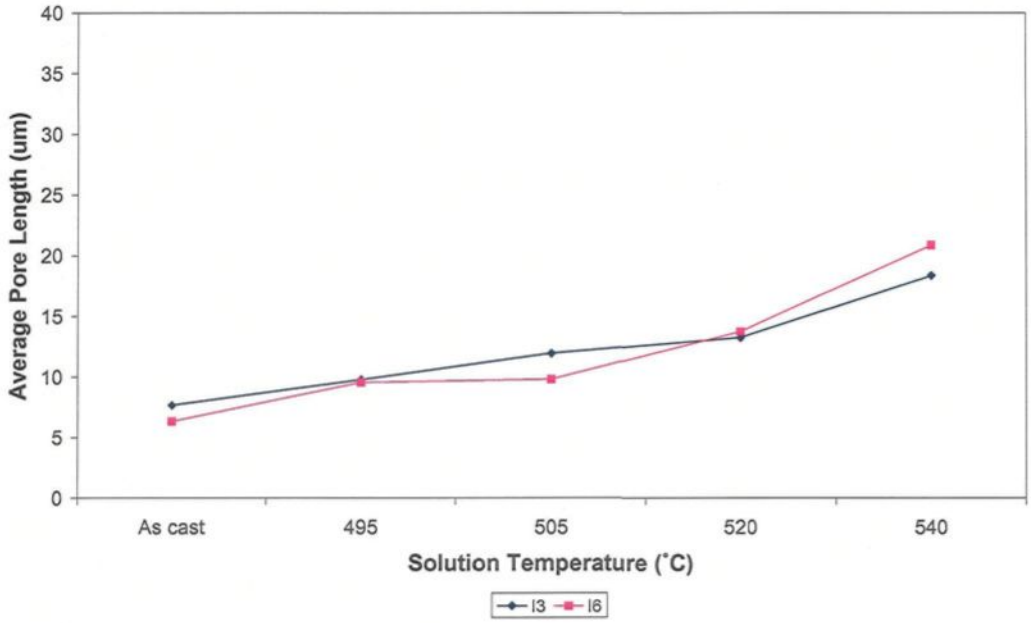


**Figure 5.6** Average pore length of industrial 319 alloys as a function of solution heat treatment temperature.

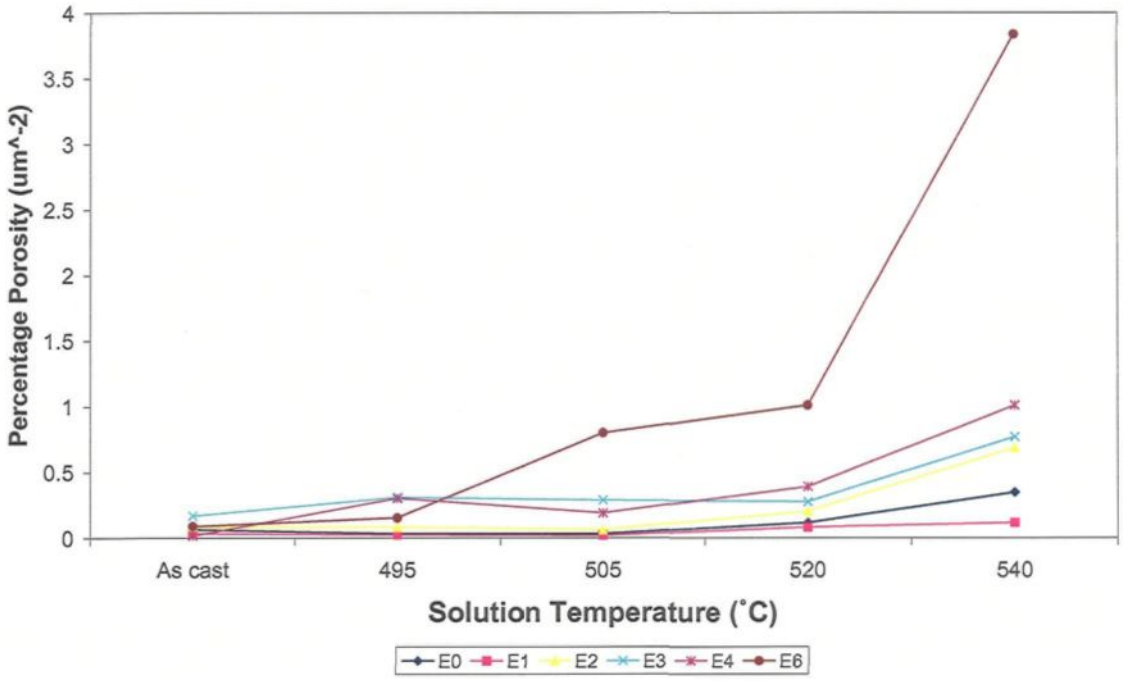


**Figure 5.7** Percentage porosity of experimental 319 alloys as a function of solution heat treatment temperature.

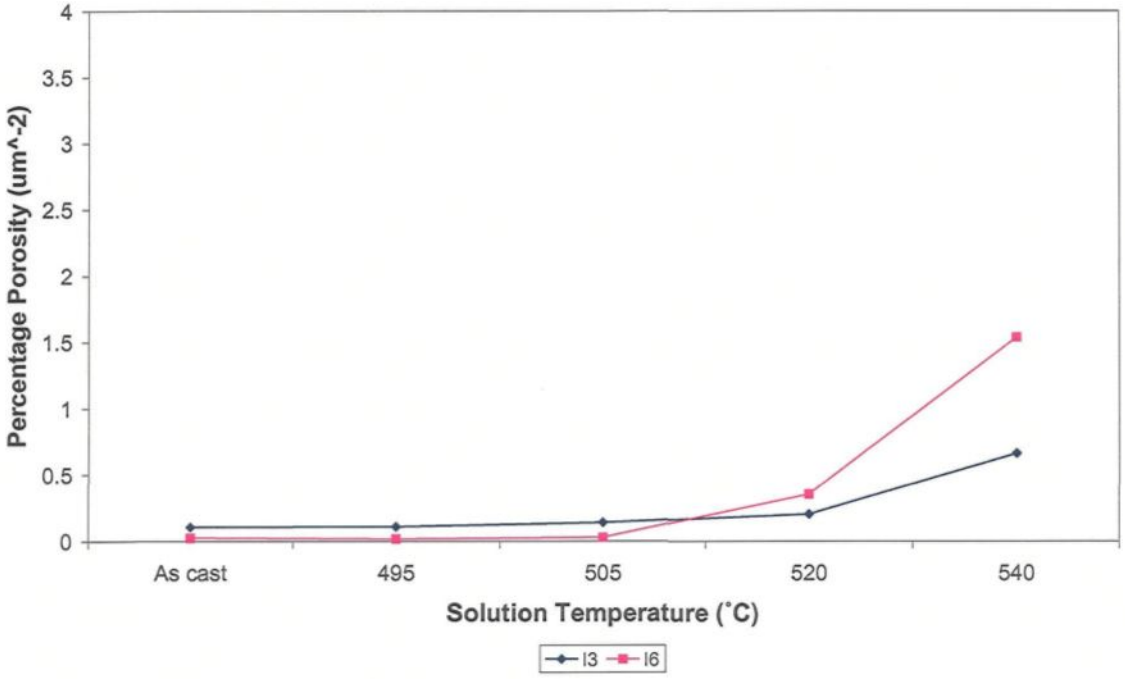


**Figure 5.8** Percentage porosity of industrial 319 alloys as a function of solution heat treatment temperature.

of the copper phase. Heating at a higher second-stage solution temperature (530°C) causes incipient melting of the copper phase, resulting in an increase in the porosity parameter values. It can also be seen that the two-stage solution treatment (505°C/8 h followed by 530°C/2 h) does not affect the porosity characteristics of E0 alloy, which matches the tensile property results. Comparing the porosity parameters of the experimental and industrial alloys containing the same Mg levels, it can be observed that the industrial alloy gives better results than the experimental alloy. This further supports the proposition that the reaction between Cu and trace elements such as Fe and Ni present in the industrial alloy would lead to an increase in the incipient melting temperature of the copper phase in the

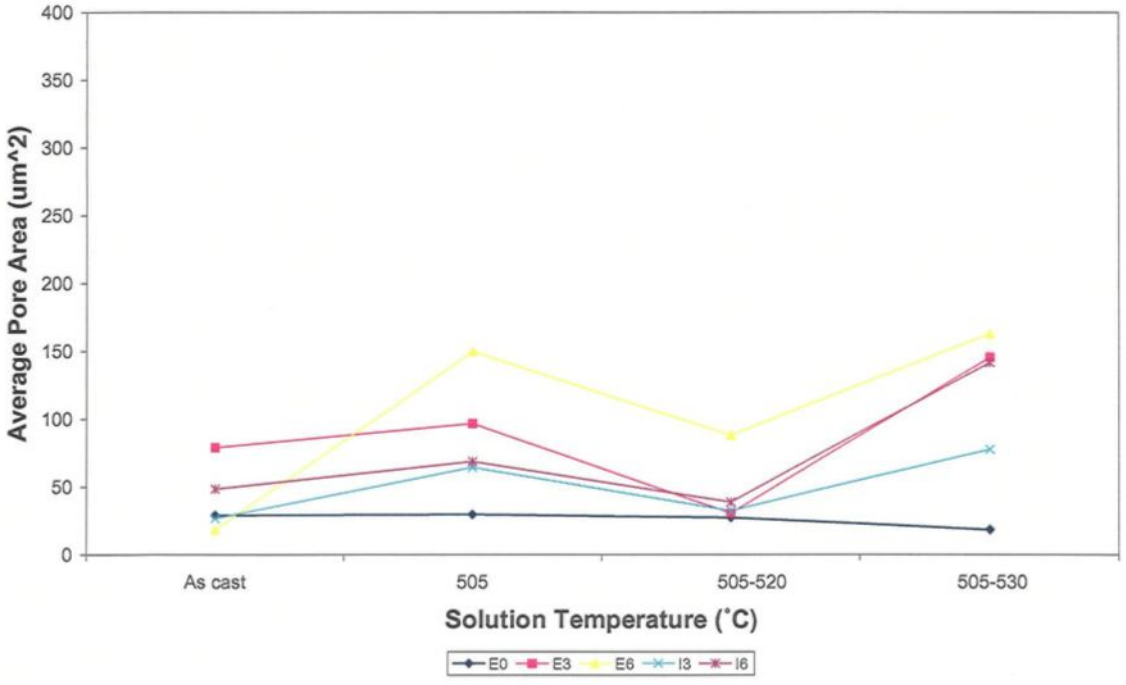


(a)

**Figure 5.9** Porosity parameters obtained from as-cast, single-stage solution heat treated and two-stage solution teat-treated alloys E0, E3, E6, I3 and I6: (a) average pore area, (b) average pore length, and (c) percentage porosity.

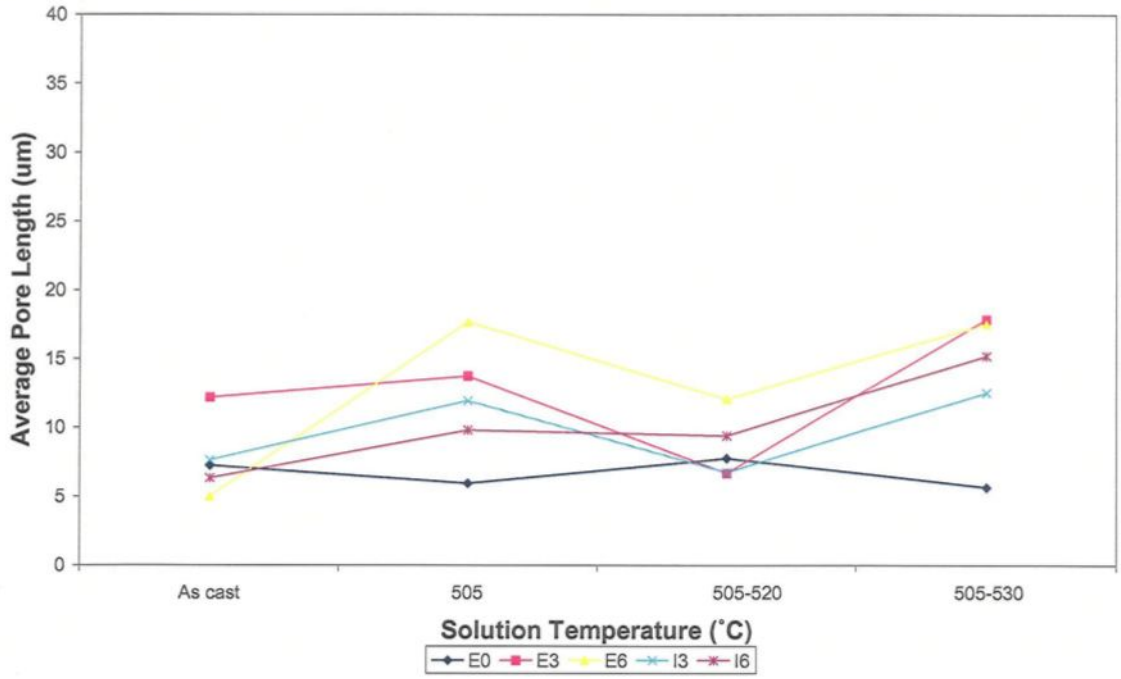


(b)

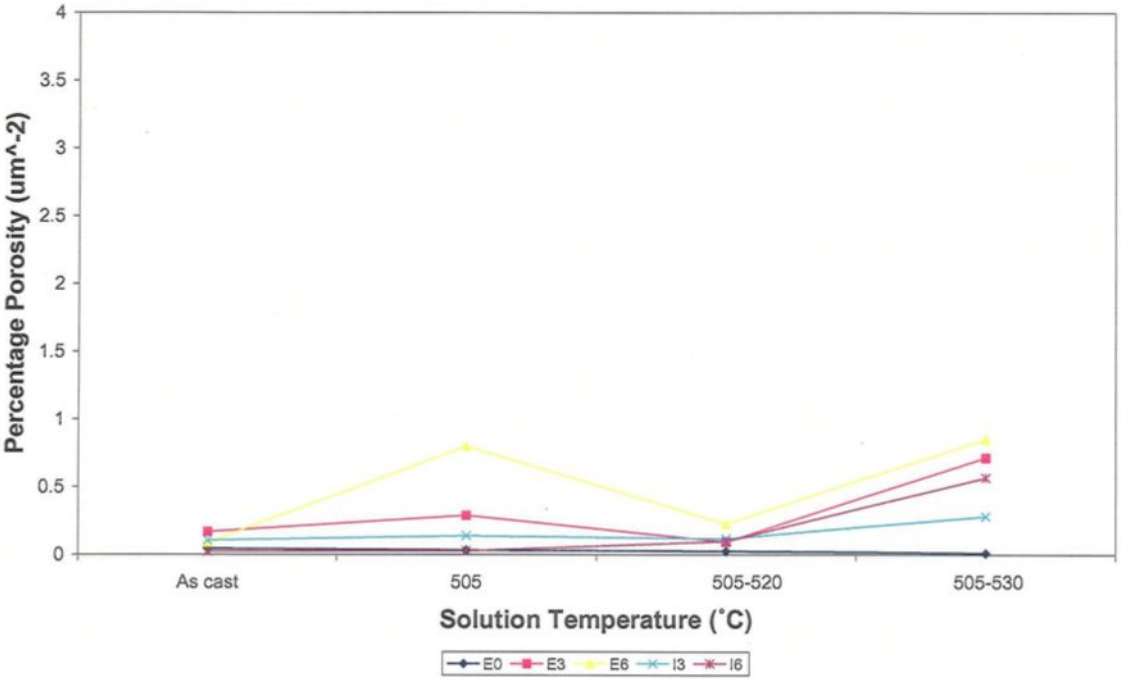


(c)

**Figure 5.9** Porosity parameters obtained from as-cast, single-stage solution heat treated and two-stage solution teat-treated alloys E0, E3, E6, I3 and I6: (a) average pore area, (b) average pore length, and (c) percentage porosity.

industrial alloy, and thereby lower the occurrence of incipient melting at the solution temperatures studied.

### 5.4.3 Microstructural Analysis

Figure 5.10 shows the microstructures of the various alloys submitted to solution heat treatment at 505°C or 530°C. Among all the alloys investigated, only E0 alloy remains sound after solution heat treatment at 530°C, which matches the results obtained from the tensile properties. It is also obvious, from a comparison of Figure 5.10(c), (d) and Figure 5.10(e), (f), that the industrial alloys show a better resistance to the melting of the copper phase.

Figure 5.11 shows the microstructures of alloys E0, E3, E6, I3 and I6 after two-stage solution heat treatments at 505°C/520°C and 505°C/530°C. As before, the E0 alloy remains sound under both solution heat treatment conditions (see Figure 5.11(a) and (b)). As for the other alloys, their microstructures remain sound after solution heat treatment at 505/520°C, due to the improvement in homogeneity on account of the dissolution of the copper phase (see Figure 5.11(c), (e), (g) and (i)), whereas increasing the second stage solution temperature to 530°C causes serious copper melting in the alloy (see Figure 5.11(d), (f), (h) and (j)). Again, as in the case of single stage solution treatment, for the two stage solution treatments also, the industrial alloys show better results than the experimental alloys for the same Mg level/solution heat treatment conditions.

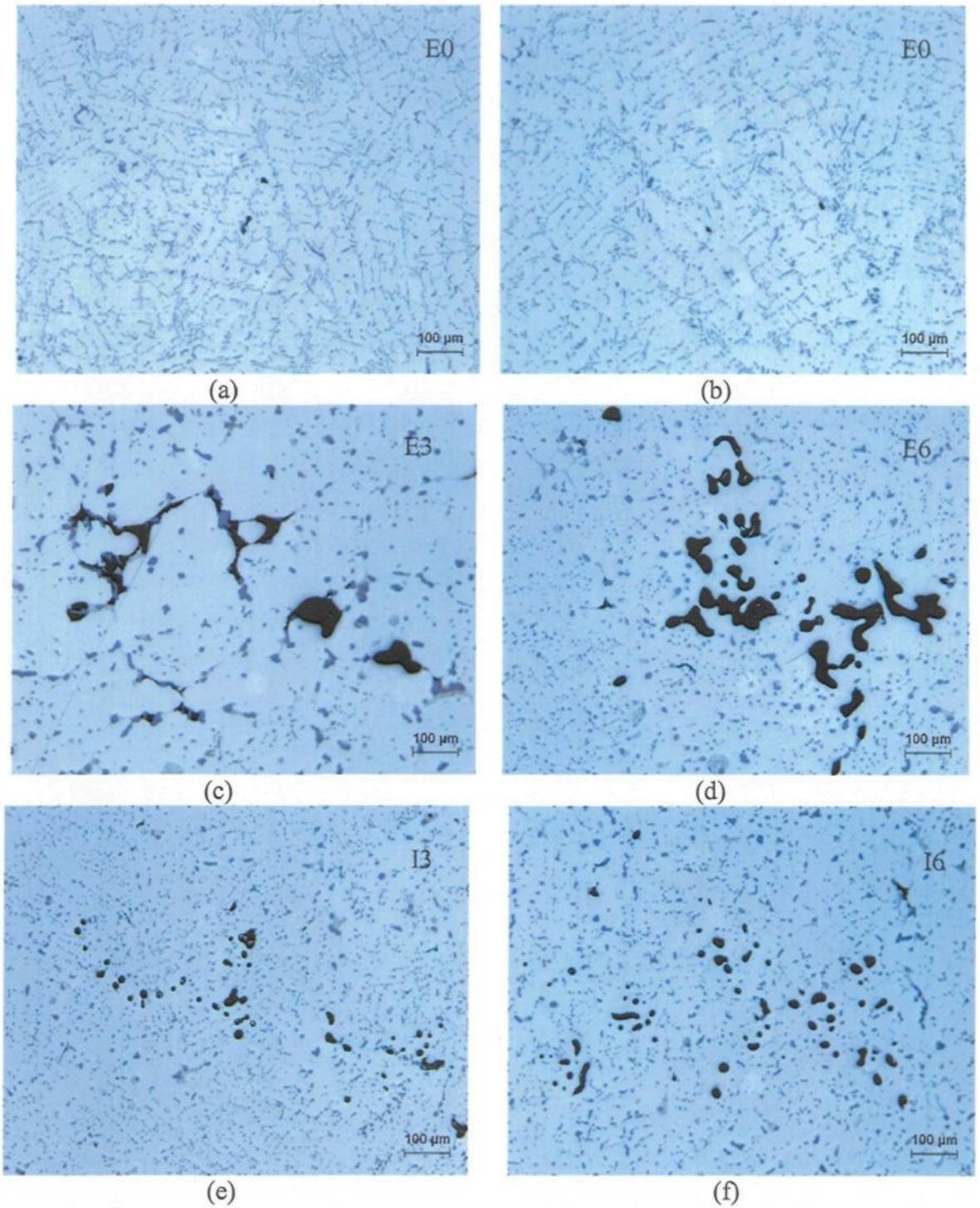


**Figure 5.10** Microstructures of samples obtained from the tensile-tested bars of (a) E0 submitted to 505°C and (b) E0, (c) E3, (d) E6, (e) I3 and (f) I6 alloys submitted to solution heat treatment at 530°C.

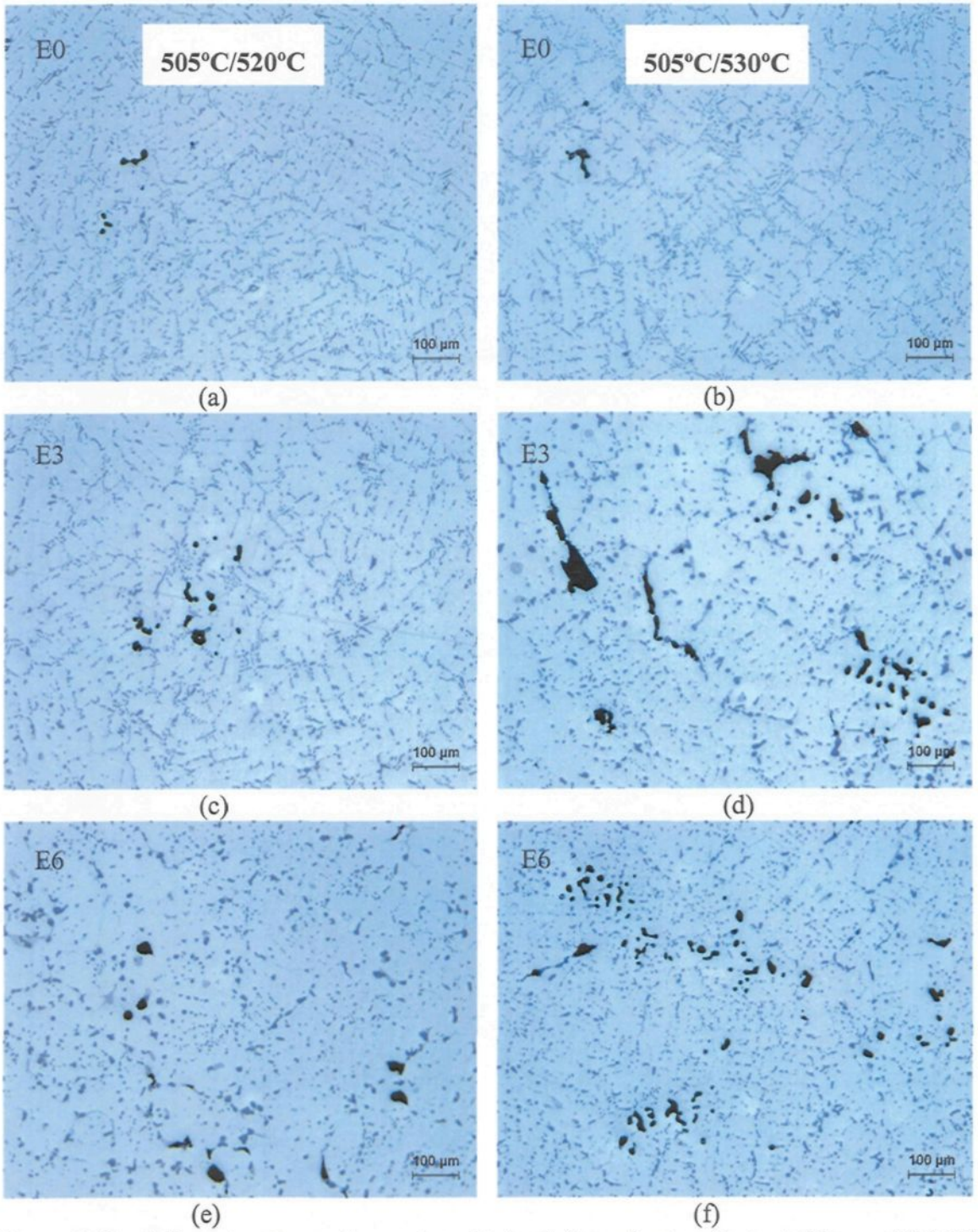


**Figure 5.11** Microstructures of samples obtained from the tensile-tested bars of (a) E0, (c) E3, (e) E6, (g) I3 and (i) I6 alloys submitted to 505°C/520°C two-stage solution heat treatment, and (b) E0, (d) E3, (f) E6, (h) I3 and (j) I6 alloys submitted to 505°C/530°C two-stage solution heat treatment.

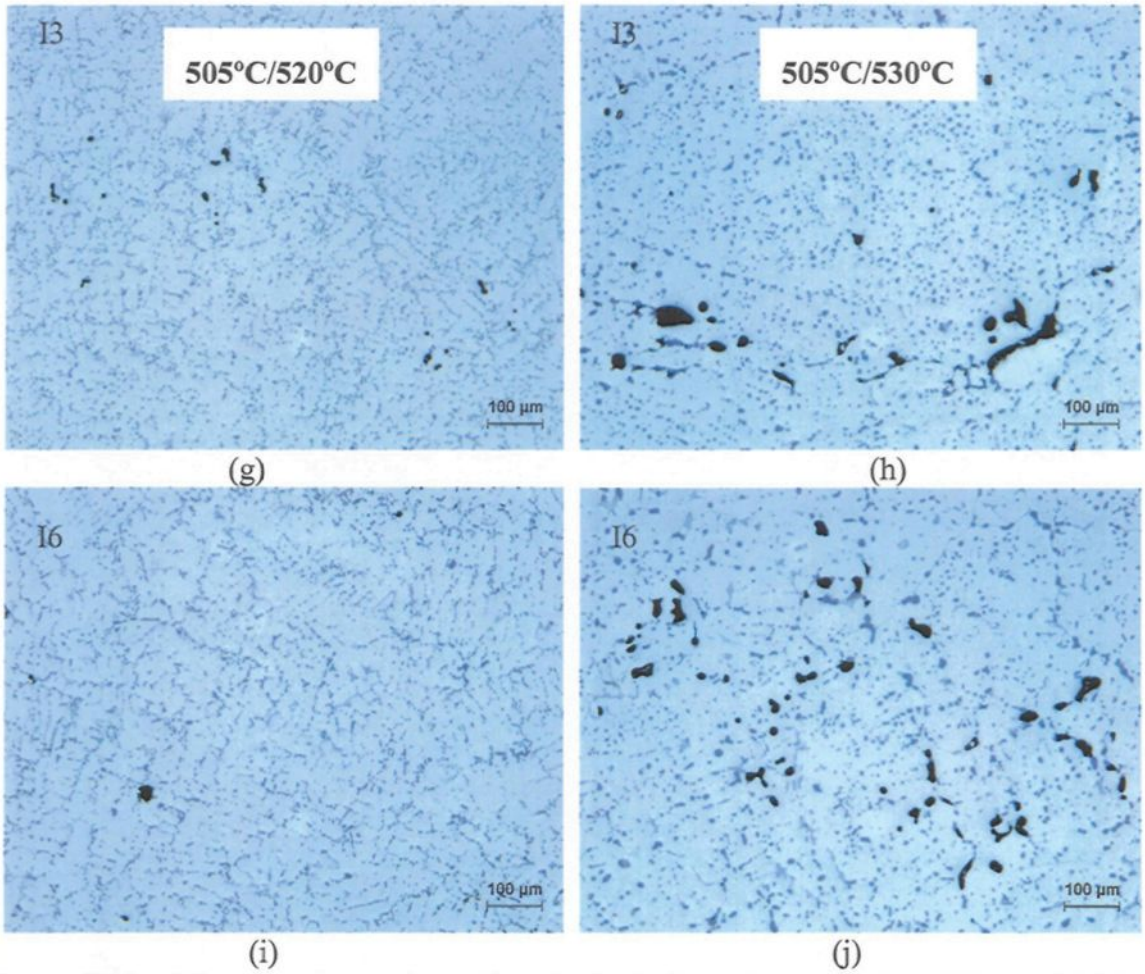


**Figure 5.11** Microstructures of samples obtained from the tensile-tested bars of (a) E0, (c) E3, (e) E6, (g) I3 and (i) I6 alloys submitted to 505°C/520°C two-stage solution heat treatment, and (b) E0, (d) E3, (f) E6, (h) I3 and (j) I6 alloys submitted to 505°C/530°C two-stage solution heat treatment.

# CHAPTER 6

# CONCLUSIONS

# CHAPTER 6

# CONCLUSIONS

A study has been carried out on the effect of Mg additions and solution heat treatment (temperature and different solution heat treatment methods) on the occurrence of incipient melting in experimental and commercial 319 type alloys. Their effect on the mechanical properties was also investigated through a study of the tensile properties. Porosity, arising as a result of incipient melting, was also measured to monitor the occurrence of the incipient melting. Based on the results obtained, the following conclusions can be made.

1. Addition of Mg to 319 alloy, irrespective of the alloy source (experimental or industrial), modifies the Si particle morphology. This effect is observed very clearly at 0.6 wt% Mg, with a corresponding decrease in the Al-Si eutectic temperature compared to the base alloy. At low cooling rate, the modification effect of Mg is not very obvious at low Mg addition, as evidenced by the corresponding microstructural analysis.

2. The addition of Mg to 319 alloy lowers the Al-$CuAl_2$ eutectic temperature; the depression increases with increasing Mg addition. The addition of Mg also causes segregation of the copper phase. This results in the precipitation of the $CuAl_2$ phase

in the block-like, rather than the eutectic-like form. In comparison, the addition of Mg does not affect the precipitation temperature of the α-Al dendrite network.

3. Addition of Mg can also lead to the precipitation of the $Al_5Mg_8Cu_2Si_6$ phase, and to the splitting of the copper phase formation temperature range into two explicit peaks representing the precipitation of $CuAl_2$ and $Al_5Mg_8Cu_2Si_6$ phases, respectively, the latter phase precipitating after the $CuAl_2$ phase. Thus, three different copper-rich phases are observed in these alloys during solidification: block-like $CuAl_2$, eutectic Al-$CuAl_2$, and $Al_5Mg_8Cu_2Si_6$.

4. When addition of Mg exceeds 0.4 wt%, the precipitation of the $Al_5Mg_8Cu_2Si_6$ phase also takes place in another reaction, *before* the precipitation of the $CuAl_2$ phase. The morphology of the $Al_5Mg_8Cu_2Si_6$ phase particles in this case is script-like rather than the irregular-shaped particles normally observed.

5. With respect to the solution treatment temperatures employed in the present study, it is observed that the $Al_5Mg_8Cu_2Si_6$ phase is insoluble, probably due to its large number of atoms.

6. Compared to the experimental alloys, the industrial alloy shows a greater resistance to the melting of the copper phase which may be accounted for in terms of the reaction between Cu and trace elements such as Fe and Ni present in the alloy, leading to an increase in the incipient melting temperature.

7. The tensile properties of the 319 alloys studied may be summarized as follows.

(i) Both the source (experimental *vs.* industrial) and the Mg level of the alloy determine which heat treatment will provide the best tensile properties.

(ii) With respect to the two-stage solution treatment, the second stage solution temperature should not exceed 520°C, particularly at Mg levels of 0.6%.

(iii) Choice of the heat treatment will also depend upon the strength-ductility combination required of the cast component.

8. Based on the results of the tensile property measurements, the tensile curves could be divided into four regions across the range of solution temperatures used. Region Ⅰ corresponds to the change in tensile properties of the alloy on going from the as-cast to the solution heat-treated condition. Region Ⅱ represents the recommended solution treatment temperature range. Region Ⅲ represents a continuation of region Ⅱ until peak properties are reached, following which incipient melting begins to occur, while Region Ⅳ corresponds directly to the progress of incipient melting with the increase in solution temperature.

9. The porosity measurements support the tensile property results in that:

(i) an increase in the solution treatment temperature results in an increase in the porosity parameters measured;

(ii) compared with the single stage solution treatment, the second stage solution-treated samples exhibit smaller porosity values, due to better dissolution of the copper phase and related improvement in homogeneity; and

(iii) for experimental and industrial alloys containing the same Mg levels, the

industrial alloys exhibit lower porosity values for the same solution heat treatment conditions.

Thus, the porosity measurements affirm the tensile property results.

10. In addition to the incipient melting, a high solution temperature also produces macrocracking and buckling (shape deformation) in the test bars.

11. The presence of polygonal Si particles is observed in the vicinity of the molten copper phase (at 530°C), which is different from the spheroidized form of the Si particles observed after solution heat treatment elsewhere in the matrix.

12. From an analysis of all the results obtained from this study, the following solution treatment temperatures are suggested for the various 319 experimental and industrial alloys, to avoid or minimize the occurrence of incipient melting. It is suggested that the temperatures used should never exceed these values.

| Alloy | E0 | E1 | E2 | E3 | E4 | E6 | I3 | I6 |
|---|---|---|---|---|---|---|---|---|
| Suggested temperature (°C) | 535 | 530 | 525 | 525 | 520 | 510 | 520 | 520 |

# SUGGESTIONS FOR FURTHER WORK

The work carried out in the present study is mainly focused on the effect of Mg addition on the occurrence of incipient melting in experimental and commercial 319 type alloys with respect to the solution heat treatment. Based on these results, further work in this area could be undertaken to:

1. Elaborate the effect of trace elements on the increase in incipient melting temperature in Al-Si-Cu-Mg alloys from the industrial point of view.

2. Study the effect of thermal gradient on the sensitivity and severity of incipient melting in Al-Si-Cu-Mg castings, on going from the casting surface to the interior of the casting.

3. Investigate the second stage solution heat temperature in detail, in the case of two-stage solution treatment.

# REFERENCES

# REFERENCES


1 Jerry H. Sokolowski, X-C. Sun, G. Byczynski, D.E. Penrod, R. Thomas and A. Esseltine, "The Removal of Copper-Phase Segregation and the Subsequent Improvement in Mechanical Properties of Cast 319 Aluminum Alloys by a Two-Stage Solution Heat Treatment", *Journal of Materials Processing Technology*, Vol. 53, 1995, pp. 385-392.

2 Z. Li, "Parameters Controlling the Precipitation and Dissolution of $CuAl_2$ Phase in 319 Alloys and Their Influence on the Alloy Performance", M.Eng Thesis, Université du Quebèc à Chicoutimi, Chicoutimi, Canada, 2003.

3 H. de la Sablonniere and F.H. Samuel, "Solution Heat Treatment of 319 Aluminium Alloy Containing ~0.5 wt% Mg", *International Journal of Cast Metals Research*, Vol. 9, 1996, pp. 151-225.

4 F.H. Samuel, "Incipient Melting of $Al_5Mg_8Si_6Cu_2$ and $Al_2Cu$ Intermetallics in Unmodified and Strontium-Modified Al-Si-Cu-Mg (319) Alloys During Solution Heat Treatment", *Journal of Materials Science*, Vol. 33, 1998, pp. 2283-2297.

5 J.L. Jorstad, "Hypereutectic Al-Si Casting Alloys: 25 Years, What's Next?", *Silver Anniversary Paper, AFS Transactions,* Vol. 104, 1996, pp. 669-671.

6 F. Paray and J.E. Gruzleski, "Factors to Consider in Modification", *AFS Transactions*, Vol. 92, 1994, pp. 833-842.

7 L. Bäckerud, G. Chai and J. Tamminen, *Solidification Characteristics of Aluminum Alloys, Vol. 2: Foundry Alloys*, AFS/Skanaluminium, Des Plaines, IL, 1990, pp. 71-84.

8 J.E. Hatch (Ed.), *Aluminum: Properties and Physical Metallurgy*, American Society for Metals, Metals Park, OH, 1984, pp. 320-350.

9 D.O. Northwood, X.C. Sun, G.E. Byczynski and J.H. Sokolowski, "A Metallurgical Study of the Heat Treatment of Aluminum Alloy 319 (Al-6Si-3.5Cu) Castings", *Proceedings of the International Symposium on Recent Metallurgical Advances in*

*Light Metals Industries*, 34th Annual Conference of Metallurgists of CIM, Vancouver, British Columbia, August 20-24, 1995, pp. 355-365.

10 J.E. Davis (Ed.), *Aluminum and Aluminum Alloys*, ASM Specialty Handbook, ASM International, Materials Park, OH, 1993.

11 H. Baker, *Alloy Phase Diagrams*, ASM Handbook, Vol. 3, ASM International, Materials Park, OH, 1992, pp. 2-86.

12 A.M. Samuel and F.H. Samuel, "Modification of Iron Intermetallics by Magnesium and Strontium in Al-Si Alloys", *International Journal of Cast Metals Research*, Vol. 10, 1997, pp. 147-157.

13 M.F. Hafiz and T. Kobayashi, "A Study on the Microstructure-Fracture Behavior Relations in Al-Si Casting Alloys," *Scripta Metallurgica et Materialia*, Vol. 30, 1994, pp. 475-480.

14 E.N. Pan, Y.C. Cherng, C.A. Lin and H.S. Chiou, "Roles of Sr and Sb on Silicon Modification of A356 Aluminum Alloys", *AFS Transactions*, Vol. 102, 1994, pp. 609-629.

15 D. Apelian, G.K. Sigworth and K.R. Whaler, "Assessment of Grain Refining and Modification of Al-Si Foundry Alloys by Thermal Analysis", *AFS Transactions*, Vol. 92, 1984, pp. 297-307.

16. Pacz, Aladar, *United States Patent* 1,387,900 (Aug. 16, 1921).

17 L.M. Hogan and M. Shamsuzzoha, "Crystallography of the Flake–Fibre Transition in the Al-Si Eutectic", *Materials Forum*, Vol. 10, 1987, pp. 270-277.

18 S.Z. Lu and A. Hellawell, "The Mechanism of Silicon Modification in Aluminum-Silicon Alloys: Impurity Induced Twinning", *Metallurgical Transactions*, Vol. 18A, 1987, pp. 1721-1733.

19 P.D. Hess and E.V. Blackmun, "Strontium as a Modifying Agent for Hypoeutectic Aluminum Silicon Alloys", *AFS Transactions*, Vol. 83, 1975, pp. 87-90.

20 R. Sharan and N.P. Saksena, "Rare Earth Additions as Modifiers of Aluminum-Silicon Alloy", *AFS International Cast Metals Journal*, Vol. 2, No. 1, 1978, pp. 29-33.

21 G.K. Sigworth, "Theoretical and Practical Aspects of the Modification of Al-Si Alloys", *AFS Transactions*, Vol. 91, 1983, pp. 7-16.

22 B.J. Ye, C.R. Loper, Jr., D.Y. Lu and C.S. Kang, "An Assessment of the Role of Rare Earth in the Eutectic Modification of Cast Aluminum Silicon Alloys", *AFS Transactions*, Vol. 93, 1985, pp. 533-544.

23 M. Garat and R. Scalliet, "A Review of Recent French Casting Alloy Development", *AFS Transactions*, Vol. 86, 1978, pp. 549-562.

24 M. Garat, G. Laslaz, S. Jacob, P. Meyer, P.H. Guerin and R. Adam, "The State of the Art of the Use of Antimony, Sodium and Strontium-Modified Aluminum Silicon Casting Alloys", *AFS Transactions*, Vol. 100, 1992, pp. 549-562.

25 C.B. Kim and R.W. Heine, "Fundamentals of Modification in the Aluminum-Silicon System", *Journal of the Institute of Metals*, Vol. 92, 1964, pp. 367-376.

26 J. Gobrecht, "The Influence of Alloying Elements on the Duration of Modification of Na and Sr in Al–Si Cast Alloys", *Giesserei*, Vol. 65, 1975, pp. 87-90.

27 J.E. Gruzleski, M. Pekguleryuz and B. Closset, in *Proceedings of the Third International Solidification Conference*, (Sheffield, UK), *Institute of Metals*, Sheffield, 1987.

28 G-Q. Wang, X-F. Bian, W-M. Wang, and J-Y. Zhang, "Influence of Cu and Minor Elements on the Solution Treatment of Al-Si-Cu-Mg Cast Alloys" *Materials Letters*, Vol. 57, Issues 24-25, August 2003. pp. 4083-4087.

29 L. Heusler and W. Schneider, "Influence of Alloying Elements on the Thermal Analysis Results of Al–Si Cast Alloys", *Journal of Light Metals*, Vol. 2, 2002, pp. 17-26.

30 Jerry H. Sokolowski, Mile B. Djurdjevic, Christopher A. Kierkus and Derek O. Northwood, "Improvement of 319 Aluminum Alloy Casting Durability by High Temperature Solution Treatment", *Journal of Materials Processing Technology*, Vol. 109, Issues 1-2, 1 February 2001, pp. 174-180.

31 N. Crowell and S. Shivkumar, "Solution Treatment Effects in Cast Al-Si-Cu Alloys", *AFS Transactions*, Vol.103, 1995, pp.721-726.

32 M. Djurdjevic, T. Stockwell, and J. Sokolowski, "The Effect of Strontium on the Misrostructure of the Aluminium-Silicon and Aluminium-Copper Eutectics in the 319 Alloys," *International Journal of Cast Metals Research*, Vol. 12 (2), 1999, pp. 67-73.

33 G. Sigworth, "Theoretical and Practical Aspects of the Modification of Al-Si Alloys", *AFS Transactions*, Vol. 91, 1983, pp. 7-16.

34 F.H. Samuel, P. Ouellet, A.M. Samuel and H.W. Doty, "Effect of Mg and Sr Additions on the Formation of Intermetallics in Al-6 Wt Pct Si–3.5 Wt Pct Cu-(0.45) to (0.8) Wt Pct Fe 319–Type Alloys", *Metallurgical and Materials Transactions A*, Vol. 29A, 1998, pp. 2871-2884.

35 L. Bäckerud, G. Chai, and J. Tamminen, *Solidification Characteristics of Aluminium Alloys, Vol. 2: Foundry Alloys*, AFS/Skanaluminium, Des Plaines, IL, USA, 1990, pp. 71-84.

36 F.H. Samuel, A.M. Samuel and H.W. Doty, "Factors Controlling the Type and Morphology of Cu-Containing Phases in 319 Al Alloy," *AFS Transactions*, Vol. 104, 1996, pp. 893-901.

37 Z. Li, A.M. Samuel, F.H. Samuel, C. Ravindran, S. Valtierra and H.W. Doty, "Factors Affecting Dissolution of $CuAl_2$ Phase in 319 Alloys", *AFS Transactions*, Vol. 111, 2003, Paper 03-100, pp.1-14.

38 L.F. Mondolfo, *Manganese in Aluminum Alloys*, The Manganese Center, Neuilly sur Seine, France, 1990, pp. 1-35.

39 W. Bonfield and B.K. Dutta, "Precipitation Hardening in an Al-Cu-Si-Mg Alloy at 130 to 220° C", *Journal of Materials Science*, Vol. 11, 1976, pp. 1661-1666.

40 J. Gauthier, P.R. Louchez and F.H. Samuel, "Heat Treatment of 319.2 Aluminium Automotive Alloy: Part 1, Solution Heat Treatment", *Cast Metals*, Vol. 8, 1994, pp. 91-114.

41 J. Gauthier, P.R. Louchez and F.H. Samuel, "Heat Treatment of 319.2 Aluminium Automotive Alloy: Part 2, Aging Behavior", *Cast Metals*, Vol. 8, 1995, pp. 107-114.

42 J.E. Hatch (Ed.), *Aluminum: Properties and Physical Metallurgy,* American Society for Metals, Metals Park, OH, 1984, p. 157.

43 A.M. Samuel and F.H. Samuel, "Review: Various Aspects Involved in the Production of Low Hydrogen Aluminum Castings", *Journal of Materials Science*, Vol. 27, 1992, pp. 6533-6563.

44 J. Campbell, "*The Solidification of Metals*," Iron and Steel Institute, Publication No. 110, London, 1967, 18 pp.

45 K. Kubo and R.D Pehlke, "Mathematical Modeling of Porosity Formation in Solidification", *Metallurgical Transactions B*, Vol. 16B, 1985, pp. 359-366.

46 G.E. Dieter, Jr., *Mechanical Metallurgy*, 2nd Edition, McGraw-Hill, New York, 1976.

47 R. Fuoco and E.R. Corrêa, "Incipient Melting During Solution Heat Treatment of Al-Si-Mg and Al-Si-Cu-Mg alloys", *AFS Transactions,* Vol. 110, 2002, pp. 1-17.

48 L. Lasa and J.M. Rodriguez-Ibabe, "Characterization of the Dissolution of the $Al_2Cu$ Phase in Two Al-Si-Cu-Mg Casting Alloys Using Calorimetry", *Materials Characterization*, Vol. 48, 2002, pp. 371-378.

49 A.M. Samuel, P. Ouellet, F.H. Samuel and H.W. Doty, "Microstructural Interpretation of Thermal Analysis of Commercial 319 Al Alloy With Mg and Sr Additions", *AFS Transactions*, Vol. 105, 1997, pp. 951-962.

50 S. Shivkumar, S. Ricci, Jr., C. Keller and D. Apelian, "Effect of Solution Treatment Parameters on Tensile Properties of Cast Aluminum Alloys", *Journal of Heat Treating*, Vol. 8, 1990, pp. 63-70.

51 Q.G. Wang and C.H. Cáceres, "Mg Effects on the Eutectic Structure and Tensile Properties of Al-Si-Mg Alloys", *Materials Science Forum,* Vol. 242, 1997, pp. 159-164.

52 A.M. Samuel, J. Gauthier and F.H. Samuel, "Microstructural Aspects of the Dissolution and Melting of $CuAl_2$ Phase in Al-Si Alloys During Solution Heat Treatment", *Metallurgical and Materials Transactions*, Vol. 27A, 1996, pp. 1785-1798.

53 Z. Poniewierski, "Effect of the Type of Modification on the Eutectic Microstructure of Aluminum-Silicon Alloys", *Revue Internationale des Hautes Températures et des Réfractaires*, Vol. 14, 1977, pp. 253-260.

54 S. Bercovici, "Control of Solidification Structures and Properties of Aluminum-Silicon Alloys", *Revue de l'Aluminium*, 1979, February, pp. 85-99.

55 A.K. Gupta, A.K. Jena and M.C. Chaturvedi, "Insoluble Phase in Al-1.52Cu-0.75Mg Alloys Containing Silicon", *Materials Scienceand Technology*, Vol. 3, 1987, pp. 1012-1018.

56 H.Y. Hunsicker, "Dimensional Changes in Heat Treating Aluminium Alloys", *Metallurgical Transactions A*, Vol. 11, 1980, pp. 759-773.

57 P. Ouellet, F.H. Samuel, D. Gloria and S. Valtierra, "Effect of Mg Content on the Dimensional Stability and Tensile Properties of Heat Treated Al-Si-Cu (319) Type Alloys", *International Journal of Cast Metals Research*, Vol. 10, 1997, pp. 67-78.

58 W.D. Walter, C.M. Adams and W.S. Pellini, "Mechanism for Pore Formation in Solidifying Metals", *AFS Transactions*, Vol. 64, 1956, pp. 658-664.

59 Q.T. Fang and D.A. Granger, "Porosity Formation in Modified and Unmodified A356 Alloy Castings", *AFS Transactions*, Vol. 97, 1989, pp. 989-1000.

60 N. Roy, A.M. Samuel and F.H. Samuel, "Porosity Formation in Al-9 Wc Pct Si-3 Wt Pct Cu Alloy Systems: Metallographic Observations", *Metallurgical and Materials Transactions A*, Vol. 27A, 1996, pp. 415-429.

61 N. Roy, "Etude parametrique de l'evolution de la porosite dans le system Al-9%Si-3%Cu", M. Eng. Thesis, UQAC, Chicoutimi, QC, Canada, December 1994.

62 G.A. Edwards, G.K. Sigworth, C.H. Cáceres, D.H. StJohn, and J. Barresi, "Microporosity Formation in Al-Si-Cu-Mg Casting Alloys", *AFS Transactions*, Vol. 105, 1997, pp. 809-818.